Generation of an antibody targeting B cell maturation antigen for the treatment of multiple myeloma and autoimmune diseases

Dissertation zur Erlangung des akademischen Grades des
Doktors der Naturwissenschaften (Dr. rer. nat.)
eingereicht im Fachbereich Biologie, Chemie, Pharmazie
der Freien Universität Berlin

vorgelegt von
Dipl. Biol. Felix Oden
aus Berlin

Berlin 2013

Die Arbeit wurde im Zeitraum Januar 2009 bis Sepember 2013 in der Abteilung Tumorgenetik und Tumorimmunologie (Abteilungsleiter Herr Dr. Martin Lipp) am Max-Delbrück Centrum (MDC) für Molekulare Medizin in Berlin Buch angefertigt.

1. Gutachter: Herr Prof. Dr. Oliver Daumke
2. Gutachter: Herr Dr. rer nat habil. Martin Lipp

Disputation am 16.12.2013

Hiermit erkläre ich, dass ich die beigefügte Dissertation selbstständig verfasst und keine anderen als die angegebenen Hilfsmittel genutzt habe. Alle inhaltlich übernommenen Stellen habe ich als solche gekennzeichnet.

Teile dieser Dissertation wurden aus dem sich in Arbeit befindenden Manuskript mit dem Titel „Potent anti-tumor response by targeting B cell maturation antigen (BCMA) in a mouse model of multiple myeloma“ und der Patentanmeldung „An antibody that binds CD269 (BCMA) suitable for use in the treatment of plasma cell diseases such as multiple myeloma and autoimmune diseases” (EP 13156091.4) übernommen.

Berlin, den_____ _____

Ort, Datum Unterschrift

Danksagung

In den nun fast fünf Jahren meiner Doktorarbeit bin ich mit vielen Personen in Kontakt gekommen und habe viele Erfahrungen im Labor, aber auch einige für das Leben sammeln können. Ich werde die Zeit am MDC sehr positiv in Erinnerung behalten und hoffe, dass so manche geschlossene Freundschaft auch in Zukunft bestehen bleiben wird! Es ist jetzt an der Zeit mich bei einigen Menschen zu bedanken, die mich in den vergangen Jahren unterstützt haben.

Mein erster Dank gilt Dr. Martin Lipp, der es mir ermöglichte in seiner Arbeitsgruppe die Idee für die Generierung eines anti-BCMA Antikörpers umzusetzen, mich meine Daten in vielen wissenschaftlichen Konferenzen innerhalb Deutschlands, Europas und den USA präsentieren ließ und auch ein Gutachter dieser Arbeit ist.

Als zweites möchte ich mich bei Prof. Dr. Oliver Daumke bedanken, mit dessen Arbeitsgruppe ich mehrfach erfolgreich zusammenarbeiten durfte und der sich bereiterklärt hat als Erstgutachter diese Arbeit zu bewerten.

In „meiner“ Arbeitsgruppe gibt es neben Dr. Lipp noch weitere Personen, bei denen ich mich bedanken will. Anfangen möchte ich bei P.D. Dr. Uta Höpken und Dr. Gerd Müller, die mir während der gesamten Doktorandenzeit mit Rat und Tat zur Seite standen. Ein besonderer Dank gilt Susanne Scheu, die mir vor allem in den letzten anderthalb Jahren eine großartige Hilfe im Laboralltag war. Auch bei Daniela Keyner, die „gute Seele“ der AG Lipp, möchte ich mich bedanken für die hervorragende Unterstützung bei allen organisatorischen Aufgaben und Fragen. Mein Dank gilt auch allen anderen Arbeitskollegen, nennen möchte ich Kerstin Krüger, Karolin Voss und Heike Schwede, die mir entweder im Laboralltag oder im Tierhaus ab und an eine große Hilfe waren.

Bei Dr. Buket Yilmaz möchte ich mich für die vielen interessanten wissenschaftlichen Diskussionen und vor allem einige „Wochenendhilfen“ im Labor bedanken. Dr. Janko Brand gilt mein Dank für die Labor- und Starthilfe zu Beginn dieses Projekts.

Mein größter Dank gilt Dr. Stephen Marino, mit dem ich die letzten anderthalb Jahre eng zusammengearbeitet habe und der auch diese Dissertation Korrektur gelesen hat. Ich habe viel gelernt und es hat richtig viel Spaß gemacht!

Zuletzt möchte ich mich bei all meinen Freunden bedanken, die mich außerhalb des Institutes unterstützt haben und sehr verständnisvoll waren, wenn ich mal wieder wegen Experimenten kurzfristig Treffen absagen musste…

Für meinen Eltern, die mich immer bedingungslos unterstützt haben.

Schön, dass es Euch gibt!

1. Index

2. Introduction

2.1 The immune system

Organisms are exposed to a variety of harmful environmental conditions including pathogenic microbes like bacteria, parasites, fungi, and viruses which are able to damage or even kill the organism if not eliminated. In addition, environmental factors such as radiation, toxins or ultraviolet light can cause pathogenic transformations of cells in the body. During evolution, vertebrates developed a very complex but effective system to protect the organism from these dangers – the immune system.

The mammalian immune system can be divided into two major arms that are closely coordinated. The first, innate immunity comprises anatomical and physiological barriers like epithelial layers, body temperature, and compartmental pH values. Furthermore, several proteins like granzymes or proteins of the complement system as well as cell types such as monocytes, macrophages, granulocytes, natural killer (NK) cells and dendritic cells are part of the innate immunity. These components are able to distinguish between self and non-self and thereby form the first line of defense against pathogenic invaders. They use mechanisms not specifically adapted to the pathogen, recruit adaptive immune cells by the secretion of chemokines and cytokines, and present parts of the pathogens to these cells for the development of a pathogen-specific immune response. The adaptive immune cells form the second arm of the immune system. Their characteristics include a high specificity towards pathogens and the ability to establish an immunological memory to enable the organism to defeat a secondary exposure to the same pathogen more effectively and rapidly.

The adaptive immune system can be further subdivided into B and T lymphocytes which develop from common lymphoid progenitor (CLP) cells in the bone marrow (BM) – together with the thymus and liver, a primary lymphoid organ. Whereas B cells pass through several developmental stages in the BM, immature T cells migrate to the thymus to become mature T helper (CD4-positive) or cytotoxic T (CD8-positive) lymphocytes. T helper cells are the main regulators of the immune system. They interact via their T cell receptor (TCR) and their CD4 receptor with class II major histocompatibility complexes (MHCII) on antigen presenting cells (APCs) like magrophages, dendritic cells and B cells. Through MHCII molecules, short peptides of pathogen-derived proteins engulfed by the APC are presented to the T helper cells. Depending on the co-stimulus of the APC which depends on the origin of the presented peptide (pathogenic or non-pathogenic) towards the T cell and on the specificity of the TCR, the T helper cell secretes cytokines which induce or inhibit an immune response. In contrast,

cytotoxic T lymphocytes (CTLs) recognize intracellularly produced peptides presented via MHCI molecules. Using MHCI, all nucleated cells display peptides of their proteome on the cell surface. Since virus infected cells synthesize viral proteins, they also display peptides of these foreign proteins via MHCI on their cell surface. The same is true for some tumors that display peptides derived from abnormal proteins caused by genetic alterations via MHCI. The CTL exhibiting the TCR specific for such a pathogenic peptide directly induces apoptosis via death receptors or lyses the cell using granzymes. (Janeway, 2001)

2.2 B lymphocytes, antibodies, and their mode of action

Due to their ability to secret antibodies, B lymphocytes are the main players of the humoral immune response. Therefore, the next section is devoted to this cell type and its special weapon(s) – the antibodies.

2.2.1 Antibody structure

Antibodies, also called immunoglobulins (Ig), are Y-shaped divalent proteins made of two identical heavy and light chains. They can either be membrane-bound as part of the B cell receptor (BCR) complex on B lymphocytes or expressed as secreted proteins (Pieper et al., 2013; Schroeder and Cavacini, 2010). In the latter case, they lack their transmembrane and intracellular domains. There are five different antibody isotypes known in humans and mice which differ in the size of their heavy chains, the number and location of disulfide bonds, the quantity of oligosaccharide moieties attached, and the length of the hinge region (Janeway, 2001; Maul and Gearhart, 2010; Schroeder and Cavacini, 2010; Stavnezer et al., 2008; Xu et al., 2013). The antibody isotypes will be introduced in more detail in section 2.2.4. In this section, the most abundant isotype in the serum (IgG) is used to describe the general features of antibody structure (**Fig. 1**).

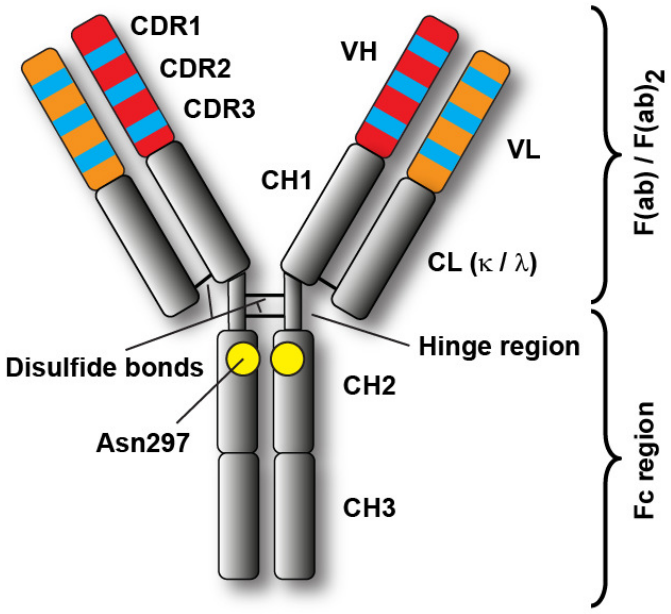

Figure 1: Structure of a human IgG1 antibody. Two identical heavy chains composed of three constant heavy (CH) domains and one variable heavy (VH) domain are linked by two disulfide bonds in the hinge region. The CH2 exhibits an N-glycosylation site at position Asn297 (yellow dots).

The two identical light chains containing one constant light and one variable light (VL) domain are linked through a disulfide bond between the constant light (CL) and CH1 domains. The CL is either of κ or λ subtype origin.

VH and VL each exhibit three complementarity determining regions (CDR; blue lines) which are important for antigen binding.

The fragment antigen binding (F(ab)) comprises the VH, CH1, VL, and CL domain. The $F(ab)_2$ additionally contains the hinge region.

The fragment crystallizable (Fc) comprises the hinge region, CH2 and CH3.

The light and heavy chains have molecular weights of 25,000 and 50,000 Dalton (Da), respectively, resulting in an overall molecular weight of approximately 150,000 Da (150 kDa). Each heavy chain (HC) contains an N-terminal variable region (VH) followed by three constant heavy chain domains (CH1-3). The hinge region is located between CH1 and CH2 and links the two heavy chains via two disulfide bonds. The CH2 domain contains an N-glycosylation site at position Asn297 (numbering according to Kabat and Wu (1991)). Each light chain (LC) also exhibit an N-terminal variable region (VL) followed by either a kappa or lambda light chain constant domain (CLκ or CLλ, respectively). The LC is linked to the HC through a disulfide bond between CL and CH1 (Schroeder and Cavacini, 2010). The two N-terminal variable regions (VR) of HC and LC each contain three complementarity determining regions (CDRs) which are important for the direct interaction with the antigen. These are the most diverse areas of the antibody and generally become mutated during affinity maturation in germinal centers after encounter with the specific antigen (Kuroda et al., 2012; Stavnezer et al., 2008). The VR together with the CH1 and CL domain comprise the

fragment antigen binding (F(ab)). Both Fabs connected via the hinge region are called $F(ab)_2$. $F(ab)_2$ fragments can be obtained through proteolytic digestion of antibodies using papain or pepsin. The remaining constant domains are called the fragment crystallizable (Fc) region. The Fc region is able to interact with the C1q protein of the complement system and Fc gamma receptors (FcγRs) on FcγR bearing cells such as monocytes, granulocytes, eosinophils, dendritic cells, natural killer (NK) cells and B cells (Nimmerjahn and Ravetch, 2007). The immune response upon Fc interaction with a C1q or an Fc receptor depends on the isotype of the antibody and its glycosylation pattern. For the interaction with FcRs, both the specific receptor (see section 2.2.7) and the specific cell type are important for the outcome of the immune response (Nimmerjahn and Ravetch, 2007, 2008; Ravetch and Nussenzweig, 2007; Xiang et al., 2007).

2.2.2 Antibody rearrangement and antibody repertoire

The great diversity of antibody specificities is based on the diversity of the BCRs which in turn is achieved by random fusion of different gene segments located on the human chromosomes 14 (heavy chain locus), 2 (κ chain locus) and 22 (λ chain locus) during B cell maturation in the BM (Matsuda et al., 1998). Heavy chain variable domains are made of three different gene segments: variable (V_H), diversity (D_H) and joining (J_H). Light chain variable domains only contain V_L and J_L gene segments. For humans, there are 44 V_H, 27 D_H and 6 functional J_H gene segments known as well as 30 Vκ, 40 Vλ, 5 Jκ and 4 functional Jλ gene segments (Hozumi and Tonegawa, 1976; Li et al., 2004; Matsuda et al., 1998). The rearrangements of the V(D)J take place during B cell development in the bone marrow (see section 2.2.3) (Pieper et al., 2013; Schroeder and Cavacini, 2010; Stavnezer et al., 2008). For this, the recombination activating gene enzymes RAG1 and RAG2, exclusively expressed in lymphocytes, recognize the so called recombination signal sequences (RSS) which flank the gene segments and introduce single strand DNA breaks followed by hairpin formation (Schatz et al., 1992; Schroeder and Cavacini, 2010). Upon random hairpin cleavage, the recombination event is facilitated through several enzymes such as Artemis, DNA Ligase IV and Cernunnos (Ma and Steinmetz, 2004). Cleavage of the hairpin results in the occurrence of palindromic sequences at the cleavage sites called P-addition. The terminal deoxynucleotidyl transferase (TdT) randomly inserts up to 15 nucleotides into the junction. This nucleotide-addition (N-addition) substantially increases the diversity of the antibody repertoire (Schroeder and Cavacini, 2010). The rearrangement starts with the D_H-J_H fusion followed by V_H-D_HJ_H fusion of the heavy chain. If the $V_HD_HJ_H$ rearrangement includes a shift in the reading frame due to P- and N-addition, the second HC locus is rearranged. Apoptosis is

induced if this second rearrangement is also not in frame. If the rearrangement was productive, a complete heavy chain can be expressed upon splicing to the Igμ constant domain gene segment. This heavy chain associates with a surrogate light chain forming the precursor B cell receptor (pre-BCR) which hinders the rearrangement of the second $V_HD_HJ_H$ locus (allelic exclusion) and induces proliferation of this pre-B cell clone (Boekel et al., 1998). After proliferation, the light chain V_LJ_L rearrangement is induced resulting in a complete B cell receptor which is tested for the binding of self-antigens in the BM microenvironment. If the newly formed BCR does recognize self-antigens, the second allele of the LC locus becomes rearranged to replace the initial LC. This process is called receptor editing and allows each pre-B cell a second attempt to become an immature B cell leaving the BM for the periphery (Pieper et al., 2013). If receptor editing does not eliminate the autoimmune danger inherent in the pre-B cell, the cell undergoes apoptosis. (Janeway, 2001; Pieper et al., 2013; Stavnezer et al., 2008)

Due to the complexity of antibody assembling and the numerous ways to introduce variation, the diversity of the human antibody repertoire is estimated to exceed $5*10^{13}$ possible antibodies. This number is further increased through somatic hypermutations which are point mutations mainly located in the CDRs and introduced during affinity maturation of the antibody in germinal centers (see section 2.2.3). (Janeway, 2001; Pieper et al., 2013; Stavnezer et al., 2008)

2.2.3 B cell development and germinal center (GC) formation

B lymphocytes arise from common lymphoid progenitor cells in the BM. Their special feature is their B cell receptor (BCR) which is expressed on the cell surface and is highly specific for one epitope. Each cell has a unique BCR which is generated during development in the BM (see section 2.2.2), modified in germinal centers (GCs) in the periphery and secreted as an antibody when the B cell reaches the plasma cell stage. (Pieper et al., 2013; Schroeder and Cavacini, 2010)

The first distinct B cell lineage cell is the progenitor B cell (pro-B cell). Pro-B cells express CD19, a component of a co-receptor of the BCR complex, on their surface (**Fig. 2**). At this stage, the rearrangement of the heavy chain locus begins (Vale and Schroeder, 2010) (see section 2.2.2). With the display of a pre-B cell receptor on the cell surface, the precursor B cell (pre-B cell) stage is reached. At this time, the expression of the B lymphocyte antigen CD20 begins. During the pre-B cell stage, rearrangement of the LC locus takes place and, if necessary, receptor editing as well (Pieper et al., 2013; Vale and Schroeder, 2010). B cells

with a complete rearranged BCR of the IgM isotype expressed on the cell surface leave the bone marrow and recirculate through the periphery as immature B cells. At this stage, they express the chemokine receptors CCR7 and CXCR5, which are required for migration to and within secondary lymphoid organs (SLOs) like the spleen, Peyer's patches or lymph nodes (Förster et al., 1999; Müller et al., 2003). SLOs contain structures comprised of T and B cell follicles. These structures are crucial for the maturation of mature B cells into memory B cells or antibody secreting plasma cells (Gatto and Brink, 2010; Klein and Dalla-Favera, 2008; Shlomchik and Weisel, 2012; Vinuesa et al., 2009, 2010). Entering SLOs is connected with the co-expression of both IgM and IgD BCRs on the surface of the mature B cells. They enter the T cell follicle via high endothelial venules (HEVs) in response to the presence of the chemokines CCL19 and CCL21, which are the ligands of CCR7. Upon entry into the T cell follicle, B cells down-regulate CCR7 expression and migrate due to CXCR5 activation towards the chemokine gradient of CXCL13, which is present in the B cell follicles (Förster et al., 1999; Müller et al., 2003). Mature B lymphocytes which encounter their specific antigen engulf it and present it via MHCII to T helper cells. In order to become activated, these B cells need to receive co-stimulatory signals from a T helper cell specific for one of the displayed MHCII peptides. If the B cell lacks co-stimulation, it becomes anergic and loses the ability to further mature. This mechanism insures that auto-reactive B cells that passed the selection in the BM are not able to induce autoimmunity (Gatto and Brink, 2010; Klein and Dalla-Favera, 2008; Vinuesa et al., 2009, 2010). B lymphocytes receiving co-stimulatory signals from a T cell upon encounter with their antigen begin to proliferate and either become short-lived low-affinity IgM-secreting extrafollicular plasma cells or migrate into the B cell follicle where they form germinal centers (GCs) together with follicular dendritic cells (FDCs) and the antigen-specific T cell (Paus et al., 2006; Vinuesa et al. 2009, 2010). The antigen-specific T cells located in GCs are called follicular B helper T cells (T_{FH}) and also express CXCR5 (Müller et al., 2003). GCs are divided into so called dark and light zones. In the dark zone, clonal expansion of B lymphocytes – which are now referred to as centroblasts – takes place (Gatto and Brink, 2010; Klein and Dalla-Favera, 2008; Vinuesa et al., 2009, 2010). During this proliferation process, centroblasts acquire somatic hypermutations (SHMs) in the variable region of their BCR due to expression of the activation-induced DNA-cytosine deaminase (AID) (Muramatsu et al., 2000). SHMs are random mutations induced mainly into the CDRs of the HC and LC and alter the affinity towards the specific antigen. Depending on the nature of co-stimulation, class switch recombination can also take place – also facilitated by AID (see section 2.2.5) (Pieper et al., 2013; Xu et al., 2013). After clonal expansion, centroblasts become centrocytes which now require survival signals delivered by FDCs and

T_{FH} cells. These signals involve B cell activating factor (BAFF)/BAFF-receptor, CD40/CD40-ligand, and inducible T cell co-stimulator (ICOS)/ICOS-ligand interactions (Rickert et al., 2011). Only centrocytes with the highest affinity for the antigen obtain these survival signals and can start a new round of clonal expansion. Cells not receiving signals undergo apoptosis. This mechanism ensures that cells which exhibit a low-affinity or auto-reactive BCR upon SHM are cleared from the system (Gatto and Brink, 2010; Klein and Dalla-Favera, 2008; Vinuesa et al., 2009, 2010). B lymphocytes which survive the selection process in the germinal center leave the B cell follicle and either develop into memory B cells or high-affinity antibody-secreting plasma cells (PCs) (Shlomchik and Weisel, 2012). Memory B cells remain recirculating for years. If they encounter their antigen a second time, they can either proliferate and mature into plasma cells immediately without T cell help or pass through a new round of GC selection. Plasma cells, upon leaving the B cell follicle migrate to the BM where they can persist for decades. (Gatto and Brink, 2010; Klein and Dalla-Favera, 2008; Shlomchik and Weisel, 2012; Vinuesa et al., 2009, 2010)

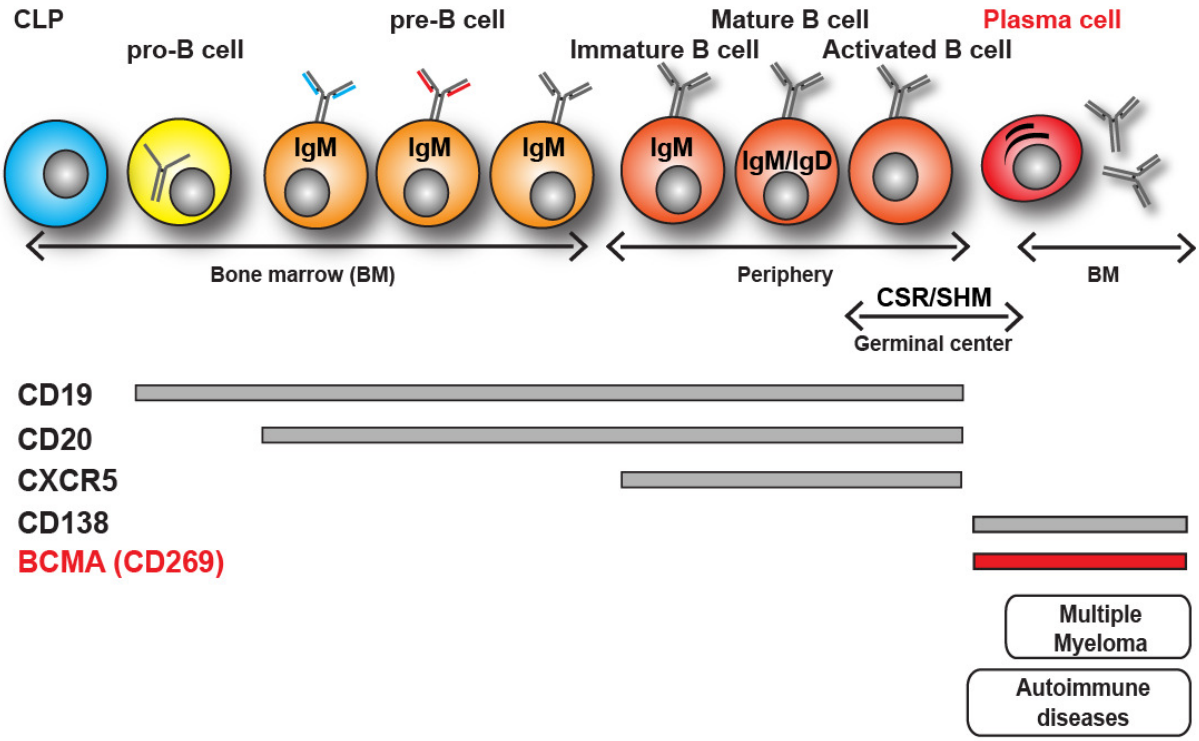

Figure 2: Development of B lymphocytes and their common surface makers. B cells arise from common lymphoid progenitor (CLP) cells in the BM. Upon VH rearrangement (pro-B cell) the pre-BCR is presented on the surface (pre-B cell; blue LC), resulting in VL rearrangement. The complete BCR is tested for self-recognition and if necessary receptor editing takes place (red LC). Non-autoimmune pre-B cells leave the BM and become immature B cells. When entering secondary lymphoid organs B cells become mature B lymphocytes and express IgM and IgD on their surface. Upon encounter of antigen and T cell help, B cells become activated and form germinal centers (GCs) with follicular B helper T cells and follicular dendritic cells. Within GCs, class switch recombination (CSR; see section 2.2.5) and somatic hypermutation (SHM) take place. High affinity B cells either become memory B cells or antibody secreting cells. Plasma cells (see section 2.2.6) are either short-lived or long-lived. Long-lived PCs migrate to the BM and are supported in special niches.

The common B cell marker is CD19, expressed from the pro-B cell stage until the B lymphocyte develops into a plasma cell. The same is true for CD20, which is expressed from the pre-B cell stage. CXCR5 is a common marker for recirculating B cells. The normal marker for PCs is Syndecan-1 (CD138). Since multiple myeloma arises from PCs and many autoimmune disorders are intensified through autoantibody production, plasma cells are interesting target cell population. Targeting B cell maturation antigen, which is also only present on B cells released from the GC reaction, is a promising option for the treatment of such diseases.

Since plasma cells are responsible for the secretion of auto-reactive antibodies in several autoimmune diseases and, in addition, can develop into malignant plasma cells responsible for multiple myeloma and plasma cell lymphoma, section 2.2.6 will focus in more detail on this cell type.

2.2.4 Antibody isotypes

As already mentioned in section 2.2.1, humans and mice produce five different antibody isotypes (IgA, IgD, IgE, IgG, and IgM), which are defined by the heavy chain (Schroeder and

Cavacini, 2010). The light chain is either of κ or λ origin and has no known impact on the effector function of an antibody.

IgA consists of the heavy chain alpha (HCα) which comprises three CH domains and a hinge region. CH2 and CH3 each contain one N-glycosylation site; the hinge regions are linked by only one disulfide bridge. There are two subclasses known (IgA1 and IgA2) which both play an important role in mucosal immunity. IgA exists either as a monomer or as dimer containing a joining chain (J-chain) which has a molecular weight of 15 kDa. It has a serum half-life of approximately 6 days and approximately 3-4 mg/ml of IgA can be found in the serum. IgA is the most abundant antibody isotype found in salvia, tears and secretions of the gastrointestinal tract, genitourinary tract and respiratory tract. Only IgA dimers are transported to the mucous through transcytosis by immature epithelial cells. This transport is facilitated by the polymeric immunoglobulin receptor (pIgR), which is proteolytically cleaved to release the IgA into the mucous. The cleaved part of the pIgR is called the secretory component. It exhibits a molecular weight of 70 kDa and remains bound to the constant domain of the antibody. (Janeway, 2001; Schroeder and Cavacini, 2010)

Only about 0.03 mg/ml of the IgD isotype is found in the serum. Its immunological role is not completely understood, since IgD deficient mice seem to have a normal humoral immune response. However, IgD is found on the surface of mature B cells together with IgM. The HCδ contains three CH domains and can be N-glycosylated once in the CH2 and twice in the CH3 domains. Like in IgA, only one disulfide bridge is formed in the hinge region to connect the two identical heavy chains. Its serum half-life is about 3 days. (Janeway, 2001; Schroeder and Cavacini, 2010)

IgE is at $5*10^{-5}$ mg/ml the least abundant isotype found in the serum with a half-life of approximately 2 days. It is built from HCε, which lacks the hinge region but contains 4 CH domains. The HCs are connected through two disulfide bonds formed between the CH2 domains. The CH1 domain exhibits three, the CH2 one and the CH3 two N-glycosylation sites. IgE plays an important role in defeating parasites. It is generally bound by the high affinity Fcε receptor 1 (FcεR1) expressed on mast cells and basophils that triggers the release of histamines, chemokines, and proteases upon cross-linking. Uncontrolled FcεR cross-linking through IgE is also known to cause type I hypersensitivities and anaphylactic reactions. (Janeway, 2001; Schroeder and Cavacini, 2010)

The most common serum isotype at approximately 14 mg/ml is IgG, which can be further subdivided into the subclasses IgG1, IgG2, IgG3 and IgG4 in humans and IgG1, IgG2a,

IgG2b and IgG4 in mice (Janeway, 2001; Schroeder and Cavacini, 2010). The half-life of this isotype is approximately 21 days. The most potent pro-inflammatory antibody isotypes in humans are IgG1 and IgG3 and, in mice, IgG2a and IgG2b. These isotypes have the greatest potential to induce antibody-dependent cellular cytotoxicity (ADCC; see section 2.2.8) and complement-dependent cytotoxicity (CDC; see section 2.2.9) (Campoli et al., 2010; Tai and Anderson, 2011). IgG antibodies normally contain several somatic hypermutations and are high affinity antibodies, as they have passed through the germinal center reaction. For these reasons the IgG1 isotype is generally used for therapeutic antibodies, where a strong immune response is desired (Jefferis, 2012; Wang and Weiner, 2008). Not only is the isotype of the antibody crucial for its effector function, but the structure of its glycan moiety is also important. For instance, IgG1 antibodies lacking the core fucose residue are much more potent in ADCC activation than fucosylated antibodies (Yamane-Ohnuki and Satoh, 2009). In contrast, antibodies lacking the entire glycan moiety are unable to induce ADCC or CDC at all (Jefferis et al., 1998; Nezlin and Ghetie, 2004; Shields et al., 2001).

IgM is the first Ig isotype expressed on immature B cells and also the first antibody isotype secreted upon the initiation of a humoral immune response. The HCμ consists of four CH domains and lacks a hinge region. IgM is highly N-glycosylated with one site in each of the CH1, CH3 and CH4 and two sites in the CH3 domains. The heavy chains are connected via one disulfide bond located at the end of CH2. Secreted IgM exists as pentameric molecules wherein five identical IgM monomers are linked through a J-chain. The molecular weight of a complete IgM is about 970 kDa, and it has a serum concentration of approximately 1.5 mg/ml, and a half-life of around 10 days. Since IgM-positive B cells do not pass through the germinal center reaction (see section 2.2.3), IgM antibodies are unmutated and generally exhibit only a low affinity towards their target molecule. They are, however, able to strongly induce the classical pathway of the complement system. (Janeway, 2001; Schroeder and Cavacini, 2010)

2.2.5 Class switch recombination (CSR)

When leaving the BM, all immature B cells express IgM on their surface (Pieper et al., 2013; Vale and Schroeder, 2010). Upon entering secondary lymphoid organs (see section 2.2.3), the surface level of IgM is reduced and partially replaced by IgD. Thus, mature B cells express both IgM and IgD on their surface. This is possible because both isotypes are splice variants encoded by the same mRNA (Stavnezer et al., 2008; Xu et al., 2013). As long as the B cell expresses IgM and/or IgD, the other isotypes are not transcribed, since they first need to become somatically recombined with the rearranged VDJ gene segments. The HCμ is

encoded directly downstream of $V_HD_HJ_H$ followed by HCδ. The other heavy chain isotypes are encoded downstream of HCδ in the following order: HCγ3, HCγ1, HCα1, HCγ2, HCγ4, HCε, and HCα2. This order ensures that once a B cell switches to IgA1, it will never be able to switch back to IgM, IgD, IgG3, or IgG1, because the B lymphocyte has then lost the genetic information for these isotypes through the recombination process. However, it has still the capability to further switch to IgG2, IgG4, IgE, or IgA2. (Janeway, 2001; Stavnezer et al., 2008; Xu et al., 2013)

When a B lymphocyte enters the germinal center reaction upon encounter of its antigen, it begins to proliferate. This clonal expansion ensures that enough copies of this unique B cell clone exist for SHMs and CSR, since both are irreversible changes on the DNA level (Gatto and Brink, 2010; Klein and Dalla-Favera, 2008; Vinuesa et al., 2009, 2010). AID, the enzyme mainly responsible for the introduction of SHMs in the variable region of the antibody, is additionally thought to play a role in CSR, as in AID-deficient mice only IgM-positive B cells are present (Muramatsu et al., 2000). CSR takes place in the dark zone of the GC through cytokines delivered by T helper cells and the interaction of CD40/CD40-ligand (Stavnezer et al., 2008; Xu et al., 2013). Thus, the co-stimulatory signals of the T cell regulate to which isotype the B cell switches and with that define the nature of the humoral immune response against the antigen (see sections 2.2.3). For instance, the release of interleukin 4 (IL-4) firstly induces the switch to IgG4 and secondly, in B lymphocytes already switched to IgG4 induces the isotype switch to IgE. In contrast, IL-5 and tumor necrosis factor ß (TNF-ß) secretion induces the switch to IgA. The expression of interferon γ (INF-γ) results in CSR to IgG1. (Janeway, 2001; Stavnezer et al., 2008; Xu et al., 2013)

2.2.6 Plasma cells (PCs)

Plasma blasts and plasma cells are both antibody secreting cells (ASCs) expressing B lymphocyte-induced maturation protein 1 (Blimp-1), the main regulator protein for ASCs (Deng et al., 2010; Pieper et al., 2013). Plasma blasts are immature plasma cells. They are either short-lived and die within several days after entering the APC stage or develop into long-lived PCs migrating to the BM (Shapiro-Shelef and Calame, 2005; Tarlinton et al., 2008). The mechanisms underlying the development from plasma blast into long-lived BM PCs are not well known, but it is thought that the affinity to the antigen and the isotype of the BCR might play a role. The initiation process of Blimp-1 expression is also not completely understood but it is known that its expression is important for the down-regulation of CXCR5, CCR7, and Bcl-2 as well as the up-regulation of CXCR4, X-box-binding protein 1 (XBP1),

and B cell maturation antigen (BCMA) (Achatz-Straussberger et al., 2008; Deng et al., 2010; Shapiro-Shelef and Calame, 2005; Tarlinton et al., 2008). The down-regulation of CXCR5 and CCR7 enables the APC to leave the GC reaction and the B cell follicle. Down-regulation of Bcl-2 induces a pro-apoptotic stage rationalizing the short lifespan of plasma blasts. XBP1 is important for expression of several genes crucial for immunoglobulin secretion (Shapiro-Shelef and Calame, 2005; Tarlinton et al., 2008). The expression of CXCR4 enables the plasma cell to migrate to the BM where the chemokine CXCL12 is present (Achatz-Straussberger et al., 2008). The BM environment features special niches which support PC survival. For instance, BM stromal cells begin secreting IL-6 upon PC contact. In addition, interaction of A proliferation-inducing ligand (APRIL; see section 2.4.1) and BAFF (see section 2.4.2) with the B cell maturation antigen (BCMA; see section 2.4.4) stimulate PC survival through induction of anti-apoptotic gene expression (Peperzak et al., 2013; Shapiro-Shelef and Calame, 2005; Tarlinton et al., 2008).

2.2.7 Fc receptors (FcRs)

The induction of an immune response upon binding of an antibody to its target depends on the isotype of the antibody (see section 2.2.4) and its interaction with the complement C1q protein (see section 2.2.9) and the corresponding Fc receptor(s) expressed by various cell types of the innate immune system and B lymphocytes (Nimmerjahn and Ravetch, 2007, 2008). With the exception of IgD, each isotype class has its own Fc receptors. Thus, IgA antibodies bind to FcαRs, IgMs recognize FcμRs, IgEs interact with FcεRs, and IgGs bind to FcγRs (Ravetch and Nussenzweig, 2007). Since this dissertation deals with an IgG1 antibody, the following section focuses on the Fcγ receptors which are expressed on basophiles, mast cells, neutrophils, macrophages, monocytes, NK cells, dendritic cells, and B lymphocytes including plasma cells (Nimmerjahn and Ravetch, 2008; Ravetch and Nussenzweig, 2007).

The FcγR network of mice and humans is fairly complex due to the presence of four different IgG subclasses (see section 2.2.4) as well as four (FcγRI, FcγRIIB, FcγRIII and FcγRIV) and six (FcγRI, FcγRIIA, FcγRIIB, FcγRIIC, FcγRIIIA and FcγRIIIB) different Fcγ-receptors expressed in mice and humans, respectively, which bind each Ig subclass with varying affinities (Nimmerjahn and Ravetch, 2007, 2008; Ravetch and Nussenzweig, 2007). In both species, the FcγRIIB (CD32B) is the only inhibitory FcγR known and this is also the only FcγR which is found on B lymphocytes and plasma cells (Xiang et al., 2007). It binds with low to medium affinity (micromolar range) to IgG immune complexes and is important for maintaining the peripheral tolerance by negative regulation of antigen uptake, antigen

presentation, cell activation and plasma cell survival (Nimmerjahn and Ravetch, 2007, 2008; Ravetch and Nussenzweig, 2007).

FcγRI (CD64) exhibits the highest affinity to IgG antibodies, followed by FcγRIIIA (CD16A). They are found on innate immune cells like granulocytes, monocytes, macrophages, dendritic cells or natural killer cells and therefore link the innate with the adaptive immune system (Nimmerjahn and Ravetch, 2007, 2008). Cross-linking of these FcγRs cause cell activation and leads to ADCC (see section 3.2.8). However, the activation of ADCC also depends on the glycosylation moiety of the antibody at Asn297 (Jefferis et al., 1998; Nezlin and Ghetie, 2004; Shields et al., 2001).

Another Fc-receptor which is able to bind IgG antibodies is the neonatal Fc receptor (FcRn) (Roopenian and Akilesh, 2007). Beside its role in supplying the fetal and the neonatal circulation with maternal IgG antibodies, it is responsible for the long serum half-life of IgG. The receptor is expressed on monocytes and endothelial cells which take up serum proteins at physiological pH and form acidified endosomes. Within these endosomes, all proteins lacking a recycling receptor become degraded. Since IgG molecules can bind to the FcRn at low pH they survive degradation and are released back to the circulation (Roopenian and Akilesh, 2007). The binding of IgG antibodies to FcRn depends on its CH3 domain and is unaffected upon changes to the glycosylation moiety (Jefferis et al., 1998; Nezlin and Ghetie, 2004; Shields et al., 2001).

2.2.8 Antibody-dependent cellular cytotoxicity (ADCC)

With regard to cell-depletion, there are two major effector mechanisms known (Campoli et al., 2010; Tai and Anderson, 2011). One is the complement-dependent cytotoxicity (CDC) towards the target cell (see section 2.2.9). The other mechanism is called antibody-dependent cellular cytotoxicity (ADCC). This effector function is characterized by the recruitment of immune cells which express Fc-receptors for the respective isotype of the antibody (see section 2.2.7). ADCC is mainly mediated upon binding of IgG1 or IgG3 to FcγRI or FcγRIIIA expressed by innate immune cells like granulocytes, monocytes, macrophages, dendritic cells or natural killer cells (Nimmerjahn and Ravetch, 2007, 2008). Depending on the cell type, there are several modes of action of FcγR-bearing cells upon recognition of an antibody-marked target cell. Granulocytes generally release vasoactive and cytotoxic substances or chemoattractants but are also capable of phagocytosis. Monocytes and macrophages respond with phagocytosis, oxidative burst, cytotoxicity or the release of pro-inflammatory cytokines, whereas NK cells release granzymes and perforin and can also trigger cell death through the

interaction with FAS on the target cell and their Fas ligand (Chavez-Galan et al., 2009; Nimmerjahn and Ravetch, 2008; Wang and Weiner, 2008).

2.2.9 Complement and complement-dependent cytotoxicity (CDC)

The complement system is the humoral part of the innate immune system which is mainly important for the fight against pathogenic microbes (Nilsson and Ekdahl, 2012). It is divided into three different protein-cascade pathways which all lead to the formation of the membrane attack complex (MAC) that results in lysis of the target cell. Activation of all three pathways results in release of the peptides C3a and C5a which serve as mediators of inflammation and recruit phagocytes (Janeway, 2001; Nilsson and Ekdahl, 2012). The alternative and mannose-binding lectin pathways directly recognize surface structures on pathogens, whereas the classical pathway, which is initiated through the binding of C1q to the Fc fragment is the only complement pathway related to antibody-mediated cytotoxicity (Wang and Weiner, 2008). Thus, binding of antibodies to the target cell enables the C1q protein to bind areas located in the CH2 domains including the glycan moiety of the antibodies – a requirement for the C1q-mediated start of the classical complement pathway (Jefferis et al., 1998; Nezlin and Ghetie, 2004; Shields et al., 2001). The most potent antibody isotypes to induce CDC are IgG1, IgG3 and IgM (Janeway, 2001; Schroeder and Cavacini, 2010).

2.2.10 Therapeutic antibodies

The use of therapeutic antibodies has dramatically increased over the last two decades. In 1986, the first monoclonal antibody (mAb) was approved by the U.S. Food and Drug Administration (FDA). This murine IgG2a anti-CD3 mAb named OKT3 was developed to dampen T cell responses upon organ transplantation (Smith, 1996). Currently, there are 31 approved mAbs on the market and more than 130 in clinical trials (Immunologylink.com, 2013). The number of antibodies currently in preclinical development may be even higher.

Today, almost all antibodies used as therapeutics are recombinantly designed, resulting in various formats differing in size, tissue penetration, half-life, cytotoxicity, functionality, and production capacity. For instance, there is a variety of small antibody formats which bind to two or more different epitopes at the same time and directly recruiting effector cells to target cells (Holliger and Hudson, 2005; Xie et al., 2005).

Therapeutic antibodies can act through several mechanisms upon binding to their target (**Fig. 3**). The binding itself can trigger signal cascades in the cell leading to programmed cell death

(Campoli et al., 2010; Chavez-Galan et al., 2009). It can also block the interaction of a receptor with its ligand by binding either to the receptor or the ligand. This interruption can cause apoptosis if signals important for survival are affected (Campoli et al., 2010; Chiu et al., 2007). However, the most common mechanisms for a therapeutic antibody are the induction of ADCC or CDC upon binding to the target (Campoli et al., 2010; Tai and Anderson, 2011). Recently, the use of antibody-drug conjugates has increased, since it was shown that these agents are more effective in depleting cancer cells. In this format, antibodies are fused to small cytotoxic agents which cause cell death upon internalization (Sievers and Senter, 2013). Additionally, some therapeutic mAbs are able to induce a CTL response against tumors. Upon labelling of the tumor cell by the mAb, the cell is taken up by APCs such as dendritic cells or B cells. These cells are able to cross-present exogenous protein via MHCI molecules to CD8-positive T cells. This cross-priming of CTLs induces a direct cell-mediated killing of the tumor by CTLs (Campoli et al., 2010).

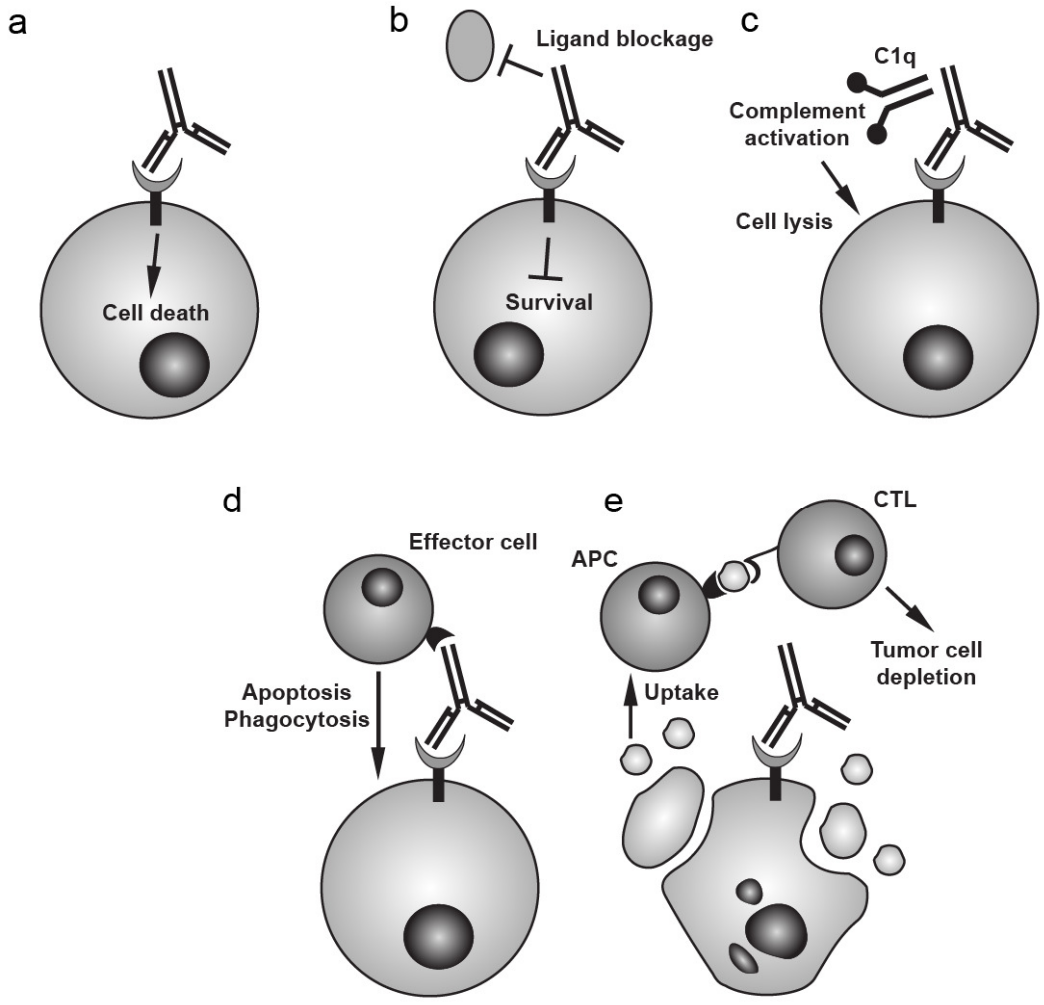

Figure 3: Mechanisms of antibody action. (a) Binding of a therapeutic antibody can directly induce cell death. **(b)** Binding of a receptor can block receptor-ligand interaction leading to a survival disadvantage. **(c)** Complement activation. **(d)** Antibody-mediated cellular cytotoxicity. **(e)** Induction of cell death by a therapeutic antibody can lead to antigen uptake and presentation on an APC which in

turn induces a CTL immune response.

The most well-known therapeutic mAb is the anti-CD20 IgG1 antibody Rituximab from Genentech (Roche) which has been very successfully used in the treatment of B cell malignancies and autoimmune diseases (Alawadhi et al., 2012; Cheson and Leonard, 2008; Gregersen and Jayne, 2012). It is a chimeric mAb consisting of a human IgG1 constant domain and a murine variable region (Leget and Czuczman, 1998). Since chimeric antibodies are partly non-self, they are prone to induce an immune response upon administration in humans. In order to avoid this immunogenicity, most antibodies developed today are either of completely human origin or chimeras that are subsequently humanized. In humanized mAbs, only the CDRs are still of foreign origin (Getts et al., 2010).

2.3 Multiple myeloma (MM)

Multiple myeloma (MM) is an aggressive neoplasm of plasma cells (PCs) constituting 13% of hematological malignancies and 1% of all cancers worldwide. It is characterized by an accumulation of abnormal PCs in the bone marrow (BM) and with disease onset also in the periphery. Since the disease interferes with many organs, patients often suffer from various symptoms like bone pain due to bone lesions caused by pathologic activation of osteoclasts. In addition, the disturbed production of normal blood cells leads to anemia and the clonal expansion of the malignant PC causes the appearance of a paraprotein in the serum. Paraproteins are either whole immunoglobulin molecules or antibody light chains secreted by the tumor cells. They are detectable in urine and blood of MM patients and can cause renal failure. (Chou, 2012; Palumbo and Anderson, 2011; Raab et al., 2009)

Surprisingly, the incidence of MM in women is less frequent than in men and the median age at diagnosis is 61 and 62, respectively. In addition, people of black African decent are twice as much affected by MM than Caucasians. The cause behind these gender and race differences is not known (Raab et al., 2009).

2.3.1 Diagnosis

The diagnostic criteria of MM proposed by the International Myeloma Working Group (IMWG) are based by the presence of at least 10% clonal plasma cells in the bone marrow and more than 30 g/l of paraprotein in the serum or urine. The classification into asymptomatic or symptomatic MM depends on the absence or presence of one or more so called CRABO criteria, respectively. These criteria include hypocalcaemia (C), renal

insufficiency (R), anemia (A), bone lesions (B) and other myeloma-related symptoms (O). The pre-stages of MM are thought to be a monoclonal gammopathy of undetermined clinical significance (MGUS) that can further develop into a smoldering MM (Kuehl and Bergsagel, 2002). In MGUS, the presence of the paraprotein is less than 30 g/l and PCs also account for less than 10% in the BM. Within the smoldering MM stage, one of these two factors exceed its threshold. (Durie et al., 2004; Kyle and Kumar, 2009)

Patients suspected of having MM are analyzed for their complete blood count, an elevated calcium level in the blood and the presence of paraprotein in serum and/or urine. In addition, blood and bone marrow are tested for the presence of MM cells, which typically express CD38, CD56 and CD138 but are negative for the cell surface markers CD19 and CD45 (Fonseca et al., 2009; Kyle and Kumar, 2009). To screen for MM-related bone lesions, conventional systemic skeletal system radiography is used often followed by magnetic resonance imaging (MRI) (Dimopoulos et al., 2011; Kyle and Kumar, 2009).

The IMWG developed a stage system based on the presence of serum ß$_2$-microgrobulin and serum albumin levels to predict the survival of MM patients. This system distinguishes three different stages (Greipp et al., 2005) (**Tab. 1**).

Table 1: Staging system of multiple myeloma

Stage	Serum level	Median survival (month)
I	ß$_2$-microgrobulin < 3.5 mg/l albumin > 3.5 g/dl	62
II	Neither stage I nor stage III	45
III	ß$_2$-microgrobulin > 5.5 mg/dl	29

2.3.2 Etiology

Several genetic abnormalities are associated with the development of multiple myeloma. Besides changes in microRNA expression and gene methylation modifications based on epigenetic changes (Roccaro et al., 2009), chromosomal translocations also frequently occur in MM cells. The most common translocations occur between the chromosomal loci 14(q32.33) and 11q13, 4p16.3, 6p21, 16q23 and 20q11 (Bergsagel and Kuehl, 2005; Kuehl and Bergsagel, 2002). In addition, hypoploidy of t(4;14) or deletion of 17p13 can also be found in MM cells (Fonseca et al., 2009).

In addition to genetic alterations, the interaction between MM cells and the bone marrow microenvironment causes the production and secretion of cytokines and growth factors such as a proliferation inducing ligand (APRIL), B cell activating factor (BAFF), interleukin-6 (IL-6), interleukin-10 (IL-10), insulin growth factor (IGF), and vascular endothelial growth factor

(VEGF). These proteins are regulated by autocrine and paracrine loops and support tumor growth, survival, and migration and additionally promote drug resistance (Claudio et al., 2002; Moreaux et al., 2004; Moreaux et al., 2009b; Podar et al., 2003). Thus, they are involved in onset, progression, and relapse of multiple myeloma.

2.3.3 Treatment

In 1962, the melphalan-prednisone (MP) combination therapy for the treatment of MM patients was introduced and prolonged survival after diagnosis to approximately 3-4 years (Bergsagel, 1962; Kumar et al., 2008). Using high dose MP chemotherapy improved the response rate but had no impact on survival. In the 1980s, high dose MP chemotherapy followed by autologous stem cell transplantation extended survival to 4-5 years (Kumar et al., 2008). Recently, the introduction of anti-angiogenic and immunomodulatory drugs like thalidomide or lenalidomide or the proteasome inhibitor bortezomib into the clinic has improved the median survival of MM patients to 5-7 years (Hideshima and Anderson, 2002; Munshi and Anderson, 2013; Palumbo and Anderson, 2011; Raab et al., 2009; Richardson et al., 2003; Yang and Yi, 2011). The current standard therapy for MM patients under the age of 65 includes administration of thalidomide, lenalidomide or bortezomib followed by autologous or allogenic hematpoietic stem cell transplantation (HSCT). For patients exhibiting serious heart, renal or liver damage, low dose MP treatment followed by autologous HSCT is indicated. Patients older than 65 years are also treated with melphalan in combination with thalidomide, lenalidomide, or bortezomib but without subsequent HSCT (Chou, 2012).

Since MM is still incurable, substantial effort is being invested in gaining a better understanding of the disease and for the development of new drugs based on antibodies (Tai and Anderson, 2011).

2.4 APRIL, BAFF, and their receptors

An effective and balanced humoral immune response is crucial not only protecting the body from pathogenic invaders but also regulating the strength of the response and avoiding autoimmune manifestations. The APRIL and BAFF ligand-receptor interaction network plays an important role in the maturation, proliferation and survival of B cells upon egress from the bone marrow. Since this network and its signalling is complex and not completely understood, and other receptor-ligand interactions are also involved in B cell development and homeostasis (such as ICOS/ICOS-ligand and CD40/CD40-ligand), the following section serves as a short introduction to this part of the tumor necrosis factor ligand and receptor

superfamilies.

2.4.1 A proliferation inducing ligand (APRIL)

The cytokine APRIL (CD256) is member 13 of the tumor necrosis factor ligand superfamily (TNFLSF) and interacts with the receptors B cell maturation antigen (BCMA) and transmembrane activator and calcium modulator and cyclophilin ligand interactor (TACI) (see section 2.4.4 and 2.4.5, respectively). It is expressed by eosinophils, macrophages, monocytes, osteoclasts, mesenchymal stromal cells of the BM and B cells (Belnoue et al., 2008; Chu et al., 2007; Chu et al., 2011; Hideshima et al., 2007; Mackay et al., 2010; Mackay et al., 2003). The biologically active form of APRIL is a homotrimer that can either be membrane bound or released into the serum in a furin-dependent manner (Lopez-Fraga et al., 2001). The membrane-bound form consists of 250 amino acids (aa) and has a molecular weight (MW) of approximately 27.4 kDa. The cleaved/secreted form of APRIL comprises amino acids 105 to 250 and has a MW of about 16.3 kDa (Uniprot.org, 2013b). In addition to its interaction with BCMA and TACI, APRIL exhibits a heparin-sulfate proteoglycan (HPSG) binding site which enables the additional recruitment of HPSG modified receptors like Syndecan-1 (CD138) on plasma cells (Ingold et al., 2005; Mackay and Schneider, 2009; Reijmers et al., 2011). Due to its interactions, APRIL plays an important role in B cell survival, especially at the plasma cell stage (Belnoue et al., 2008; O'Connor et al., 2004; Rickert et al., 2011).

2.4.2 B cell activating factor (BAFF)

BAFF (CD257) which shares 33% homology with APRIL is member 13B of the TNFLSF and also interacts with BCMA and TACI (Mackay and Schneider, 2009; Rickert et al., 2011). In addition, it binds to BAFF receptor (BAFF-R; see section 2.4.3). This additional interaction makes BAFF crucial for the maturation and homeostasis of peripheral B cells (Coquery and Erickson, 2012; Mackay et al., 2010; Mackay and Schneider, 2009; Mackay et al., 2003; Rickert et al., 2011). As with APRIL, the active form of BAFF is a homotrimer which is found either membrane-bound or secreted (Bossen et al., 2011). There is also a BAFF 60mer complex form which is thought to be more effective than the BAFF trimer in engaging TACI (Bossen et al., 2008). The membrane bound form consists of 285 aa and has a MW of about 31.2 kDa; the secreted form contains aa 134 to 285 and has a MW of approximately 16.3 kDa (Uniprot.org, 2013a). BAFF is expressed by several cell types including follicular dendritic cells (FDCs), macrophages, monocytes, neutrophils, mesenchymal stromal cells of the BM and also B lymphocytes and MM cells have been shown to secret BAFF (Chu et al., 2011;

Hideshima et al., 2007; Mackay et al., 2003; Rickert et al., 2011).

2.4.3 BAFF receptor (BAFF-R)

The only known ligand for the BAFF receptor (CD268), which is member 13C of the tumor necrosis factor receptor superfamily (TNFRSF), is BAFF. The expression of BAFF-R starts on immature B cells leaving the BM and lasts during their maturation into germinal center B cells. The maturation of transitional B cells into follicular B lymphocytes is connected with an up-regulation of BAFF-R (Hsu et al., 2002; Meyer-Bahlburg et al., 2008), whereas germinal center B cells and plasma cells as well as MM cells show reduced levels (Coquery and Erickson, 2012; Mackay et al., 2003; Ng et al., 2004; O'Connor et al., 2004; Rickert et al., 2011). As with its expression on recirculating B cells, BAFF-R is important for the differentiation of immature B cells into follicular and mantle zone (MZ) B lymphocytes as well as the proliferation and survival of the peripheral B cell populations (Moore et al., 1999; Schneider et al., 1999).

Unlike the majority of TNF receptors which bind their ligands via multiple cysteine-rich domains (CRDs), BAFF-R possesses only a partial CRD. However, mutational analysis of BAFF-R revealed that the presence of aspartic acid (D) at position 26 and leucine (L) at position 28 of the extracellular domain is essential for binding to BAFF (Gordon et al., 2003). This D*x*L motif is also found in the B cell maturation antigen (BCMA; see section 2.4.4) and the transmembrane activator and calcium modulator and cyclophilin ligand interactor (TACI; see section 2.4.5) which are both interaction partners of BAFF. Interaction of BAFF with BAFF-R causes oligomerization of the receptor and leads to the expression of anti-apoptotic genes like members of the B cell lymphoma 2 (Bcl-2) family such as Bcl-2, Bcl-w, Bcl-x_L and myeloid cell leukemia 1 (Mcl-1) (Mackay et al., 2010; Mackay et al., 2003; Peperzak et al., 2013; Rickert et al., 2011). The major player of the signaling cascade is the protein complex nuclear factor kappa-light chain-enhancer of activated B cells (NF-κB). This transcription factor is found in almost all human cell types and controls the expression of various genes involved in development, cell adhesion, proliferation, the innate and adaptive immune responses, and apoptosis (Perkins, 2007; Rickert et al., 2011). Since the NF-κB pathway is very complex, highly regulated by other cellular pathways, and differs by cell type and induction, the following section only describes the main events of the canonical NF-κB signal transduction pathway upon BAFF-R engagement. BAFF interaction with BAFF-R recruits the TNF receptor associated factors 2 and 3 (TFARF2, TRAF3) to the intracellular domain of the receptor. They associate with different proteins leading to the activation of inhibitor NF-κB

kinase (IKK). The IKKs phosphorylate serines of inhibitors of NF-κB (IκB), for instance, serines 32 and 36 of IκBα (Perkins, 2007; Rickert et al., 2011). These phosphorylations lead to ubiquitination and finally degradation of IκBα in proteasomes (DiDonato et al., 1995). The degradation of IκBα activates NF-κB which migrates into the nucleus and initiates the transcription of Bcl-2 family member genes, thereby supporting cell survival. Engagement of BAFF with BAFF-R was also shown to activate the non canonical NF-κB signal transduction pathway (Shen et al., 2011). The main proteins involved herein are the NF-κB-inducing kinase (NIK) and IKK1 which are responsible for the phosphorylation of p100, which in turn leads to its degradation and the release of NF-κB.

2.4.4 B cell maturation antigen (BCMA)

The B cell maturation antigen (CD269) is TNFRSF member 17. Although it was described before BAFF-R, BCMA signaling and function are less well understood than these of BAFF-R. One reason might be that BCMA can interact with both BAFF and APRIL (Marsters et al., 2000; Patel et al., 2004). For both ligands, the crystal structures of the receptor-ligand complex have been solved and revealed that APRIL and BAFF share more than 95% of their BCMA epitope but strongly vary in their affinity to it (Bossen and Schneider, 2006; Hymowitz et al., 2005; Liu et al., 2003). In contrast to BAFF-R, BCMA is expressed in fewer cell populations (Coquery and Erickson, 2012; Marsters et al., 2000) and was detected first in the Golgi apparatus in cells of the B cell lineage. Therefore, BCMA was thought to play a role in antibody secretion (Gras et al., 1995). BCMA mRNA levels can be found in splenic and memory B cells, plasma blasts and plasma cells, but expression of BCMA protein on the cell surface is almost exclusively detected on antibody secreting plasma blasts, plasma cells and in multiple myeloma (Benson et al., 2008; Coquery and Erickson, 2012; Darce et al., 2007; Good et al., 2009; Novak et al., 2004; O'Connor et al., 2004). Due to its surface expression pattern, BCMA is, unlike BAFF-R, not involved in the maturation, proliferation, and homeostasis of transitional B cells but is important for the survival of plasma blasts and long-lived BM plasma cells (Coquery and Erickson, 2012; Mackay et al., 2003; O'Connor et al., 2004; Rickert et al., 2011).

The BCMA epitopes of APRIL and BAFF are nearly identical and both contain the D*x*L motif (Gordon et al., 2003). Therefore, it is not surprising that interactions of APRIL or BAFF with BCMA are redundant. Both ligands induce the expression of anti-apoptotic genes as seen by engagement of BAFF-R with BAFF. In plasma cells, high levels of Mcl-1 protein are found associated with BCMA signaling (Peperzak et al., 2013; Rickert et al., 2011). Signal

transduction via BCMA also involves the canonical NF-κB pathway. But, as mentioned above NF-κB signaling differs by cell type and stimulus. Thus, it was shown that upon engagement, BCMA can interact with TRAF1, 2, 3, 5 and 6, whereas the role of TRAF1 in NF-κB activation is not completely understood and TRAF3 is thought to regulate TRAF2- and 5-mediated NF-κB activation (Coquery and Erickson, 2012; Hatzoglou et al., 2000; Hauer et al., 2005; Shen et al., 2011).

2.4.5 Transmembrane activator and calcium modulator and cyclophilin ligand interactor (TACI)

TACI (CD267) is member 13B of the TNFRSF and like BCMA interacts with APRIL and BAFF. It is expressed on mature B cells and plasma cells and shows variable expression in MM (Mackay and Schneider, 2008; Moreaux et al., 2005). It is up-regulated on activated B cells upon Toll-like receptor (TLR) stimulus (Groom et al., 2007). Since mutations of TACI are found in about 10% of patients with common variable immunodeficiency (CVID), it is thought to play an important role in isotype class switching (Castigli et al., 2005; Salzer et al., 2005). Like BAFF-R and BCMA, TACI signals via NF-κB. Unlike BAFF-R and BCMA, TACI exhibits the capacity to intracellularly interact with the myeloid differentiation primary response gene 88 (MyD88) and activate the NF-κB pathway synergistically with TLRs (Groom et al., 2007).

2.5 Aim of the project

Plasma cell malignancies like multiple myeloma or plasma cell leukemia (PCL) are still incurable (Palumbo and Gay, 2011; Raab et al., 2009) and some autoimmune diseases like systemic lupus erythematosus and rheumatoid arthritis often depend on autoantibody-secreting plasma cells (Chan et al., 2013; Schett and Gravallese, 2012; Wofsy, 2013). Therefore, plasma cells are an attractive target for the treatment of such diseases.

During the past two decades, monoclonal antibodies have increasingly been used for the treatment of hematological malignancies. For example, treatment with Rituximab, a monoclonal antibody (mAb) against CD20, in combination with chemotherapy, has dramatically improved the long-term survival of patients suffering from Non-Hodgkin's Lymphoma (Cheson and Leonard, 2008), However, MM patients treated with Rituximab showed no clinical improvement (Tai and Anderson, 2011), since the majority of PCs are CD20-negative. Therefore, other mAbs targeting cell surface molecules expressed on MM cells like CD38, CD70 or CD138 are currently in preclinical development or in early phase

clinical trials. Strategies interfering with the tumor growth-promoting BM microenvironment by targeting B cell growth factors such as IL-6 or BAFF have also reached the clinic (Munshi and Anderson, 2013; Tai and Anderson, 2011; Yang and Yi, 2011). However, there are as yet no approved antibody-based therapies for MM. In addition, the epitopes of mAbs in clinical development are not exclusively present on MM cells. CD38, for instance, is also expressed on activated B and T cells (Malavasi et al., 2008) and CD138 is present on epithelial cells (Inki and Jalkanen, 1996). For these reasons, the aim of this thesis was to generate a monoclonal antibody against the B cell maturation antigen which is almost exclusively expressed on PCs, plasma blast and in MM (Benson et al., 2008; Carpenter et al., 2013; Coquery and Erickson, 2012; Darce et al., 2007; O'Connor et al., 2004). In addition, BCMA has been previously investigated as a potential therapeutic target for the treatment of MM (Carpenter et al., 2013; Ryan et al., 2007).

3. Material

3.1 Antibodies

Abcam (Cambridge): purified rat-anti-human CD269

AbD serotec (Düsseldorf): purified mouse-anti-6xHis

Cell Signaling (Boston): purified rabbit-anti-IκBα

Jackson ImmunoResearch (Suffolk): allophycocyanin (APC)-conjugated goat-anti-rat IgG, phycoerythrin (PE)-conjugated goat-anti-human IgG, PE-conjugated goat-anti-mouse IgG, horseradish peroxidase (HRP)-conjugated goat-anti-rabbit IgG

3.2 Bacteria

Escherichia coli (*E. coli*) DH5α (F- Φ80d*lac*ZΔM15 endA1 recA1 hsdR17(r_K^- r_K^+) supE44 thi-1 d^- gyrA96 Δ(*lac*ZYA-argF)U169), *E. coli* BL21/Rosetta (F- ompT $hsdS_B$ (r_B^- m_B^-) gal dcm pRARE (Cam^R)

3.3 Bacterial media and antibiotics

Luria-Bertani (LB): 10 g/l tryptone, 10 g/l NaCl, 5 mM NaOH, 5 g/l yeast-extract

Merck (Darmstadt): Ampicillin

Sigma-Aldrich (Munich): Chloramphenicol

Terrific Broth (TB): 4 g/l glycerol, 17 mM KH_2PO_4, 72 mM K_2HPO_4, 25 g/l tryptone, 24 g/l yeast-extract

3.4 Cell culture media, supplements and antibiotics

Life Technologies (Darmstadt): FreeStyle™ F17, Geneticin (G418), Pluronic F-68

Organotechnie (La Courneuve): Tryptone N1

PAA Laboratories (Pasching): Dulbecco's Modified Eagle Medium (DMEM), fetal calf serum (FCS), L-glutamine, Penicillin/Streptomycin 100x solution, Roswell Park Memorial Institute (RPMI) 1640 medium, Trypsin-Ethylenediaminetetraacetic acid (Trypsin-EDTA) solution

3.5 Cell lines

MDC for Molecular Medicine (Berlin): Human Embryonic Kidney 293 (HEK293)-T, Jurkat,

Jurkat-Luc, MM.1S, MM.1S-Luc

National Research Council of Canada (Montreal): 293-6E

3.6 Chemicals

Chemicals were used from the following companies: Biochrom AG (Berlin), Biosynth (Staad), Fluka (Germany), Lonza (Cologne), Merck (Darmstadt), Roth (Karlsruhe), and Sigma-Aldrich (Germany).

3.7 Consumables

Consumables from the following companies were used: Becton Dickinson (Franklin Lakes), Bio-Rad (Munich), Braun (Kronberg/Taunus), Corning (New York), Eppendorf AG (Hamburg), GE Healthcare Life Science (Solingen), Gilson, Inc (Villiers le Bel), Greiner Bio-One International AG (Kremsmünster), Imtech Deutschland GmbH & Co. KG (Düsseldorf), Microflex (Vienna), Miltenyi Biotec (Bergisch Gladbach), Nunc (Waltham), Pechiney (Paris), Qiagen (Venlo), Sartorius (Göttigen), Thermo Fisher Scientific (Waltham), TPP (Trasadingen), Watts Microflex NV (Rotselaar).

3.8 DNA vectors

MDC for Molecular Medicine (Berlin): pCMV-VSG-G, pFU, pLP1, pLP2

MPI for Infectious Biology (Berlin): human γ1 heavy chain vector, human κ light chain vector

National Research Council of Canada (Montreal): pTT5, pTTo/GFP

3.9 Enzymes

GE Healthcare Life Science (Solingen): PreScission protease

Life Technologies (Darmstadt): SuperScript™ III reverse transcriptase

New England Biolabs (Schwalbach): Antartic phosphatase, PNGase F, restriction enzymes, T4 DNA ligase, Phusion high-fidelity DNA polymerase

Roboklon (Berlin): Taq DNA polymerase

Roche Applied Science (Indianapolis): RNase A

3.10 Inhibitors

Roche Applied Science (Indianapolis): Complete Protease Inhibitor Cocktail Tablets,

PhosSTOP Phosphatase Inhibitor Cocktail Tablets

3.11 Installations and devices

Installations and devices were used from the following companies: BDK Luft- und Reinraumtechnik GmbH (Sonnenbühl-Genkingen), Becton Dickinson (Franklin Lakes), Binder (Tuttlingen), Biometra (Göttingen), Bio-Rad (Munich), Canon (Krefeld), Eppendorf AG (Hamburg), Gesellschaft für Labortechnik mbH (Burgwedel), Gilson, Inc (Villiers le Bel), Heraeus (Hanau), HP Germany (Böblingen), Infors-HT (Hamburg), Kleinfeld Labortechnik (Gehrden), Leica Microsystems (Wetzlar), Liebherr (Biberach an der Riss), neoLab (Heidelberg), PEQLAB (Erlangen), PerkinElmer (Waltham), Scientific Industries, Inc (New York), Severin (Sundern), Syngene (Cambridge), Tecan Group Ltd. (Crailsheim), Thermo Fisher Scientific (Waltham), VWR International (Darmstadt).

3.12 Kits

Life Technologies (Darmstadt): SuperScript™ III First-Strand Synthesis Sytem for RT-PCR

Qiagen (Hilden): EndoFree Plasmid Maxi/Mega Kit, RNeasy Micro/Mini Kit, RNase-free DNase Set

Roche Applied Science (Indianapolis): IsoStrip Mouse Monoclonal Antibody Isotyping Kit

Zymo Research (Irvine): DNA Clean & Concentrator™ Kit, Zyppy™ Plasmid Miniprep Kit

3.13 Mice

Charles River (Wilmington): CB17.Cg-Prkdscid Lystbg/Crl (SCID Beige)

The Jackson Laboratory (Maine): NOD.Cg-Prkdcscid Il2rgtm1Wjl Tg(CSF2)2Ygy Tg(IL3)1Ygy Tg(KITL)3YgyJGckRolyJ (NSG)

3.14 Peripheral blood mononuclear cells (PBMCs)

Charité Campus Mitte (Berlin): Filter buffy coats (FBCs)

3.15 Primer

BioTeZ (Berlin): The detailed primer list can be found in the appendix (see section 10.2).

3.16 Recombinant proteins

Biomol (Hamburg): B cell activating factor His-tagged (BAFF)

3.17 Software

Adobe (Munich): Illustrator, Photoshop, Reader

Caliper LifeScience (Waltham): Living Image 3.0

GraphPad Softwae (La Jolla) : Prism 5

Microsoft (Redmond): Office 2007, Windows XP

PerkinElmer (Waltham): FinchTV

Tree Star (Ashland): Flowjo 7.6

4. Methods

4.1 Molecular biology methods

4.1.1 Isolation of plasmid DNA

Depending on the amount of plasmid DNA needed either the DNA Zyppy™ Plasmid Miniprep Kit (Zymo Research) or the EndoFree Plasmid Maxi/Mega Kit (Qiagen) was used according to the manufacturers' protocol. The Zyppy™ Plasmid Miniprep Kit was used for cloning, sequencing and small scale transfection experiments, the EndoFree Plasmid Maxi/Mega Kit was used for large scale transfection experiments.

4.1.2 Polymerase chain reaction (PCR)

To amplify DNA fragments for cloning experiments the Phusion high-fidelity DNA polymerase (NEB) was used; for colony screening, Taq DNA polymerase from Roboklon was used. The PCR was carried out according to standard procedures (Mülhardt, 2006) and the enzyme manufacturer's protocols. The annealing temperature depended on primer length and nucleotide composition (see section 10.2).

4.1.3 Isolation of RNA

For the isolation of RNA the RNeasy Micro/Mini Kit in combination with the RNase-free DNase Set (both Qiagen) were used according to the manufacturer's protocols.

4.1.4 Reverse transcription PCR (RT-PCR)

For synthesis of cDNA, isolated RNA was reversed transcribed using SuperScript™ III First-Strand Synthesis System for RT-PCR (Life Technology) according to the manufacturer's protocol.

4.1.5 DNA digestion

The digestion of DNA fragments was performed using restriction enzymes from New England Biolabs (NEB) with the appropriate buffer according to the manufacturer's protocol.

4.1.6 Agarose gels

To separate DNA fragments by size, 0.8 % agarose gels were prepared and gel-electrophoresis was performed according to standard procedures (Mülhardt, 2006). Depending on the number of samples 50 ml (1 to 10 samples), 170 ml (11 to 32 samples) or 300 ml (33 to 90 samples)

agarose gels were cast.

4.1.7 DNA ligation

For DNA ligation, vector and insert were extracted from agarose gels and purified using the DNA Clean & Concentrator™ Kit from Zymo Research according to the manufacturer's protocol. DNA concentrations were measured using the NanoDrop 2000. The applied molecular mass ratio of vector to insert was 1 to 4. Ligations of DNA fragments were performed using the T4 DNA ligase from NEB at room temperature (RT) overnight (O/N).

4.1.8 DNA sequencing

For sequencing DNA samples and sequencing primers were sent to Eurofins MWG Operon (Ebersberg). Concentrations were adjusted according to the manufacturer's requirements.

4.1.9 Transformation

For the transformation of plasmid DNA into *E. coli*, the heat shock method was performed according to standard protocols (Mülhardt, 2006). For the amplification of DNA *E. coli* DH5α was used, for protein expression *E. coli* BL21/Rosetta was transformed.

4.1.10 Competent bacteria

To prepare competent bacteria, 4 ml LB medium were inoculated with *E. coli* DH5α or *E. coli* BL21/Rosetta and incubated at 240 rotations per minute (rpm) at 37 °C O/N. The next day, the 4 ml were used to inoculate 200 ml LB medium. Cells were grown to an OD_{600} of between 0.4 and 0.6. Bacteria were centrifuged at 3000 x g for 10 min (4 °C) and washed twice with and resuspended in 15 ml ice-cold PC buffer (50 mM $CaCl_2$, 10 mM Pipes). After O/N incubation on ice, cells were centrifuged at 3000 x g (4 °C), resuspended in PCG buffer (50 mM $CaCl_2$, 10 mM Pipes, 15 % glycerol), flash frozen and stored at -80 °C.

4.1.11 Storage of bacteria

For the storage of transformed bacteria, 800 µl of an O/N culture was mixed with 200 µl of ice-cold 70 % glycerol, flash frozen and stored at -80 °C.

4.1.12 Generation of the chimeric antibodies J6.5-xi and J22.9-xi

Upon RNA extraction and cDNA synthesis (see section 4.1.3 and 4.1.4, respectively), the variable regions of the light and heavy chains of the mouse hybridomas J6.5 and J22.9 were amplified. The primers (see section 10.2) described by Tiller and colleagues (2009) were used

for nested PCR. Heavy and light chain PCR products were digested with AgeI/SalI and AgeI/BsiWI, respectively, and cloned upstream of the human kappa and the human IgG1 constant domain genes, respectively.

4.2 Biochemical methods

4.2.1 SDS-PAGE

To separate proteins by their molecular weight, denaturing and discontinuous SDS-polyacrylamide gel electrophoresis (SDS-PAGE) according to standard protocols (Rehm, 2006) was performed. Samples were prepared either under reducing or nonreducing conditions.

4.2.2 Expression and purification of BCMA

Human BCMA (residues 1-54; approximately 6 kDa) was expressed from the pGEX6p-1 vector (GE Healthcare) with an N-terminal glutathione-S-transferase (GST) fusion followed by a PreScission cleavage site. Proteins were expressed in *E. coli* host strain BL21/Rosetta, and bacteria were cultured in TB medium at 37 °C to an OD_{600} of 0.5 followed by induction with 60 µM Isopropyl β-D-1-thiogalactopyranoside (IPTG) and temperature shift to 18 °C for overnight expression. Cells were resuspended in buffer A (50 mM HEPES/NaOH (pH 7.5), 500 mM NaCl 1 µM DNase (Pham et al.), 500 µM Pefabloc (Roth) and disrupted by a microfluidizer (Microfluidics). Cleared lysates (95,000 x g, 1 h, 4 °C) were incubated with Benzonase (Novagen) for 30 min at 4 °C prior to application to a GSH column (Clontech). Protein was eluted with buffer A containing 20 mM GSH. Fractions containing BCMA were incubated with His_6-tagged Prescission protease overnight at 4 °C. Non-cleaved BCMA and the free GST were removed by a second application to a GSH column. The flow-through and four column volumes of washing buffer A were collected and concentrated using 3 kD molecular weight cut-off concentrators (Amicon). Finally, BCMA was purified by size exclusion chromatography on a Superdex200 column (GE Healthcare) in buffer containing 20 mM HEPES/NaOH (pH 7.5), 300 mM NaCl. Fractions containing BCMA were pooled, concentrated and flash-frozen in liquid nitrogen.

4.2.3 Expression and purification of the chimeric antibodies J6.5-xi, J22.9-xi and isoAb

293-6E cells at 1.7 x 10^6 cells/ml in serum free Freestyle F17 medium were transfected using polyethyleneimine (PEI) at a 1:2.5 ratio with plasmid DNA carrying the heavy and light chain genes with N-terminal secretion signal peptides, at a final concentration of 1 µg/ml culture.

Two days after transfection cells were fed with 100% of the transfection volume of Freestyle F17 medium containing 1% tryptone N1 (Organo Technie). At day 7 cells were harvested by centrifugation and the filtered (0.45 µm) culture medium was passed over 3.5 ml Protein A Sepharose (Bio-Rad). The column was washed with 10 ml phosphate buffered saline (PBS) and antibody eluted by addition of 20 mM sodium acetate, 150 mM NaCl, pH 3.5. 2 ml fractions were collected directly into tubes containing 100 µl 1 M HEPES, pH 7.5 for neutralization. The final yield of full length IgG was approximately 40 mg/l culture.

The isotype control antibody comprising the J22.9-xi heavy chain and a random chimeric kappa light chain was produced in parallel with the J22.9-xi antibody. This antibody was shown by ELISA and flow cytometry to be unable to bind to BCMA.

4.2.4 Deglycosylation of J22.9-xi

The N-linked oligosaccharide chains at Asn297 of J22.9-xi were removed enzymatically using N-Glycosidase F (PNGase F) (NEB). 10 mg of J22.9-xi were incubated with 15,000 units PNGase F in 500 µl PBS (pH 7.4) for 36 hours at 37 °C followed by buffer exchange into sterile PBS.

4.2.5 Generation of F(ab) and F(ab):BCMA complexes

These experiments were mostly performed by Dr. Stephen Marino

$F(ab)_2$ fragments were generated from full length J22.9-xi IgG by incubation with pepsin. Pepsin was added at 30 µg per milligram J22.9-xi in 50 mM sodium acetate, pH 3.5. Incubation at 37 °C for 2.5 hours was sufficient to completely digest the Fc and pepsin was inactivated by exchange over a PD-10 column into PBS. The reduction of the $F(ab)_2$ fragments to individual Fabs was accomplished in PBS by addition of 2-Mercaptoethylamine to 50 mM in the presence of 5 mM ethylenediaminetetraacetic acid (EDTA). After incubation for 90 minutes at 37 °C, the reduced cysteines were blocked by alkylation with 500 µM iodoacetamide for 30 minutes followed by buffer exchange into fresh PBS. The Fab fragments were combined with 1.5 molar equivalents of purified BCMA and the complexes isolated by size exclusion chromatography on a Superdex 75 16/60 column. Fractions were analyzed on 4-12% SDS polyacrylamide gels and fractions containing both Fab and BCMA were pooled and concentrated for crystallization trials.

4.2.6 Crystallization of F(ab):BCMA complexes

These experiments were performed in cooperation with Dr. Stephen Marino

Concentrated complexes were supplemented with 0.5 molar equivalents of pure BCMA to ensure saturation and were subjected to crystallization screening. Initial F(ab):BCMA crystallization conditions were identified from commercial screens in 96-well sitting drop format plates using a Gryphon pipetting robot (200 nl drops) and optimized in 24 well plates in hanging drops (3 µl). Crystals were grown by mixing 1 µl of the complex at a concentration of 8 mg/ml with 2 µl of 21% PEG 3350, 0.1 M BisTris pH 6.5 and 5 mM $CuCl_2$ at 20°C. Crystals appeared after three days as clusters of thin plates and attained their final size (0.2 – 0.3 mm) within approximately 7 days. Clusters were separated and individual plates were flash-frozen in liquid nitrogen in mother liquor with 20% glycerol as cryoprotectant. Complete diffraction data from 42 Å- 1.74 Å resolution were collected from a single crystal at BL14.1 at BESSY II, Berlin. Data were processed using the XDS program suite (Kabsch, 2010), and the structure was solved by molecular replacement with MOLREP (Vagin and Teplyakov, 2010), using the structure of Efalizumab (pdb i.d. 3EO9) as the search model. The model was built with COOT (Emsley et al., 2010) and iteratively refined using PHENIX (Adams et al., 2010). The final model comprises two heavy chains (amino acids 1-133, and 139-220 in chain A and amino acids 1–135 and 141-220 in chain H), two light chains (amino acids 1-213 in chain B and amino acids 1-213 in chain L) and two BCMA molecules (amino acids 6-41 in chain F and amino acids 8-37 in chain K). 98% of all residues are in the most favored regions of the Ramachandran plot with no residues in the disallowed regions, as analyzed by MolProbity (Chen et al., 2010). Figures were prepared using the PyMOL Molecular Graphics System, Version 1.5.0.4 and domain superpositions were performed with COOT (Emsley et al., 2010).

4.3 Cell culture methods

4.3.1 Thawing, freezing and maintenance of cell culture cell lines

The thawing, freezing and maintenance procedures of all cell lines used were performed in the cell line specific medium (**Tab. 2**) according to standard protocols (Schmitz, 2009).

Tabelle 2: Cell lines and their culture media

Cell line	Medium	Supplements
293-6E	Freestyle F17	7.5 mM L-Glutamine, 0.1% Pluronic F68, 25 µg/ml G418
HEK293-T	DMEM high glucose	10% FCS
Jurkat(-Luc)	RPMI 1640	10% FCS, Penicillin, Streptomycin
MM.1S(-Luc)	RPMI 1640	10% FCS, Penicillin, Streptomycin
X63.Ag8.653	DMEM high glucose	20% FCS

4.3.2 Cell fusion

This experiment was performed by P.D. Dr. Uta Höpken

To obtain hybridomas, the splenocytes of immunized mice were extracted and fused to the murine myeloma cell line X63.Ag8.653 using polyethylene glycol (PEG). The procedure was performed according to Yokoyama (Yokoyama, 2006).

4.3.3 Hypoxantine-aminopterin-thymidine (HAT) selection

For the positive selection of hybridomas, HAT medium was used. This medium contains aminopterin which blocks the normal synthesis of the nucleotides guanine thriphosphate (GTP) and thymidine triphosphate (TTP). Unlike B cells, which express hypoxanthine-guanine phosphoribosyltransferase (HGPRT) and are able to use hypoxanthine for the synthesis of GTP, the X63.Ag8.653 myeloma cells are deficient in HGPRT and only survive when fused to a B cell. Unfused B cells or B cell/ B cell fusions have a median survival of approximately 7 to 10 days in cell culture. Thus, only hybridomas are able to survive in HAT medium (Luttman, 2006; Yokoyama, 2006).

4.3.4 Screening of hybridomas

Fourteen days after cell fusion the supernatants of the hybridomas were screened for the presence of anti-BCMA antibodies by ELISA (see section 4.4.2) on BCMA coated microtiter plates (1 µg/ml in PBS). Anti-BCMA positive supernatants were further analyzed by flow cytometry (see section 4.4.3).

4.3.5 Subcloning of hybridomas

Since the hybridomas are polyclonal after cell fusion, the hybridomas of anti-BCMA positive supernatants were diluted to 5 cells/ml and 100 µl were added to each well of a 96well plate (0.5 cells/well). Between days 5 and 14 after the dilution the wells were microscopically analyzed. Wells which contained only one cell clone were again analyzed for the presence of

anti-BCMA antibodies by ELISA and flow cytometry (see sections 4.4.2 and 4.4.3, respectively). In the case of positive clones another round of subcloning was performed (Luttman, 2006; Yokoyama, 2006).

4.3.6 Transfection

The transient transfection of 293-6E cells was performed using polyethyleneimine (PEI) according to Pham and colleagues (Pham et al., 2006).

4.3.7 Isolation of human peripheral blood mononuclear cells (PBMCs)

For the isolation of human PBMCs, filter buffy coats (FBCs) from the blood transfusion service of the Berlin Charité Campus Mitte (Berlin) were collected. FBCs were handled according to Meyer and colleagues (Meyer et al., 2005).

4.3.8 Ficoll-Hypaque gradient

To isolate PBMCs from whole blood samples a Ficoll-Hypaque gradient was used according to standard procedures (Luttman, 2006).

4.4 Immunological methods

4.4.1 Western blot (WB)

Western blot analysis was done with whole cell lysates from MM.1S cells incubated with either J22.9-xi or isoAb for 30 or 60 minutes. For detection of IκBα, unconjugated rabbit-anti-IκBα antibody was used (Cell Signaling, dilution 1:1000) followed by HRP-conjugated goat-anti-rabbit secondary antibody (Jackson ImmunoResearch, dilution 1:5,000). Experiments were performed according to standard procedures (Luttman, 2006).

4.4.2 Enzyme-linked immunosorbent assay (ELISA)

Microtiter plates were coated with 1 µg/ml of the extracellular domain of human BCMA. Detection was done with serial dilutions of J22.9-xi or isoAb ranging from 1 to 1000 ng, followed by HRP-conjugated goat-anti-human secondary antibody (Jackson ImmunoResearch, dilution 1:5,000). ELISAs were performed according to standard procedures (Luttman, 2006). All ELISAs were developed using BD OptEIA reagents A and B (BD Bioscience) and quantitated using a microplate spectrophotometer (BioTek) at 450 nm and 570 nm.

4.4.3 Flow cytometry

For cell surface antigen detection experiments, the self-made (J22.9-xi, isoAb) and commercially available PE-conjugated goat-anti-human IgG1 (Jackson ImmunoResearch, dilution 1:400) antibodies were used. Flow cytometry analyses were performed according to standard procedures (Luttman, 2006) on a FACSCalibur or a FACSCanto II flow cytometer (BD Bioscience). To detect apoptotic cells, propidium iodide (Life Technologies) staining was performed. The data were analysed with Flowjo software version 7.6 (TreeStar Inc.).

4.4.4 Fluorescence-activated cell sorting (FACS)

Fluorescence-activated cell sorting was performed on a FACSAria cell sorter (BD Bioscience). GFP expressing cells were washed twice and resuspended in FC buffer (PBS pH 7.4, 3% FCS, 0.01 M EDTA). Cells emitting at 509 nm after excitation with 488 nm were sorted into RPMI 1640 medium (10% FCS, Penicillin/Streptomycin 1x).

4.4.5 Isotype determination

For determination of the isotype of the monoclonal hybridoma antibodies the IsoStrip Mouse Monoclonal Antibody Isotyping Kit (Roche Applied Science) was used according to the manufacturer's protocol.

4.4.6 Affinity determination of J22.9-xi to BCMA

The binding affinity of J22.9-xi was determined by surface plasmon resonance (Moreaux et al.) using a ProteOn^{TM} XPR36 (Bio-Rad). 50 µg/ml of J22.9-xi were immobilized through amine coupling to a GLC Sensor Chip (Bio-Rad). BCMA concentrations ranging from 1 to 90 nM were applied to the chip. Coupling and measurements were performed according to the manufacturer's protocol.

4.4.7 Apoptosis assay

$1*10^7$ MM.1S cells were cultured without FCS in RPMI 1640. B cell activating factor (BAFF), J22-9-xi or isoAb were added (30 pmol each) at day 0, 3 and 5. Propidium iodide (PI) staining and flow cytometry were performed on day 7. To calculate the percentage of living cells, the percentage of PI-positive cells was subtracted from 100.

4.4.8 Blocking assay

To check the blocking capacity of J22.9-xi, BCMA was coated on microtiter plates and preincubated with either J22.9-xi or isoAb for 30 minutes. After washing, 1 mg/ml

recombinant human BAFF (Biomol) containing an N-terminal 6xHis tag was incubated and detected using the horseradish peroxidase (HRP)-conjugated mouse anti-His tag antibody (AbD Serotec, dilution 1:5000). The assay was developed using BD OptEIA reagents A and B (BD Bioscience) and quantitated using a microplate spectrophotometer (BioTek) at 450 and 570 nm.

4.4.9 Cytotoxicity assays

In order to test the cytotoxic potential of J22.9-xi, a luciferase-based cytotoxicity assay was established using luciferase transduced MM.1S-Luc cells (**Fig. 4**). In this assay only the bioluminescence of living cells is detected, whereas luciferase released by dead cells is nonfunctional due to insufficient ATP in the medium (Fu et al., 2010). For ADCC determination, peripheral blood mononuclear cells (PBMCs) from healthy donors were isolated and mixed with MM.1S-Luc cells in a ratio of 20 to 1. To test for CDC, human blood serum was extracted.

Human serum was prepared or PBMCs were adjusted by dilution in RPMI/10% FCS w/o phenol red to $1x10^7$ cells/ml. $5x10^4$ MM.1S-Luc cells in 50 µl RPMI were plated in microtiter plates. Ten minutes prior to the addition of 100 µl PBMCs or serum, the MM.1S-Luc cells were incubated with J22.9-xi, J22.9-xi-N-glycan or isoAb serial dilutions in a sample volume of 200 µl. After addition of target cells, antibodies and effector cells, microtiter plates were centrifuged (300 x g) for 2 minutes at room temperature (RT) and stored at 37 °C with 5 % CO_2. Control wells for complete lysis were treated with 1 % Triton X instead of antibody. After 4 hours of incubation to test for ADCC or 1 hour incubation for CDC, 25 µl of PBS with luciferin (250 ng/ml) were applied to each well, and the bioluminescence of the living cells was measured in a bioluminescence reader (Tecan Infinite). Cytotoxicity relative to isoAb was calculated according to the following formula:

$$100 - [\text{value (J22.9-xi)} - \text{value (total lysis)}] / [\text{value (isoAb)} - \text{value (total lysis)}] \times 100$$

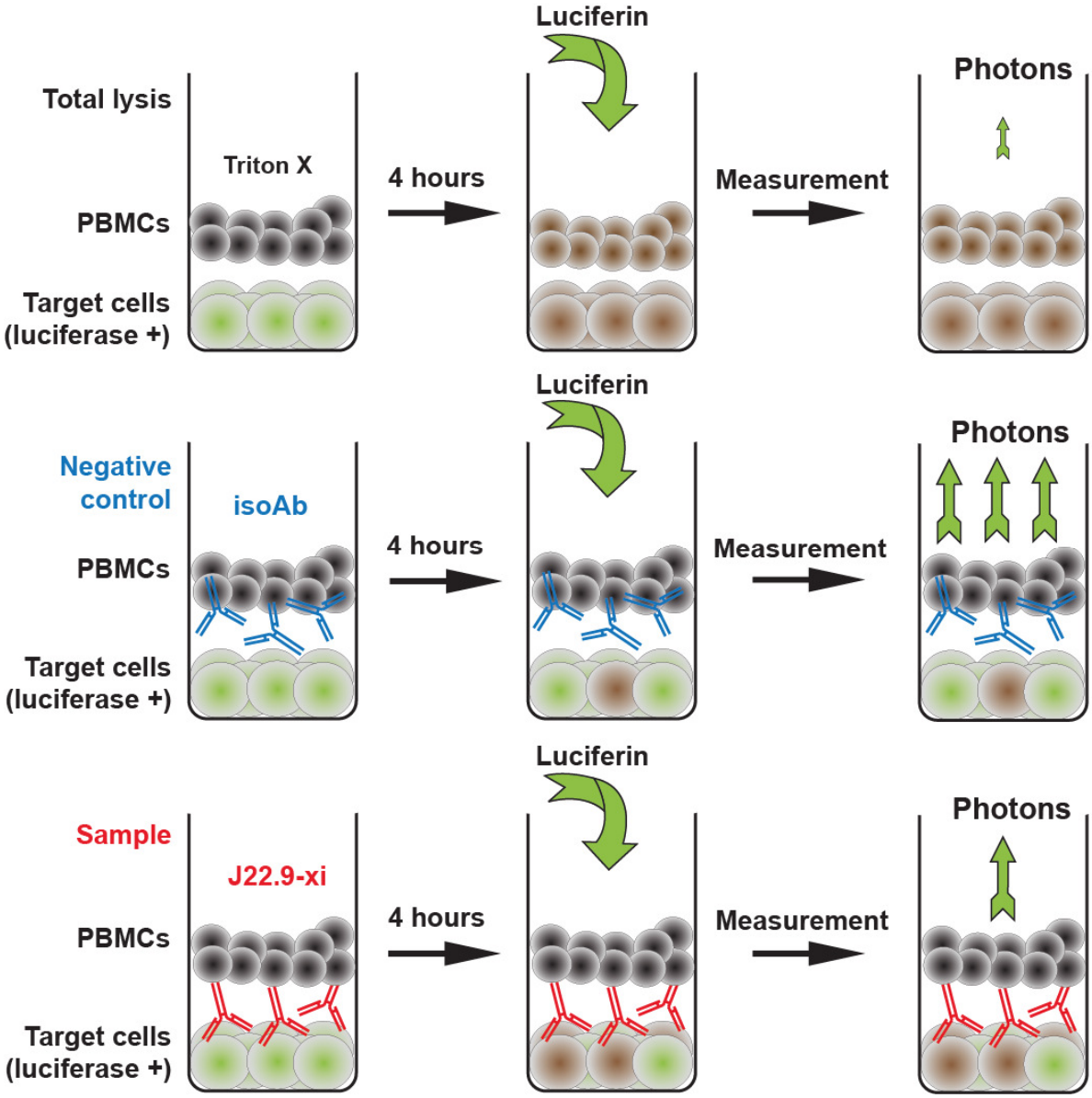

Figure 4: Schematic diagram of the luciferase-based cytotoxicity assay. Luciferase-positive target cells are incubated with effector cells (PBMCs) and either Triton X (total lysis), isoAb (negative control) or J22.9-xi (sample) for 4 hours. After luciferin is added, the bioluminescence of living cells is measured. This assay can also be used with serum instead of effector cells. In this case the bioluminescence is measured after a one hour incubation.

4.5 Animal experimental methods

4.5.1 Mouse handling procedures

All animal studies were performed on female mice according to institutional and state guidelines, under specific pathogen-free conditions.

4.5.2 Mouse strains

Severe combined immunodeficient (SCID) Beige mice (CB17.Cg-Prkdscid Lystbg/Crl; strain code: 250) were purchased from Charles River Laboratories (Sulzfeld). The SCID mutation

results in an immunodeficiency affecting the B and T cell compartment. The Beige mutation also causes a loss of functional natural killer (NK) cells.

A second strain, the SCID, Non-Obese Diabetic (NOD), common gamma chain (gamma) mice (NSG; NOD.Cg-Prkdcscid Il2rgtm1Wjl Tg(CSF2)2Ygy Tg(IL3)1Ygy Tg(KITL)3YgyJGckRolyJ; stock number: 011066), was purchased from The Jackson Laboratory (Maine). NSG mice also lack functional B, T and NK cells and, in addition, support engraftments through transgenic expression of the cytokines IL-3, CSF2 and stem cell factor (KITLG).

Since both strains lack a functional adaptive immune system, they are typically used for xenograft tumor models.

4.5.3 Immunization

To induce an immune response against BCMA four C57BL/6 mice were immunized with 50 µg of GST-BCMA diluted in 250 µl PBS and 250 µl incomplete Freund's adjuvant (IFA). The water-oil emulsion was sonicated at 70 W for 1 min before immunization.

4.5.4 Isolation of peritoneal macrophages

Three days before cell fusion or subcloning of hybridoma cells, growth factor-secreting peritoneal macrophages, which are important for the support of freshly fused hybridomas, were extracted from the peritoneum of female C57BL/6 wild type mice. Mice were euthanized with isofluorane, fixed and the macrophages flushed out by injection of 5 ml cold DMEM containing 10% FCS into the peritoneum. Cells were centrifuged at 300 x g for 5 min, counted and diluted in DMEM (10% FCS) to $1.5*10^5$ cells/ml. From this cell suspension 100 or 1000 µl/well were added to 96-well plates or 24-well plates, respectively.

4.5.5 Intravenous (i.v.) injection

For the intravenous injection of tumor cells, mice were put into a mouse-restrainer. Dilation of the veins was accomplished by warming the tail in warm water. Each mouse was injected with $1x10^7$ MM.1S-Luc-GFP cells resuspended in 200 µl RPMI 1640 using a 26 gauge needle.

4.5.6 Intraperitoneal (i.p.) injection

For immunization and the application of luciferin or antibodies, intraperitoneal injection was performed. The back of the mouse was fixed with the left hand and flipped over. Injection was performed directly into the peritoneum.

4.5.7 *In vivo* imaging

Mice injected with 150 µg luciferin (Biosynth) intraperitoneally were put into the *in vivo* imaging system (IVIS) induction chamber and anesthetized through inhalation of isofluorane at 2.5% with 1 l/min flow of oxygen. After 5 minutes, anesthetized mice were placed on the 37 °C heated imaging platform of the IVIS Spectrum imaging station (Caliper LifeScience) at 1.5% with 1 l/min flow of oxygen. A white light image was obtained followed by 3 bioluminescence images with an exposure time of 5, 15 and 30 seconds. Thereafter, mice were placed back into their cages. Images were analyzed using Living Image 3.0 software (Caliper LifeScience).

4.5.8 Xenograft mouse model

Experiments were performed on mice between 6 and 8 weeks old weighing 18-22 g. The xenograft model of multiple myeloma was induced by intravenous injection of $1*10^7$ MM.1S-Luc cells in the tail vein at day zero. Tumor challenged animals developed hind limb paralysis within 6 to 8 weeks – the experimental endpoint of survival.

For the efficacy studies, the antibodies were administered intraperitoneally (i.p.) twice a week or on 5 consecutive days starting at day zero. J22.9-xi was given in doses of 2 µg, 20 µg or 200 µg per injection; for isoAb, 200 µg/injection was used. The bioluminescence of the MM.1S-Luc cells was measured after i.p. injection of 150 µg luciferin (Biosynth) using an IVIS Spectrum (Caliper Life Sciences). Measurements were done weekly. At each time point, 3 untreated mice were also administered luciferin. Total flux values of these animals were either subtracted from each measurement or are shown in the graphs. Images were analyzed with Living Image 3.0 software (Caliper LifeScience).

To treat established tumors, antibody therapy was started 5 or 12 days after tumor challenge, and 200 µg isoAb or J22.9-xi per injection administered twice a week for a period of 6 weeks.

4.6 Safety level 2 (S2)

4.6.1 Generation of lentiviral vectors

To generate recombinant lentiviral vectors HEK293-T cells were transiently transfected with pFU-luciferase-GFP and the pCMV-VSG-G, pLP1 and pLP2 ViraPower Sytem vectors (Life Technology) using polyethylenimine (PEI) by following the protocol of Auer and colleagues (2010). In the pFU vector luciferase and green fluorescent protein (GFP) are connected by a 2A/2B junction resulting in a simultaneous expression of both proteins with an approximately

2- to 5-fold molar excess of luciferase over GFP (Donnelly et al., 2001). This difference is not of importance, as GFP was only needed for FACS. Since lentiviral vectors belong to safety class 2 all the procedures were carried out in accordance with S2 guidelines in S2 laboratories.

4.6.2 Transduction and establishment of luciferase expressing cell lines

To $5*10^6$ MM.1S or Jurkat cells, approximately $2.5*10^7$ of luciferase-GFP lentiviral vectors were added and gently shaken at 150 rpm for 3 min. After incubation at 37°C and 5% CO_2 for 3 days, cells were washed 3*3 times with RPMI 1640 (10% FCS) over a period of 1 week to remove remaining lentiviral vectors. After the last washing step the cultures were considered to be safety class 1 again and were fluorescence-activated cell sorted for the expression of GFP. Afterwards, the cells were diluted to 5 cells/ml in RPMI (10% FCS) and manually seeded into 96well plates (100 µl/well) to obtain monoclonal cell lines.

4.7 Statistics

Prism software Version 5.0 (GraphPad) was used to analyze data and to determine the statistical significance of differences between groups by applying a 2-tailed t-test. Kaplan Meier plots were applied to analyze survival. Comparisons of survival curves were made using the Logrank test (Mantel, 1966). P values <0.05 were considered significant.

5. Results

5.1 Establishment of a luciferase-based cytotoxicity assay

The aim of this study was to generate an antibody directed against BCMA for the depletion of multiple myeloma cells. The therapeutic potential of such an antibody must be tested *in vitro* and *in vivo*. Therefore, studies giving information about target cell depletion needed to be performed. The most effective readout in such assay is bioluminescence, as it has a very low background and can be used both *in vitro* and *in vivo*. Hence, the initial step was to establish assays in which bioluminescence measurements could be used to accurately determine the efficacy of the therapeutic antibody.

5.1.1 Establishment of monoclonal cell lines expressing luciferase and GFP

In order to use bioluminescence as readout for cytotoxicity assays, the target cell line (MM.1S) and a control cell line (Jurkat) were transduced with recombinant lentiviral vectors (see section 4.6.1) containing RNA coding for luciferase and GFP. GFP was used for the establishment of monoclonal cell lines expressing luciferase. Fluorescence-activated cell sorting (see section 4.3.4) was performed one week after transduction (see section 4.6.2). The gating strategy excluding dead cells and doublets is seen in **Fig. 5a**. 8.1% GFP-positive MM.1S cells and 24.6% GFP-positive Jurkat cells were sorted. To obtain monoclonal cell lines, the sorted cells were diluted to single cell stage. After three weeks, these cell lines were analyzed by flow cytometry to confirm their monoclonality. The cell lines which were used in this dissertation are shown in **Fig. 5b**. Due to their expression of luciferase, they are referred to as MM.1S-Luc and Jurkat-Luc cells, respectively.

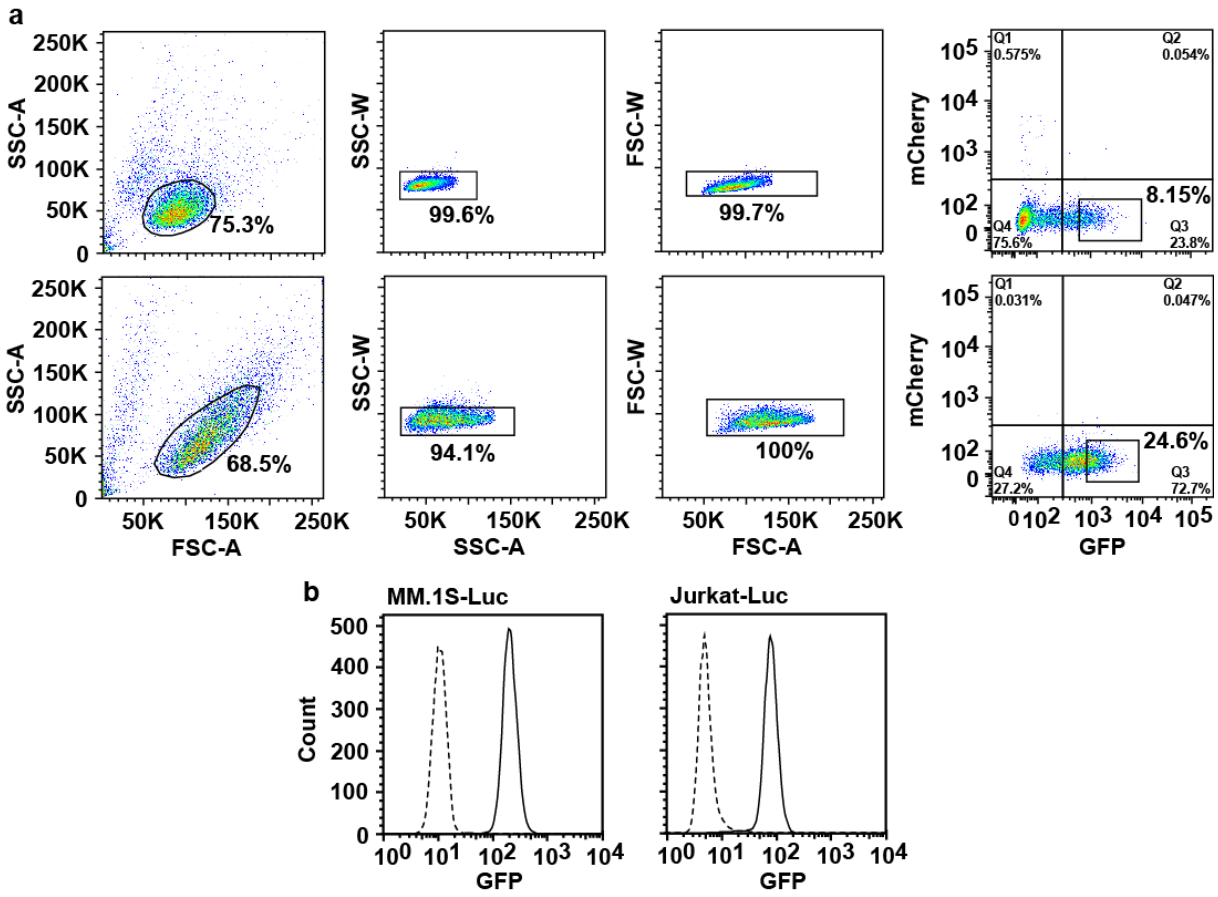

Figure 5: FACS-gating strategy and monoclonal Luc cell lines. (a) Using side scattering (SSC) and forward scattering (FSC) light of the FACS beam the main cell populations were selected excluding cell debris (first column). The same filters were used to exclude cell doublets (column 2 and 3). Gates in quadrant 3 (Q3) of the 4th columns show the sorted GFP-positive cells. Top row, MM.1S cells, bottom, Jurkat cells. **(b)** Upon dilution to single cells and expansion, cell lines were checked by flow cytometry for clonality. Dashed lines represent the original cell lines; solid lines are the cell lines which were used for all *in vivo* and some *in vitro* studies. Shown is one out of three independent experiments.

5.1.2 Cell number of luciferase-expressing cells correlates with bioluminescence

Most therapeutic antibodies induce their cytotoxic potential through the recruitment of effector cells or via interaction with the complement protein C1q (Campoli et al., 2010; Tai and Anderson, 2011). Therefore, these possibilities were assessed *in vitro* using cytotoxicity assays. Today's most popular cytotoxicity assay is still the chromium (^{51}Cr)-release assay (Brunner et al., 1968). The advantages of this assay are the low background, the high sensitivity and its effectiveness with different cell types. The clear disadvantage of this assay is the handling of radioactive material. The luciferase expressing cell lines were mainly generated to monitor tumor growth *in vivo*. But since the measured bioluminescence after addition of luciferin correlates with the number of plated cells (**Fig. 6a**), it is possible to use the bioluminescence values to back calculate the number of living cells. As luciferase activity depends on the presence of luciferin and ATP, the use of luciferin (250 ng/ml) in PBS without

additional adenosine triphosphate (ATP) reduces the background bioluminescence to a minimum (**Fig. 6b**). With these findings, a luciferase-based cytotoxicity assay with very low background was established using MM.1S-Luc or Jurkat-Luc cells (**Fig. 4**, section 4.4.9).

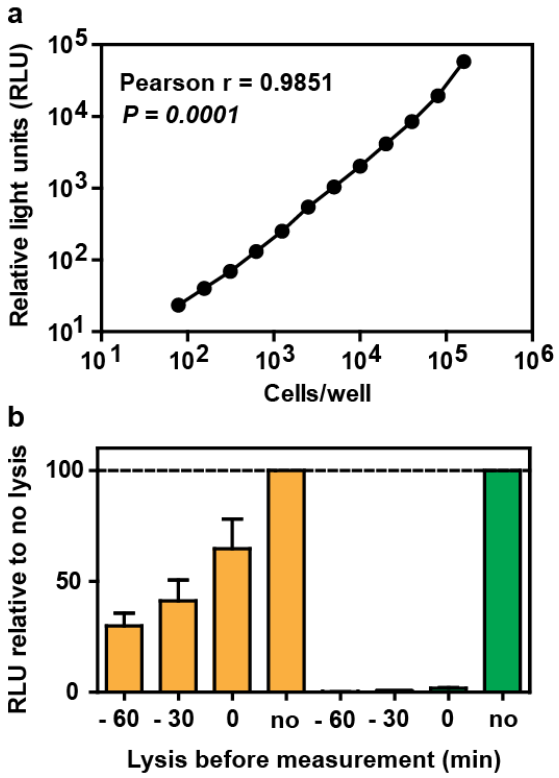

Figure 6: Basis for establishment of luciferase-based cytotoxicity assay. (a) Different cell numbers of luciferase-transduced cell lines were plated per well and bioluminescence of cells was measured upon administration of luciferin. Shown is one out of two independent experiments. Experiments were performed in triplicates for MM.1S-Luc (shown) and Jurkat-Luc. Correlation was calculated using the Pearson's correlation coefficient. **(b)** $1*10^6$ MM.1S-Luc cells/well were seeded and lysed with 1% Triton X at indicated time points prior to measurement. To test the influence of additional ATP in the luciferin mixture on the bioluminescence upon lysis, luciferin + ATP (orange columns) and luciferin w/o ATP (green columns) were used. Values obtained from unlysed wells were set to 100%. Values of different time points were calculated relative to unlysed wells. Shown is one out of two independent experiments. Experiments were performed in triplicates for MM.1S-Luc (shown) and Jurkat-Luc.

5.2 Generation of J22.9-xi a chimeric anti-BCMA antibody

The best established method for obtaining monoclonal antibodies is the immunization of mice (see section 4.5.3) with an external immunogen, followed by hybridoma technology (see sections 4.3.2 to 4.3.5).

5.2.1 Production of BCMA proteins for immunization and screening procedures

In cooperation with Dr. Janko Brand

In order to induce a humoral immune response in mice directed against BCMA, which is suited for the generation of a therapeutic antibody, the extracellular domain of BCMA

(residues 1-54; approximately 6 kDa, from here on referred to as BCMA) was purified as immunogen. Due to the low molecular weight of the extracellular domain of BCMA, it was expressed as a GST-BCMA fusion protein in *E. coli*. The protein was purified by affinity chromatography, followed by gel filtration (see section 4.2.2) (**Fig. 7a**). If required, the GST-tag was removed by PreScission protease, employing a PreScission protease cleavage site between the GST-tag and BCMA. From 10 l of bacteria cell culture, about 18 mg of purified BCMA were obtained. The purity of GST-BCMA and BCMA after gel filtration was controlled by SDS-PAGE (**Fig. 7b**). The purified GST-BCMA construct was used to immunize mice, whereas the purified BCMA was used for ELISA, affinity measurements and blocking assays (see sections 5.3.1, 5.3.2 and 5.3.3, respectively).

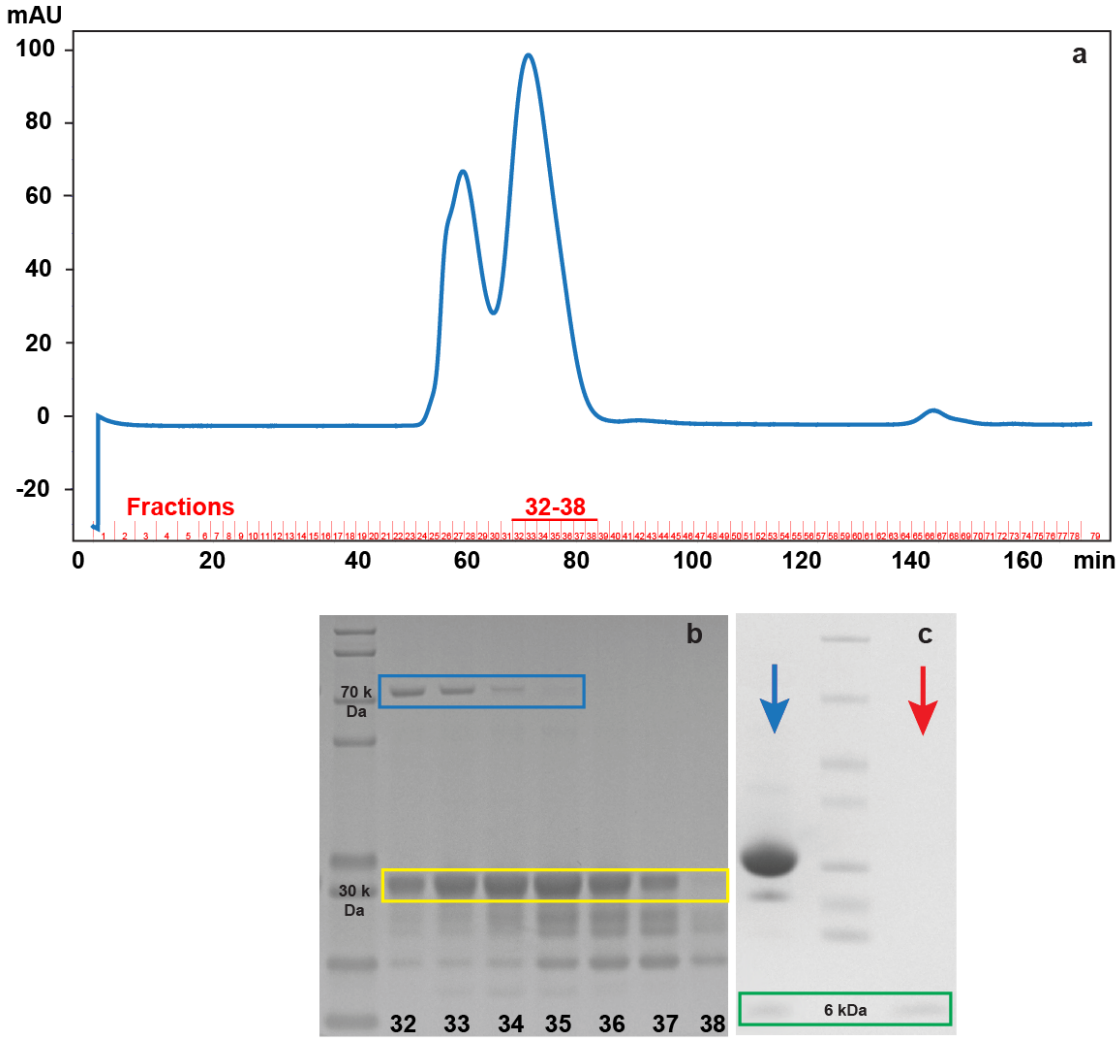

Figure 7: Purification of BCMA. (a) Chromatogram of the GST-BCMA gel-filtration. Fractions 32 to 38 were further analyzed by SDS-PAGE. **(b)** Fractions 32 to 38 after gel-filtration. All fractions contain GST-BCMA (~ 32 kDa; yellow box). Due to contamination with heat shock protein 70 (blue box), only fractions 35 to 37 were used for immunization. **(c)** Cleaved GST-BCMA fusion protein before (blue arrow) and after (red arrow) GSH-column purification. The green box indicates free BCMA. In the purified fraction, no contamination is visible. This fraction was used for all *in vitro* studies.

5.2.2 Cell fusion and screening of BCMA-positive hybridoma supernatants

To generate anti-BCMA antibody secreting hybridomas, a standard protocol was performed in cooperation with P.D. Dr. Uta Höpken (see section 4.3.2). Thus, splenocytes from mice immunized with GST-BCMA for eight weeks were fused with the murine myeloma cell line X63.Ag8.653 and cultured on peritoneal macrophages (see section 4.5.4). Fourteen days after cell fusion, 209 out of 240 supernatants were analyzed by ELISA on BCMA coated microtiter plates (see section 4.4.2) for the presence of anti-BCMA antibodies due to the presence of hybridoma clones. 32 supernatants showed a positive signal for the binding to BCMA in ELISA (data not shown). These supernatants were further tested by flow cytometry (see section 4.3.3) using BCMA-positive MM.1S cells to check the ability of the antibodies to also recognize the native protein present on the cell surface. BCMA-negative Jurkat cells served as control for the binding specificity. None of the supernatants which were positive on MM.1s cells showed a signal on Jurkat cells (data not shown). Seven of the 32 supernatants showed clear binding to MM.1S cells (**Fig. 8**).

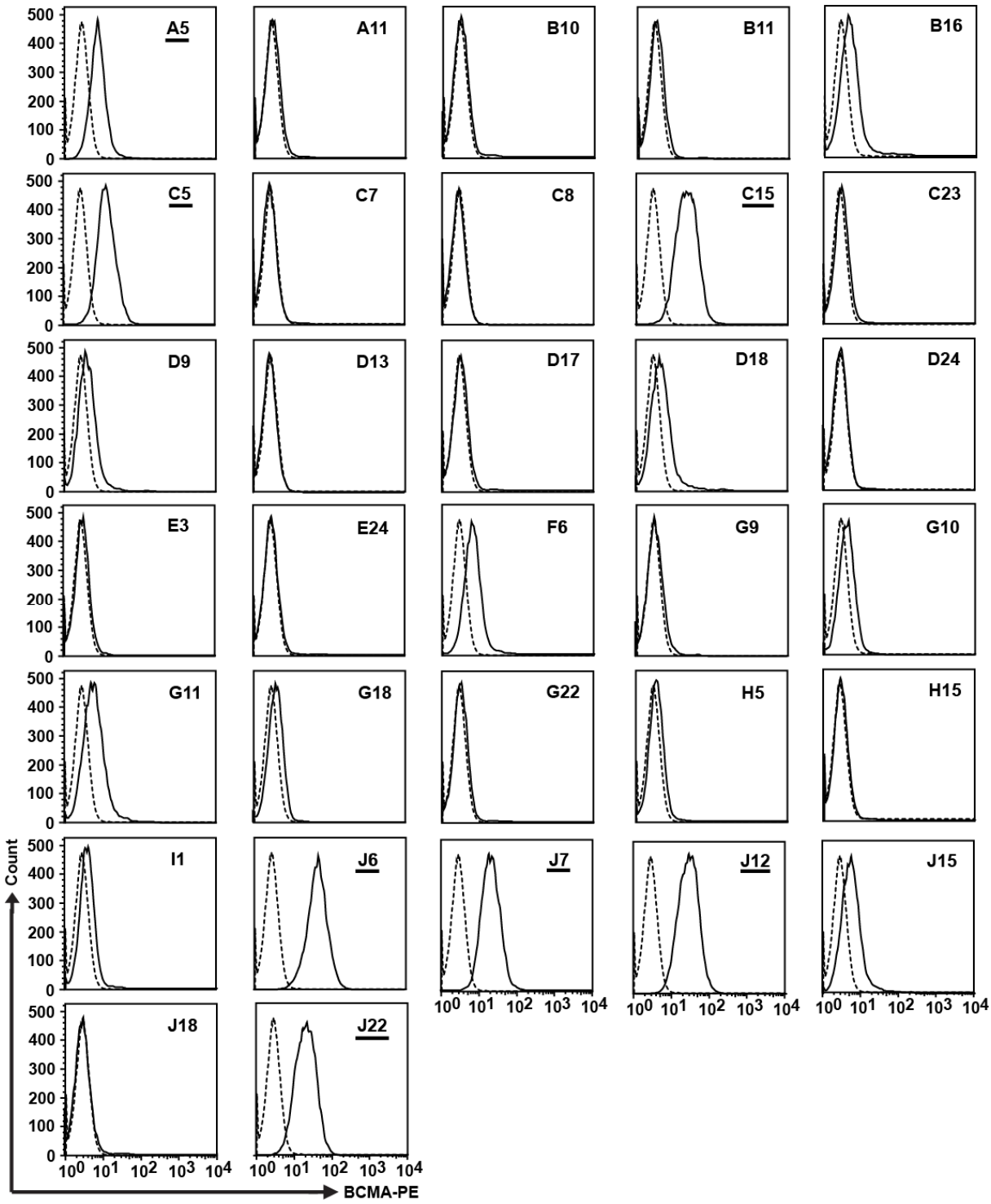

Figure 8: Flow cytometry screening of hybridoma supernatants. Hybridoma supernatants testing positive for BCMA-binding antibodies in ELISA were assessed on BCMA-positive MM.1S cells using flow cytometry. Seven out of 32 positive supernatants were able to bind MM.1S cells (A5, C5, C15, J6, J7, J12, and J22). These hybridomas were subcloned (see section 4.3.5).

The hybridoma cells of positive supernatants (A5, C5, C15, J6, J7, J12, and J22) were diluted in two rounds to finally obtain monoclonal anti-BCMA antibody secreting hybridomas (see section 4.3.5). Two of the seven clones maintained anti-BCMA antibody secretion during the dilution process. The positive hybridomas were named J6.5 and J22.9 according to the

subcloning procedure. Both hybridomas secreted antibodies of the IgG1 and kappa light chain isotype (**Fig. 9**).

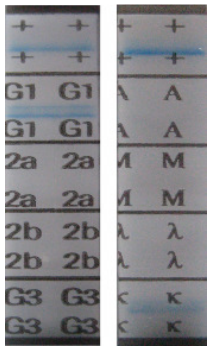

Figure 9: Determination of antibody isotype. Upon subcloning the two monoclonal hybridomas (J6.5 and J22.9) were analyzed for their isotype using the IsoStrip Mouse Monoclonal Antibody Isotyping Kit. The antibodies secreted by both hybridomas consist of an IgG1 constant heavy chain and a kappa light chain, indicated through the blue lanes within the fields of G1 and κ. Abbreviations: G1 (IgG1), 2a (IgG2a), 2b (IgG2b), G3 (IgG3), A (IgA), M (IgM), λ (LCλ), κ (LCκ), + (appearance of a blue lane in these fields indicates that the test was functional). The IsoStrips of the hybridoma clone J22.9 are shown here.

5.2.3 Amplification and cloning of the murine variable regions to human constant domains

Although J6.5 and J22.9 were able to produce monoclonal anti-BCMA antibodies, neither clone was stable when cultured for several weeks. Therefore, the variable regions of the heavy and light chains of both hybridomas were amplified by PCR and cloned upstream of the human IgG1 and human kappa constant domains, respectively, to generate the chimeric antibodies J6.5-xi and J22.9-xi (see section 4.1.12). For cloning of the HC, the restriction endonucleases AgeI and SalI were used; for the LC AgeI and BsiWI. The VDJ and VJ rearrangement of the heavy and light chain, respectively, of J6.5 and J22.9 is depicted in **Table 3**.

Table 3: VDJ and VJ rearrangement of J6.5 and J22.9

	Heavy chain			Light chain	
	Variable	Diversity	Joining	Variable	Joining
J6.5	J558.4.93	DFL16.1j	JH2	21-12	JK2
J22.9	X24.2.50	DSP2.2	JH4	19-15	JK5

5.2.4 Expression and purification of J6.5-xi and J22.9-xi

In cooperation with Dr. Stephen Marino

The antibodies were each produced by transient co-transfection of their heavy and light chain into 293-6E cells and purified using immobilized Protein A (see section 4.2.3). The protein yield of J22.9-xi was sufficient for all *in vitro* and *in vivo* analyses, whereas production of J6.5-xi was negligible. The swapping of the antibody chains between both antibodies revealed that the LC of J6.5-xi prevents antibody production, since the J6.5-xi-LC/J22.9-xi-HC antibody was hardly produced, whereas J22.9-xi-LC/J6.5-xi-HC showed a similar protein yield as J22.9-xi. The purity of the final antibody pool was verified by SDS-PAGE (**Fig. 10**). The protein yields were determined from absorption at 280 nm using a Nanodrop. Both, J22.9-xi and J22.9-xi-LC/J6.5-xi-HC were produced at a concentration of approximately 40 mg/l 293-6E cell culture. The antibodies were stored aliquoted in PBS either at 4 °C or flash frozen in liquid nitrogen, and stored at -80 °C.

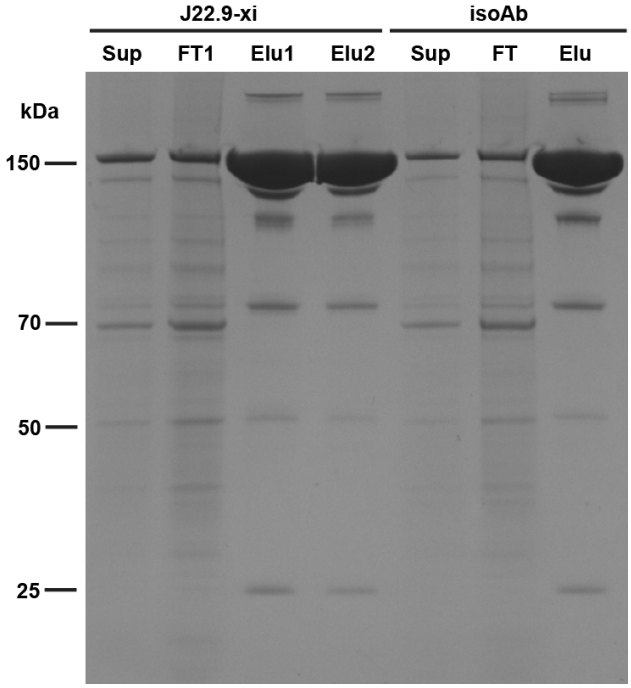

Figure 10: SDS-PAGE of antibody purification procedure. 10 µl samples of the transfection supernatants (Sup), the Protein A column flow through (FT), and the column elution (Elu) of J22.9-xi and isoAb were loaded. Protein A binding of antibodies was incomplete, since clearly visible in FT1 and FT. Therefore, J22.9-xi was applied a second time to the column and eluted (Elu2). Contaminants from the 293-6E cells were efficiently removed during the Protein A purification step. Remaining bands are most likely due to antibody aggregation or degradations, respectively. However, these bands accounted for less than 10% of the protein yield.

5.3 In vitro characterization of J22.9-xi

After the generation of J22.9-xi, the *in vitro* characteristics of this chimeric human-mouse antibody were analyzed.

5.3.1 Specific binding of J22.9-xi to BCMA

To test whether the chimerization had an effect on the specific binding of J22.9-xi to BCMA, it was again tested by ELISA on BCMA-coated microtiter plates and by flow cytometry using MM.1S cells. The same was done for the J22.9-xi-LC/J6.5-xi-HC antibody to assess whether the chain exchange had an impact on the binding to BCMA. Both ELISA and flow cytometry clearly revealed that J22.9-xi is still able to recognize BCMA, whereas J22.9-xi-LC/J6.5-xi-HC completely lost this ability (**Fig 11**). Therefore, the J22.9-xi-LC/J6.5-xi-HC antibody served as an isotype control antibody (isoAb).

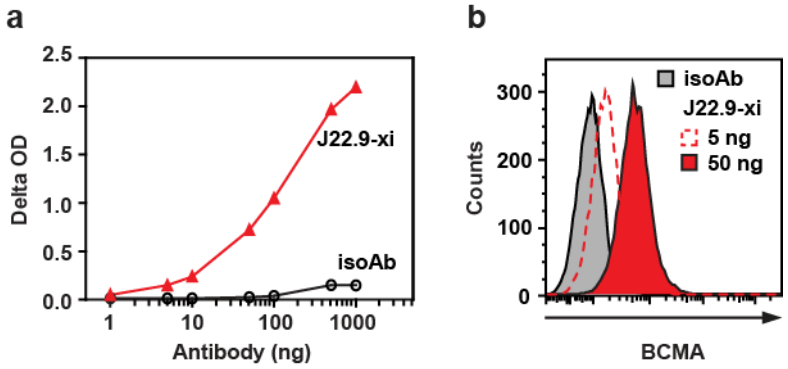

Figure 11: J22.9-xi specifically binds human BCMA. (a) ELISA on BCMA-coated microtiter plates and **(b)** flow cytometry analysis using BCMA-positive MM.1S cells. Chimeric antibodies were detected in ELISA and flow cytometry using an HRP-conjugated or PE-conjugated goat anti-human secondary antibody, respectively and experiments were done in sextuplicate and triplicate, respectively. Shown is one out of three independent experiments.

5.3.2 J22.9-xi binds BCMA with exceptionally high affinity

Having confirmed the specificity of J22.9-xi to its target, the affinity of the binding interaction was next determined using surface plasmon resonance (see section 4.4.6). Although the affinity of IgG1 antibodies on average ranges between µM and nM, the affinity of J22.9-xi to BCMA was measured to be 54 pM (**Fig. 12**). Thus, there is an above average affinity between these two partners.

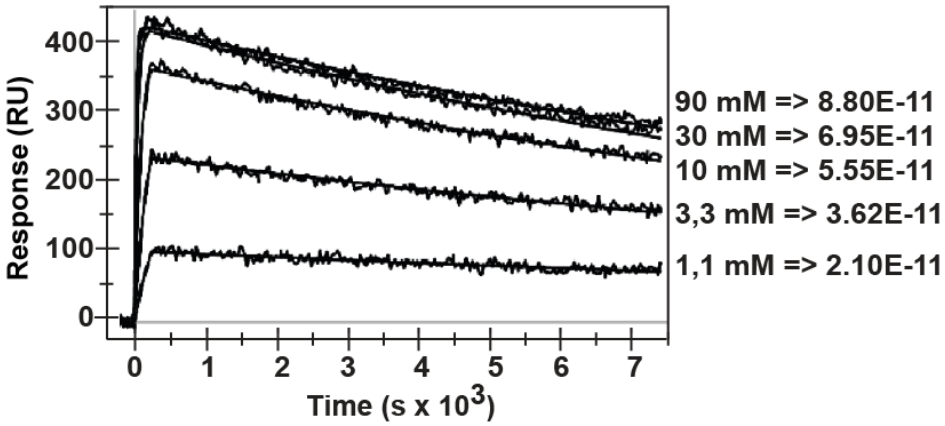

Figure 12: J22.9-xi is a high affinity antibody for human BCMA. Binding affinity was determined from surface plasmon resonance measurements. J22.9-xi was immobilized and indicated concentrations of BCMA were used as soluble binding partner. Shown is one out of two independent experiments.

5.3.3 J22.9-xi is able to block interaction of BAFF with BCMA

BCMA is known to trigger signals important for the survival of multiple myeloma and plasma cells *in vivo* through interaction with BAFF and/or APRIL. An *in vitro* blocking assay was therefore performed with BCMA and recombinant BAFF (see section 4.4.8). The binding of J22.9-xi to BCMA completely blocks the interaction between BAFF and the receptor, while no blocking effect was observed with isoAb (**Fig. 13**). This finding implies at least a partial overlap between the epitopes of J22.9-xi and BAFF on BCMA.

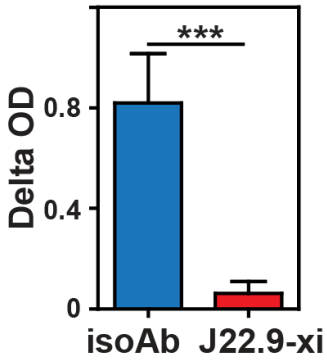

Figure 13: Blocking capacity of J22.9-xi. J22.9-xi blocks the interaction of BAFF and BCMA adsorbed onto microtiter plates. After pre-incubation with J22.9-xi or isoAb, His-tagged BAFF was applied to the wells and detected using a HRP-conjugated anti-His-tag antibody. Error bars indicate the standard error of the mean (SEM) of triplicates (***P < 0.001, t-test); shown is one out of three independent experiments.

5.3.4 Binding of J22.9-xi to BCMA induces NF-κB activation in MM.1S cells

Based on the knowledge that BCMA triggers survival signals through the NF-κB pathway upon interaction with BAFF, the question arising from the blocking experiment was whether J22.9-xi, which potentially shares parts of the BAFF epitope on BCMA, was also able to activate the NF-κB pathway. Therefore, serum starved MM.1S cells incubated with BAFF,

J22.9-xi or isoAb were analyzed by western blot for the presence of IκBα (see section 4.4.1). A reduction of the IκBα level is known to indicate NF-κB activation. Thus, consistent with what is known about the interaction of BAFF with BCMA, a reduced IκBα level in MM.1S cells was observed after one hour incubation with BAFF. Surprisingly, an equally strong reduction in the NF-κB level after incubation of MM.1S cells with J22.9-xi alone was also observed (**Fig. 14**), indicating that the antibody itself can activate the NF-κB pathway.

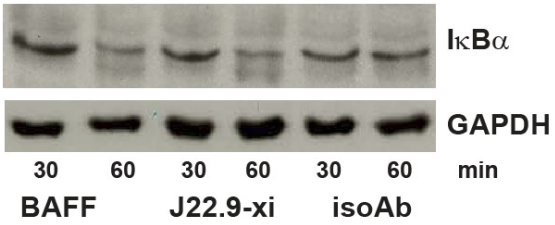

Figure 14: NF-κB activation upon binding of J22.9-xi to BCMA. Western blot analysis reveals a reduced IκBα level in MM.1S cells 60 minutes after incubation with either BAFF or J22.9-xi as compared to isoAb treated cells, indicating NF-κB activation. Shown is one representative blot of three independent experiments.

5.3.5 Incubation of MM.1S cells with J22.9-xi promotes apoptosis

To determine whether NF-κB activation upon binding of J22.9-xi to BCMA provides a survival advantage for the cells, serum starved MM.1S cells were incubated alone and in the presence of BAFF, J22.9-xi or isoAb for one week and then analyzed for apoptotic cells (**Fig. 15**). Although J22.9-xi showed an agonistic effect upon binding to BCMA on MM.1S cells (see section 5.3.4), significantly fewer cells were alive after incubation with J22.9-xi for one week compared to incubation with isoAb and BAFF. This finding shows that binding of J22.9-xi to BCMA on MM.1S cells does not confer a survival advantage.

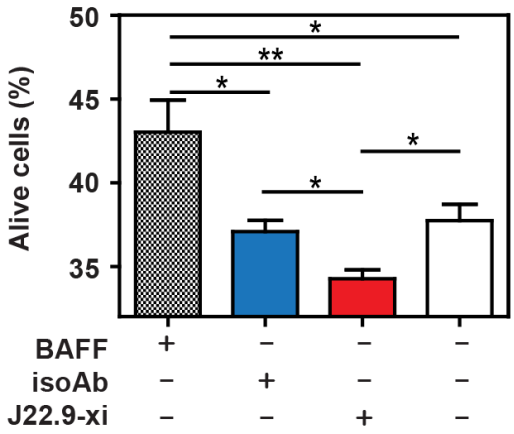

Figure 15: J22.9-xi induces apoptosis in MM.1S cells. MM.1S cells were cultured in RPMI (without FCS). Indicated substrates were added (30 pmol each) on day 0, 3 and 5. Propidium iodide (PI) staining and flow cytometry analysis were performed on day 7. To calculate percentages of living cells, the percentage of PI-positive cells was subtracted from 100. Error bars indicate SEM of sextuplicates (*$P < 0.05$, **$P < 0.01$, t-test). Shown is one of two independent experiments.

5.4 Crystallization of the J22.9-xi-F(ab):BCMA complex

The following data were generated in cooperation with Dr. Stephen Marino.

To gain more insight into the binding characteristics of J22.9-xi to BCMA, the J22.9-xi F(ab) fragment in complex with the purified 54 amino acid residue BCMA extracellular domain was crystallized (**Fig. 16a**). The structure was solved to 1.9 angstroms (Å) resolution (see **Table 4** for complete data collection and refinement statistics). Two identical BCMA:F(ab) complexes were present in the asymmetric unit, and in the following, the complex with the better resolved BCMA molecule is described.

Direct contacts in the 740 $Å^2$ interface are primarily hydrophobic, with the bulk occurring between BCMA and residues from all three complementarity determining regions (CDRs) of the light chain of the antibody (data not shown). Although the heavy chain contributes only six residues in total, at least one residue from each CDR is involved in the interaction. The BCMA epitope surface features the D*x*L motif (Gordon et al., 2003) which protrudes into a central cavity of the antigen binding site (**Fig. 16a/b/c**).

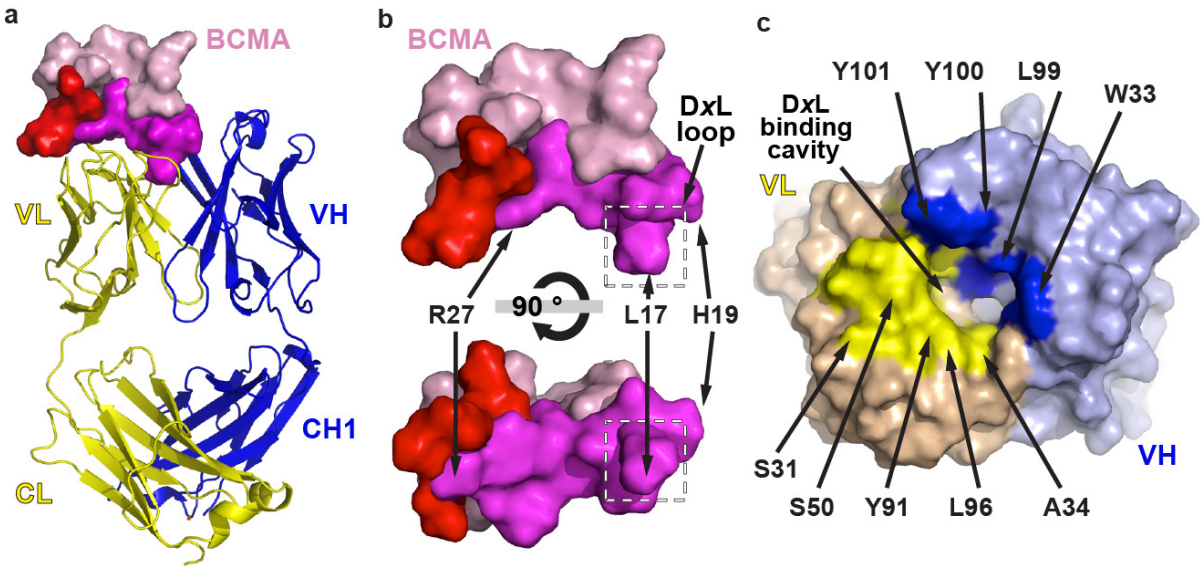

Figure 16: J22.9-xi binds the same BCMA epitope as APRIL and BAFF. (a) Structure of the J22.9-xi Fab:BCMA complex. The heavy (blue) and light (yellow) chains of the Fab fragment are shown in ribbon-type and BCMA in surface representation. **(b)** J22.9-xi recognizes the same epitope as APRIL and BAFF. Orthogonal views of the BCMA binding face, with colors as in (a). Residues contacted by APRIL, BAFF and J22.9-xi are colored magenta and residues exclusively contacted by APRIL or BAFF are colored red. L17 of the D*x*L motif is at the apex of the protruding loop of BCMA that fits into a cavity in J22.9-xi. Interface residues R27 and H19 are shown for orientation. **(c)** Surface view of the binding site in J22.9-xi, colored as in (a). Residues contacting BCMA are labeled.

Abbreviations: A (alanine), H (histidine), L (leucine), R (arginine), S (serine), W (tryptophan), Y (tyrosine)

Table 4: Data collection and statistic refinements

Data collection	**BCMA:J22.9-xi-F(ab)**
Space group	$P2_12_12_1$
Cell dimensions	
a, *b*, *c* (Å)	72.801, 110.139, 137.279
α, β, γ (°)	90, 90, 90
Resolution (Å)	1.78 (2.09) *
R_{sym} or R_{merge}	16.2 (69.9)
$I / \sigma I$	12.8 (3.04)
Completeness (%)	99.9 (99.4)
Redundancy	6.7 (6.7)

Refinement	
Resolution (Å)	1.9
No. reflections	87918
R_{work} / R_{free}	0.182/0.216
Molecules per asymmetric unit	2 heavy chains (H, A), 2 light chains (L, B), 2 BCMA (F, K)
No. atoms	
Protein	7160
Ligand/ion	2 BisTris/3 Cu^{2+}
Water	726
B-factors	
Protein	22.14
Ligand/ion	37.1/35.9
Water	27.2
R.m.s. deviations	
Bond lengths (Å)	0.013
Bond angles (°)	1.16

*Values in parentheses are for highest-resolution shell.

Interestingly, the interaction with J22.9-xi covers most of the BCMA epitope also targeted by APRIL (Hymowitz et al., 2005) (10 of 14 residues) and BAFF (Liu et al., 2003) (10 of 16 residues) (**Fig. 16a/b/c**). As with APRIL and BAFF, the D*x*L motif is completely surrounded by the ligand also in the J22.9-xi F(ab) structure. This provides clear rationalization of the blocking effect of J22.9-xi seen in the *in vitro* assay with BAFF. The overall conformation of BCMA in all three structures is very similar, with a root mean square deviation (rmsd) of the C-alpha atoms of 1.4 Å between the J22.9-xi and APRIL complexes and 1.5 Å between the J22.9-xi and BAFF complexes (**Fig. 17**). Strikingly, the respective C-alpha rmsds for the J22.9-xi BCMA binding epitope (residues 13 – 30) are only 0.98 and 0.88 Å. This indicates that J22.9-xi recognizes a functional BCMA signaling conformation and explains why its

binding can activate the NF-κB pathway.

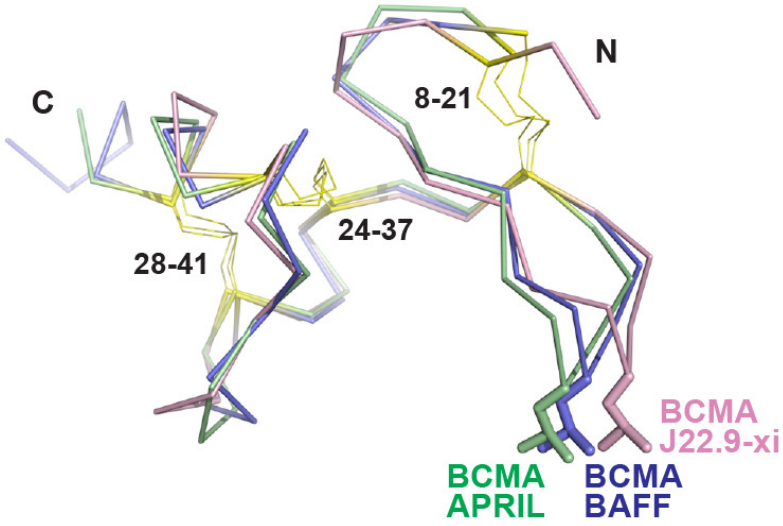

Figure 17: Backbone superposition of BCMA from three crystal structures. BCMA from the complex with APRIL (green, pdb i.d. 1XU2), from the complex with BAFF (blue, pdb i.d. 1OQD) and from the J22.9-xi complex (magenta). The side chain of Leu17 from the DxL motif is explicitly shown and the N- and C-termini are indicated, as are the three disulfide bonds (yellow) and their respective residue numbers.

5.5 J22.9-xi strongly induces ADCC and CDC in vitro

The most important feature for a therapeutic antibody is its cytotoxic activity on the target cell. Cytotoxicity can be achieved through blocking or activation of distinct signal cascades or through antibody-dependent cellular cytotoxicity (ADCC) or complement-dependent cytotoxicity (CDC). Whereas the blocking and activation mechanisms of an antibody depend on the epitope recognized by the variable region, ADCC and CDC are mediated through the constant domain (Campoli et al., 2010; Tai and Anderson, 2011). Therefore, the isotype of the antibody is important. J22.9-xi possesses the human IgG1 isotype constant domain which is the most potent human isotype known for ADCC and CDC (Jefferis, 2012; Wang and Weiner, 2008).

In order to test the cytotoxic potential of J22.9-xi, a luciferase-based cytotoxicity assay (see section 4.4.9) was established using luciferase transduced MM.1S-Luc cells (see section 5.1). In this assay, only the bioluminescence of living cells is detected, whereas luciferase released by dead cells is non-functional due to insufficient ATP in the medium (Fu et al., 2010). Peripheral blood mononuclear cells (PBMCs) from five healthy donors were isolated and mixed with MM.1S-Luc cells at a ratio of 20:1 and bioluminescence was measured after 4 hours. Lysis of MM.1S cells reached 18-35% in the presence of 125 ng/ml J22.9-xi. Increasing the concentration to 1 µg/ml increased cell lysis up to 56% (**Fig. 18a**). The lysis of tumor cells was dependent on BCMA expression, since BCMA-negative Jurkat cells were not

depleted by J22.9-xi (**Fig. 18b/c**).

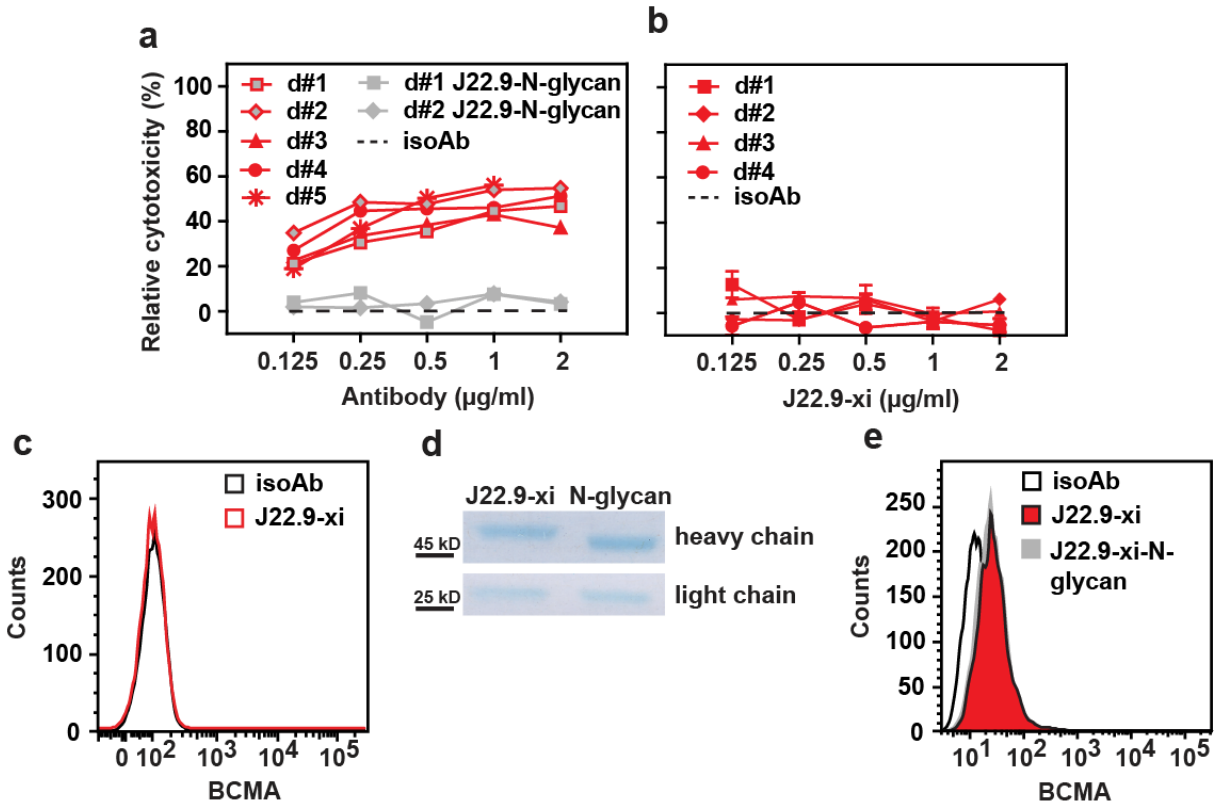

Figure 18: J22.9-xi mediates strong cytotoxic effects *in vitro*. **(a)** BCMA-positive MM.1S-Luc cells were mixed with unstimulated human PBMCs (from 5 donors (d#1-d#5)) at an effector to target ratio of 20:1 and incubated with the indicated concentrations of J22.9-xi for 4 hours (red). Grey symbols indicate the cytotoxic activity of J22.9-xi-N-glycan when incubated with PBMCs from donor 1 or 2 (red with filled grey). Cytotoxicity was calculated relative to isoAb and subtracted from 100 using bioluminescence measurements of the living cells. **(b)** No cytotoxic effect of J22.9-xi is seen when incubated on BCMA-negative Jurkat cells using unstimulated human PBMCs from 4 healthy donors. Error bars indicate SEM of triplicates. **(c)** No surface expression of BCMA on Jurkat cells is detectable using flow cytometry. Shown is one of two independent experiments. **(d)** Size comparison of J22.9-xi (left) and J22.9-xi-N-glycan using SDS-PAGE. Shown is one of two independent experiments. **(e)** No detectable difference in binding to BCMA-positive MM.1S cells between J22.9-xi and J22.9-xi-N-glycan using flow cytometry. Shown is one of two independent experiments.

Productive interaction of IgG1 with Fcγ receptors (FcγR) on effector cells or with the C1q protein of the complement cascade is dependent on glycosylation of the antibody at position 297 in the heavy chain constant region (Jefferis et al., 1998; Nezlin and Ghetie, 2004; Shields et al., 2001). To assess the proportion of cytotoxicity in this assay coming from ADCC, J22.9-xi was deglycosylated with PNGase F (J22.9-xi-N-glycan). Deglycosylation was verified by a shift in the apparent molecular mass of the heavy chain on an SDS gel (**Fig. 18d**). Although deglycosylation had no impact on the ability of J22.9-xi-N-glycan to bind to BCMA, as analyzed by flow cytometry (**Fig. 18e**), the antibody-mediated cytotoxicity decreased to below 8% (**Fig. 18a**). This observation reveals that cell lysis is due primarily to ADCC. By using serum instead of PBMCs, it was also possible to determine the CDC of J22.9-xi and

J22.9-xi-N-glycan. As expected, approximately 45% of MM.1S-Luc cells were depleted after one hour of incubation with J22.9-xi but less than 10% CDC was seen for J22.9-xi-N-glycan (**Fig. 19**). Both the ADCC and CDC assays reveal a strong cytotoxic potential for J22.9-xi against MM.1S-Luc cells *in vitro* and indicate that glycosylation of J22.9-xi is required for efficient recruitment of effector cells and activation of the complement system.

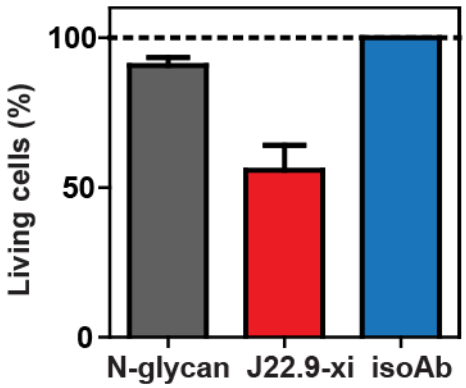

Figure 19: CDC assay. MM.1S-Luc cells incubated with serum from 4 healthy donors and either J22.9-xi-N-glycan, J22.9-xi or isoAb for one hour. Detected bioluminescence of isoAb samples was set to 100% living cells.

5.5.1 Storage conditions have no impact on cytotoxic activity

The stability of therapeutic antibodies is also of great interest, since a degraded product will have a negative impact on its performance. Therefore, the cytotoxic activity of antibodies stored at two different temperatures (4°C and -80°C) for six weeks, without additives, was assessed using the luciferase-based cytotoxicity assay (**Fig. 20**). Independent of the storage condition, J22.9-xi depleted up to 55% of MM.1S-Luc cells within 4 hours of incubation. The cytotoxic potential of frozen material is therefore comparable with that of J22.9-xi stored at 4°C. This finding was especially important for planning and performing the *in vivo* studies (see section 5.6).

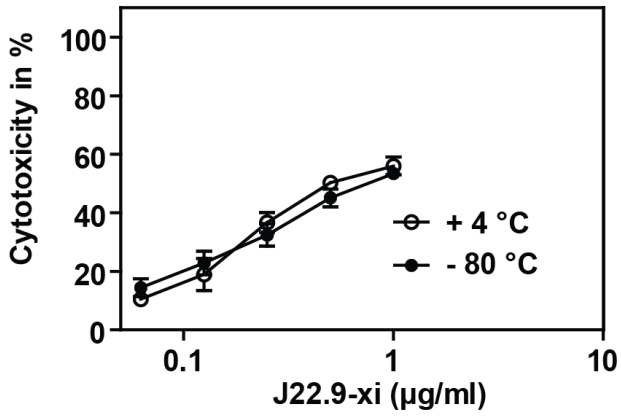

Figure 20: ADCC upon storage. BCMA-positive MM.1S-Luc cells were mixed with unstimulated human PBMCs at an effector to target ratio of 20:1 and incubated with the indicated concentrations of J22.9-xi for 4 hours. J22.9-xi was taken from samples stored for 6 weeks either at 4°C (open circles) or at -80°C (filled circles). Cytotoxicity was calculated relative to isoAb values and subtracted from

100 using bioluminescence measurements of the living cells.

5.6 J22.9-xi shows strong cytotoxic effect in vivo

Since J22.9-xi showed promising *in vitro* characteristics and strong cytotoxicity against the MM.1S cell line, the next step was to determine its *in vivo* efficacy.

5.6.1 J22.9-xi decreases tumor burden in xenografted mice and significantly prolongs survival

Next, the cytotoxic activity of J22.9-xi *in vivo* using a xenograft tumor model was tested. Six to eight week old SCID Beige female mice were intravenously (i.v.) injected with $1*10^7$ MM.1S-Luc cells (see section 4.5.5). Survival as the primary endpoint was defined by the onset of hind limb paralysis, indicating tumor growth in the bone marrow, at which point mice were euthanized.

After tumor cell challenge, mice were divided randomly into 5 groups. Groups one, two (each *n=5*) and three (*n=4*) were treated with 2, 20 and 200 µg of J22.9-xi per injection, which equates to approximately 0.1, 1 and 10 mg/kg bodyweight, respectively. To determine whether the activation of the NF-κB pathway upon binding of J22.9-xi to BCMA has any impact on tumor development, J22.9-xi-N-glycan, which neither efficiently recruits effector cells nor activates the complement system (see section 5.5.1), was administered at 200 µg per injection to group 4 (*n=6*). As control, group five (*n=5*) was treated with 200 µg isoAb. The antibodies were administered intraperitoneally (i.p.) for five succeeding days starting with the day of tumor challenge (**Fig. 21a**). Tumor growth was monitored once a week via bioluminescence measurement (see section 4.5.7) beginning on day nine post tumor cell injection. To estimate the background bioluminescence at each time point, 3 mice without tumor cells were measured. The tumor load of group five treated with isoAb increased steadily from week 2 forward, whereas tumor-derived bioluminescence was nearly undetectable at day 44 in any of the groups receiving intact J22.9-xi (**Fig. 21b/e**). Consistent with this finding, the overall tumor load was significantly reduced in J22.9-xi treated mice (**Fig. 21c**) and their survival time was nearly tripled (**Fig. 21d**). Tumor growth in animals treated with J22.9-xi-N-glycan was decelerated (**Fig. 21b**) but the overall tumor load was not significantly different from that of animals receiving isoAb (**Fig. 21c**). However, their mean lifespan was measurably prolonged by 35% (**Fig. 21d**), indicating that binding of J22.9-xi-N-glycan to BCMA alone has a negative impact on MM.1S-Luc cell survival *in vivo*.

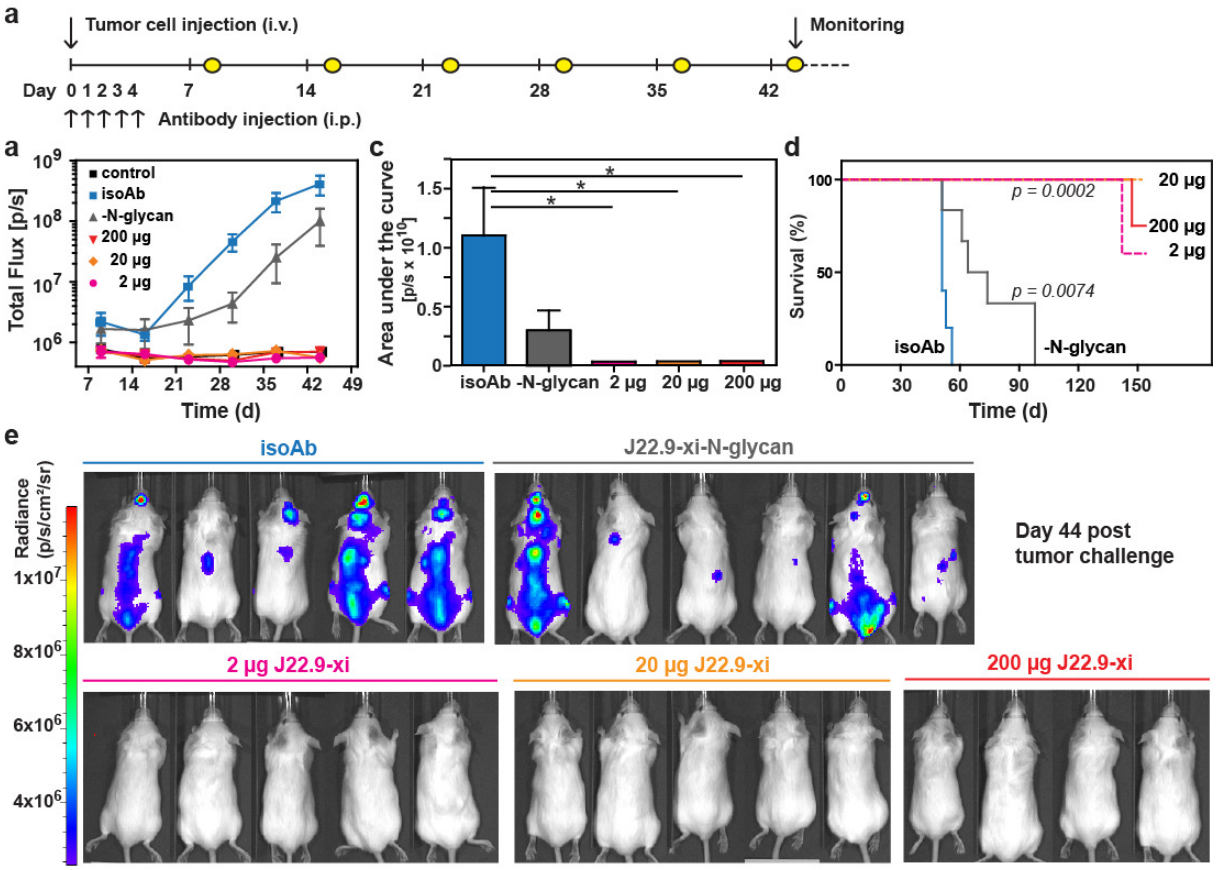

Figure 21: J22.9-xi is effective against tumors in a xenografted mouse model. **(a)** Experimental timeline: antibody treatment of xenografted SCID Beige mice for the first 5 days beginning on the day of tumor cell challenge ($1*10^7$ cells/mouse). Yellow circles indicate days of bioluminescence measurements. **(b)** Course of tumor growth in mice treated with 2 (*n=5*), 20 (*n=5*) or 200 µg (*n=4*) of J22.9-xi or 200 µg of either isoAb (*n=5*) or J22.9-xi-N-glycan (*n=6*), and without tumor (*n=3*; control). **(c)** Tumor development over time, represented as area under curve of (B), between days 9 and 44. Mean of total flux of unchallenged mice was subtracted. Shown are the mean values with SEM (*$P < 0.05$, 2-tailed t-test). **(d)** Survival of antibody-treated and control xenografted SCID Beige mice. The *P* values were calculated using the Log-rank (Mantel-Cox) Test. **(e)** Distribution of MM.1S-Luc cells in the indicated groups at day 44 post tumor challenge; dorsal view.

In a second experiment, NOD scid gamma (NSG) mice which also lack functional B, T and NK cells but support engraftments through transgenic expression of the cytokines IL-3, CSF2 and KITLG were used. Tumor cells grow faster in these mice and hind limb paralysis begins 6 weeks after tumor challenge. A repetitive antibody administration of 10 mg/kg per injection of either J22.9-xi (*n=6*) or isoAb (*n=5*) twice weekly for a period of 6 weeks was chosen, starting with the day of tumor challenge (**Fig. 22a**). Mice injected with J22.9-xi showed strongly decelerated tumor growth for the first 5 weeks (**Fig. 22b**) and a significant reduction in the overall tumor load compared with the isoAb group (**Fig. 22c**). The effectiveness of the antibody is reflected in the median survival, which was extended in J22.9-xi treated mice by 55% (**Fig. 22d**).

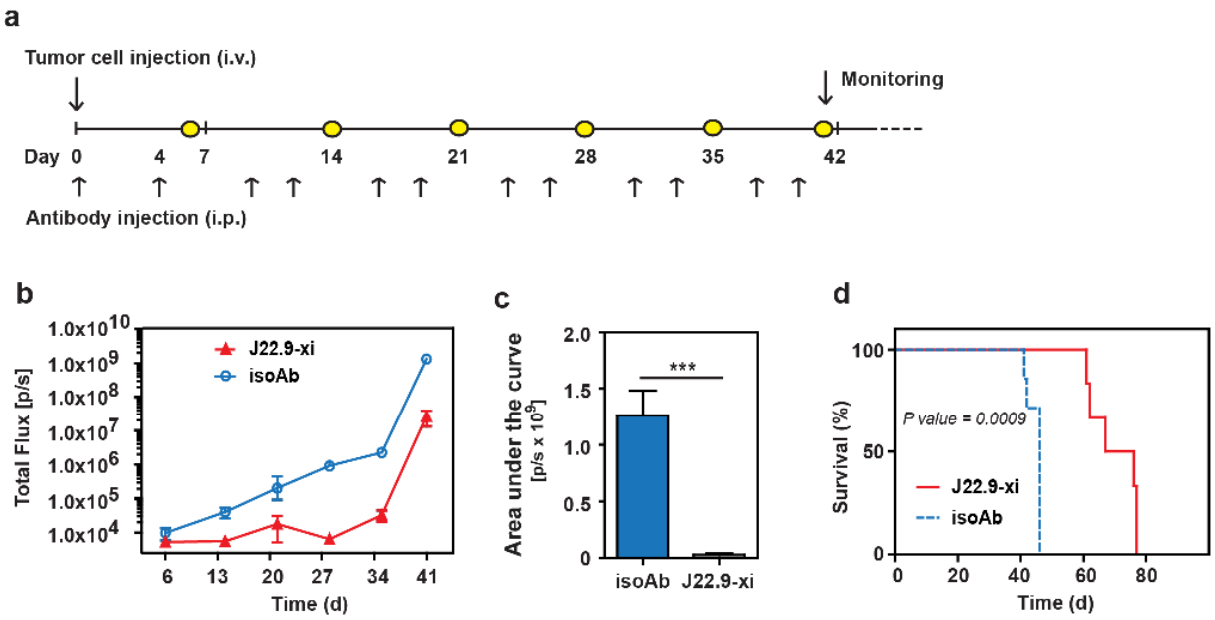

Figure 22: J.22.9-xi *in vivo* efficacy in NSG transgenic mouse strain. (a) Experimental timeline: antibody treatment twice a week beginning on the day of tumor cell challenge ($1*10^7$ cells/mouse). Yellow circles indicate days of bioluminescence measurements. **(b)** Tumor development over time with administration of 200 µg of J22.9-xi (*n=6*) or isoAb (*n=5*) twice weekly. **(c)** Total tumor burden between days 6 and 41 (Area under the curve (AUC) of (b)). Plotted are the mean values with SEM (***$P < 0.001$, 2-tailed t-test). **(d)** Overall survival. The *P* value was calculated using the Log-rank (Mantel-Cox) Test.

In both studies, all animals responded to J22.9-xi treatment and showed a strikingly decreased tumor burden and increased lifespan. These results demonstrate the *in vivo* potency of J22.9-xi either as an intact or deglycosylated antibody.

5.6.2 J22.9-xi substantially increases the lifespan of xenografted mice in model therapeutic settings

Since the outcome of the former *in vivo* experiments was positive, the *in vivo* efficacy of J22.9-xi was further investigated in a model therapeutic approach by delaying the start of antibody treatment to 5 days after tumor cell challenge (**Fig. 23a**). Xenografted mice were divided into 2 groups. The animals received 200 µg per injection of either isoAb (*n=6*) or J22.9-xi (*n=5*) twice per week. The first measurement was performed on day 8 post tumor cell injection. While there was no tumor-derived bioluminescence measurable before day 35 in the group receiving J22.9-xi, a steady increase in tumor load was seen in animals receiving isoAb (**Fig. 23b/e**), resulting in a significantly increased overall tumor load (**Fig. 23c**). Tumor challenged mice treated with isoAb survived on average 56 days, while the median lifespan of mice receiving J22.9-xi was more than tripled (**Fig. 23d**).

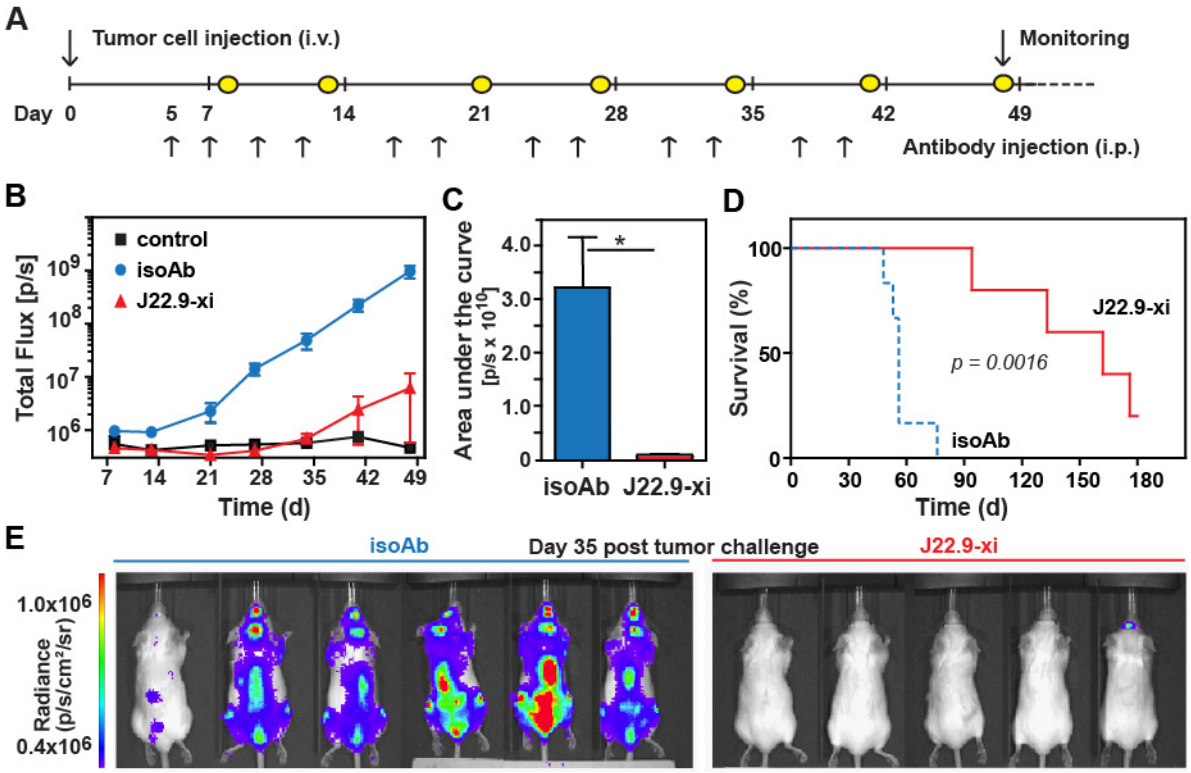

Figure 23: J22.9-xi prolongs the lifespan of SCID Beige mice in a therapeutic approach. **(a)** Experimental timeline: antibody treatment twice a week beginning on day 5 post tumor cell challenge ($1*10^7$ cells/mouse). Yellow circles indicate days of bioluminescence measurements. **(b)** Tumor development over time with administration of 200 µg of J22.9-xi (*n=5*) or isoAb (*n=6*) twice weekly beginning on day 5 post tumor challenge. Background of bioluminescence was determined using NSG mice not challenged with MM.1S-Luc cells (*n=3*; control). **(c)** Tumor development over time between days 9 and 48 of J22.9-xi and isoAb treated mice, represented as area under the curve of B). Mean of total flux of unchallenged mice was subtracted. Plotted are the mean values with SEM (*$P < 0.05$, 2-tailed t-test). **(d)** Overall survival of J22.9-xi treated SCID Beige mice. The *P* value was calculated using the Log-rank (Mantel-Cox) Test. **(e)** Distribution of MM.1S-Luc cells in the indicated groups at day 35 post tumor challenge; dorsal view.

Using the NSG mouse strain and beginning the J22.9-xi antibody treatment on day 12 after tumor challenge (**Fig. 24a**) extended the lifespan of mice by about 18% compared to mice receiving isoAb (**Fig. 24b**). These two studies confirm the anti-tumor efficacy of J22.9-xi *in vivo* and underscore the benefit of the chimeric J22.9-xi antibody in these therapeutic models.

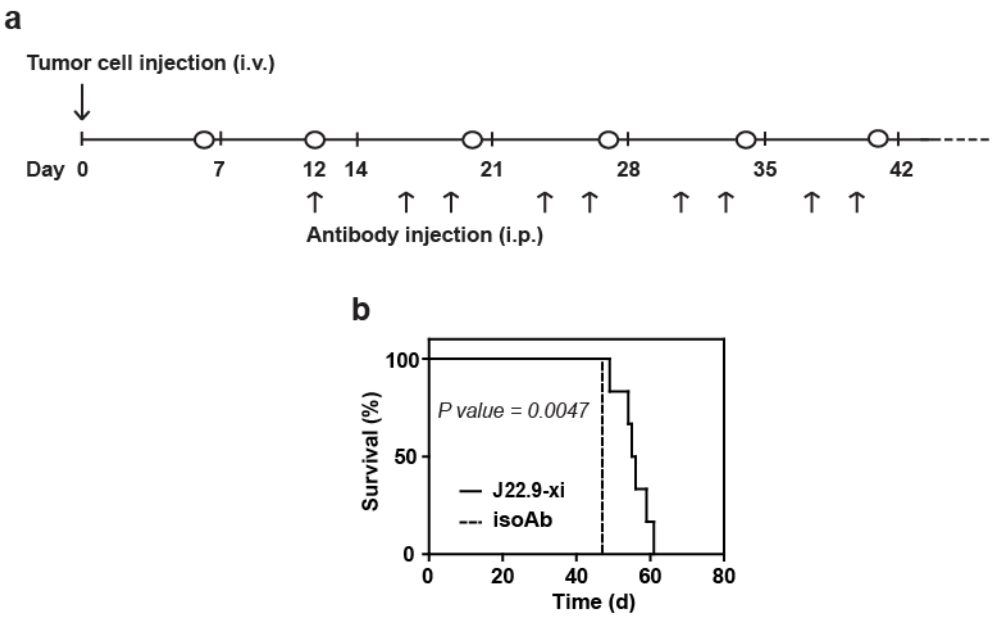

Figure 24: Treatment of NSG mice with J22.9-xi under model therapeutic conditions. (a) Experimental timeline: antibody treatment twice a week beginning on day 12 post tumor cell challenge ($1*10^7$ cells/mouse). Open circles indicate days of bioluminescence measurements. Animals were injected with 200 µg of either J22.9-xi (*n=6*) or isoAb (*n=5*) twice weekly. **(b)** Overall survival. The *P* value was calculated using the Log-rank (Mantel-Cox) Test.

6. Discussion

Due to the lack of an approved antibody therapy against MM, the aim of this study was the generation of an antibody directed against the B cell maturation antigen, which is exclusively expressed on plasma cells and in MM. This goal was achieved using hybridoma technology with subsequent cloning of the variable regions upstream the human IgG1 and kappa constant domains. The resulting human-mouse chimeric antibody, J22.9-xi, specifically binds the extracellular domain of human BCMA with an affinity exceeding that of the average antibody affinity by approximately 100 fold. Additionally, the binding of J22.9-xi to BCMA blocks the interaction with its native ligand BAFF, and leads to the activation of the canonical NF-κB signaling pathway *in vitro*. In contrast to the known anti-apoptotic effect of BCMA signal transduction, MM.1S cells incubated with J22.9-xi showed a survival disadvantage. In luciferase-based cytotoxicity assays, the antibody was able to deplete more than 50% of MM.1S cells within four hours. In addition, in a xenograft mouse model of multiple myeloma, all mice receiving the J22.9-xi antibody treatment had a significantly prolonged lifespan even in a model therapeutic approach. Moreover, experiments with a deglycosylated version of J22.9-xi, which lacks proper effector functions, revealed that the blocking and/or NF-κB activation might also have an effect *in vivo*.

6.1 Bioluminescence as an effective alternative to radioactivity-based assays

Although the gold standard of cytotoxicity assays is still the chromium (^{51}Cr)-release assay (Brunner et al., 1968), the demand for non-radioactive assays is steadily increasing due to simplicity of handling and disposal of wastes. Since the assay requires luciferase to be expressed by the cell itself, cells must either be transfected or transduced with nucleic acid encoding an expression cassette including at least a promoter and the luciferase gene. In addition, as neither method achieves 100% efficacy, luciferase-positive cells need to be selected before the assay. Moreover, the copy number of the luciferase expressing cassette will likely differ across the cell population, causing variation in luciferase expression which in turn leads to discrepancies in bioluminescence. Therefore, the establishment of a stable monoclonal cell line is advisable. Although the administrative effort for working with viral vectors for transduction is substantial, it requires less labor handling time and transduced cells remain stable even without the usage of a selection marker like geneticin (G418). Due to these reasons, it was decided to use a lentiviral system for the establishment of the luciferase-positive tumor cell lines MM.1S-Luc and Jurkat-Luc. The co-expression of GFP was useful for the sorting of transduced cells and for checking the cell lines for monoclonality. Since the

measured bioluminescence of transduced cells correlates with the cell number, and the background is nearly absent when adding luciferin without additional ATP, the luciferase-based cytotoxicity assay is a convenient alternative to the chromium (^{51}Cr)-release assay. In addition, the luciferase-transduced cell lines can be applied and monitored *in vivo* models, which is impossible with ^{51}Cr labeled cells.

6.2 Using BCMA as an antibody-target to treat multiple myeloma

In screening the literature, it becomes obvious that the need for newly developed or improved therapies is still very high with regard to multiple myeloma, although improvements in patient median survival have been realized in the past few decades (Hideshima and Anderson, 2002; Munshi and Anderson, 2013; Palumbo and Anderson, 2011; Raab et al., 2009; Richardson et al., 2003; Yang and Yi, 2011). Since MM is a hematological malignancy, the use of therapeutic antibodies is promising, as evidenced of the effectiveness of Rituximab against Non-Hodgkin's Lymphoma (Cheson and Leonard, 2008). Therefore, the list of antibodies against MM or tumor growth-promoting BM microenvironment targets in preclinical studies or early phase clinical trials is long (Munshi and Anderson, 2013; Tai and Anderson, 2011; Yang and Yi, 2011). Although some promising results have already been obtained from these studies, the problem in many cancers, including MM, is to find a target specific for this disease. Thus, many antibody-based therapies for MM accept target expression in other cell populations or body tissues that can result in severe side effects, risking the discontinuation of the study or clinical trial (Tai and Anderson, 2011; Tassone et al., 2004). Therefore, in this study B cell maturation antigen was chosen to serve as the antibody target. It is a pro-survival receptor binding the cytokines APRIL and BAFF, both of which induce expression of anti-apoptotic genes like members of the Bcl-2 family upon binding to BCMA (Coquery and Erickson, 2012; Mackay et al., 2003; Novak et al., 2004; O'Connor et al., 2004; Peperzak et al., 2013; Rickert et al., 2011). Its suitability as a target is due to the fact that it was shown to be restricted to terminally differentiated cells of the B cell lineage and MM cells. Its expression on memory B cells is controversially discussed, not least because these cells survive independently of the presence of APRIL and BAFF (Benson et al., 2008; Carpenter et al., 2013; Coquery and Erickson, 2012; Darce et al., 2007; Good et al., 2009; O'Connor et al., 2004). In addition, its function as pro-survival receptor adds the possibility of making target cells prone to apoptosis by blocking its binding. Moreover, some patients responding favorably to allogenic hematopoetic stem cell transplantation develop graft versus tumor response based on anti-BCMA antibodies in the serum (Bellucci et al., 2005). Finally, the pharmaceutical company Seattle Genetics has already developed an anti-BCMA antibody

with decent *in vitro* cytotoxic and blocking potential (Ryan et al., 2007). Although it is not known why the company halted development of their antibody at the pre-clinical, all of these facts support the idea that BCMA is an attractive antibody target for the treatment of multiple myeloma.

6.2.1 Humoral immune memory and anti-BCMA treatment

An interesting question regarding the use of anti-BCMA antibody remains: Since plasma cells can survive for decades in their niches and secrete antibodies, what will happen to the body's humoral immune memory upon depletion of all these cells and after the remaining antibodies have been cleared from the serum? If memory B cells are BCMA-negative, they will develop into antibody-secreting cells and take over the available plasma cell niches in the bone marrow. In this scenario it is likely that the immune response is only minimally disturbed, if at all. But in the case where memory B cells are also depleted by an anti-BCMA antibody, the body no longer retains protection against pathogens which were previously cleared immediately due to immune memory (e.g. vaccination). To address this question, one could immunize immune-competent mice for three to four weeks with an antigen known for the induction of a humoral immune response (e.g. GST). Sera of immunized mice can be analyzed for the presence of antigen-specific IgG antibodies throughout the whole experiment. After the immunization period, the mice would be treated with an anti-mouse-BCMA antibody (e.g. clone # 161616; R&D). When no antigen-specific antibodies can be detected in the sera, the mice would be challenged again. The time until the antigen-specific IgG titers newly emerge will indicate whether it is a primary or a secondary immune response against this antigen.

Should the antigen-specific antibody titer not decrease upon anti-BCMA antibody treatment, plasma cell depletion can be considered insufficient. This finding could indicate that long-lived plasma cells, although BCMA-positive, are somehow protected from antibody depletion. This could be due to the environment of their bone marrow niche. A related observation was made by Bellucci and colleagues (2005) in MM patients receiving allogenic hematopoetic stem cell transplantation. These patients developed a graft versus tumor response and anti-BCMA antibodies were found in their sera. This implies that these patients harbor anti-BCMA antibody secreting cells, which were protected from their own antibodies.

Independent of the outcome of such an experiment, BCMA is an attractive antibody target for the treatment of MM, since current treatments bring the risk of adverse events. Apart from the common side effects of antibody therapy like headache, fever and chills, patients treated with

Rituximab are immunosuppressed due to the depletion of all pre-B cell and recirculating B cell stages (see section 2.2.3). However, considering the severity of the disease facing patients treated with Rituximab and MM patients, the risk of such adverse events appears acceptable.

6.3 Binding, blocking, activation – the features of J22.9-xi

The basis for a therapeutic antibody is its specificity towards its antigen. This was proven for the BCMA-specific antibody J22.9-xi by flow cytometry using BCMA-positive and -negative cells, ELISA with immobilized BCMA and direct affinity measurements using SPR. J22.9-xi exhibits the highest affinity known towards BCMA, which makes it unlikely to be cross-reactive and captured by other cells or tissues.

J22.9-xi was shown to block the interaction of the BAFF and BCMA *in vitro*. This finding was rationalized by the crystal structure of the Fab:BCMA complex showing that J22.9-xi binds the majority of the interaction surface contacted by the native ligands of BCMA, APRIL and BAFF, as determined from their respective crystal structures (Hymowitz et al., 2005; Liu et al., 2003). Therefore, it is reasonable to assume that J22.9-xi also blocks APRIL, as the affinity of J22.9-xi exceeds that of APRIL and BAFF by 300- and 30,000-fold (Bossen and Schneider, 2006), respectively.

It is known that BCMA triggers the expression of anti-apoptotic genes through the activation of the NF-κB pathway upon binding of APRIL and BAFF. From the comparison of the crystal structures of J22.9-xi-F(ab):BCMA complex with the APRIL:BCMA and BAFF:BCMA complexes, it is not surprising that binding of J22.9-xi to BCMA also activates NF-κB signaling. J22.9-xi contacts most of the interaction surface of the native ligands and recognizes the functional signaling conformation seen in the cocrystal structures with APRIL and BAFF. The cell culture experiments described in section 5.3.5 show a negative effect upon J22.9-xi binding to MM.1S cells, suggesting that the activation of the NF-κB pathway upon binding of J22.9-xi to BCMA *in vitro* is responsible for the anti-tumor effect. Although activation of NF-κB is known to cause expression of pro-survival and proliferation genes, activation has also been shown to trigger expression of pro-apoptotic genes (Klapproth et al., 2009). In addition, the signals coming from binding of J22.9-xi to BCMA might be incomplete as, for instance, APRIL normally cross-links BCMA and CD138 (Ingold et al., 2005; Reijmers et al., 2011). Moreover, BCMA is a single pass transmembrane protein which needs to be cross-linked for activation, providing one explanation for the 60mer complex formation of BAFF (Mackay and Schneider, 2009). It is also possible that the high affinity of J22.9-xi towards BCMA causes changes in the activation level and/or duration. Due to these

reasons and given that NF-κB signaling is complex and heavily controlled, the downstream signaling cascade which leads to apoptosis in MM.1S cells after binding of J22.9-xi requires further investigation.

6.4 Strong cytotoxicity of J22.9-xi depends on glycosylation

Beside all of the positive features of J22.9-xi regarding its effect upon binding to BCMA, a therapeutic antibody must be able to induce a strong immune response against the marked target cells. This is facilitated through the interaction with FcγR on effector cells like macrophages, neutrophils or NK cells and/or through interaction with the complement protein C1q. These two mechanisms, ADCC and CDC, were tested in the luciferase-based cytotoxicity assays established as part of this work. In both assays, the human IgG1 constant domain revealed a strong activating potential as long as BCMA was present on the cell and the glycan moiety on Asn297 was present. Upon deglycosylation of J22.9-xi, the cytotoxic effect was abrogated as expected (Jefferis et al., 1998; Nezlin and Ghetie, 2004; Shields et al., 2001). Although J22.9-xi appears to induce apoptosis in MM.1S cells *in vitro* (see section 5.3.5), the incubation time was likely too short to measure an effect in these assays. The reason why J22.9-xi-N-glycan was tested in these assays was to make sure that the effector function was eliminated upon deglycosylation. This was important since the blocking and activating effect of J22.9-xi seen *in vitro* was to be tested *in vivo* with an antibody lacking proper effector functions but exhibiting the same half-life – a property not affected by deglycosylation in this case (Nezlin and Ghetie, 2004; Roopenian and Akilesh, 2007; Shields et al., 2001).

6.5 Xenograft mouse models confirm anti-tumor potential of J22.9-xi

In order to justify further development of J22.9-xi, it was essential to determine whether the strong cytotoxic effects towards MM cells *in vitro* could be confirmed *in vivo*. Therefore, a xenograft mouse model was established using the immunodeficient mouse strains SCID Beige and NSG. Whereas, both strains lack functional B, T and NK cells, the NSG mice additionally support engraftments due to the transgenic expression of cytokines.

The *in vitro* cytotoxicity assays reveal a strong ADCC and CDC induction upon J22.9-xi binding to MM.1S-Luc cells. This may also be the main mode of action *in vivo* where a substantial prolongation of median survival for J22.9-xi treated animals was observed. The initial boost-administration of this antibody over the first 5 successive days efficiently suppressed MM.1S-Luc tumor cell growth even at a dose as low as 0.1 mg/kg body weight

per injection. This might be attributed to the high affinity of J22.9-xi to BCMA which hinders dissociation of the antibody from tumor cells, increasing its half-life. Independent of the dose, the lifespan of all mice receiving J22.9-xi was prolonged by more than 150%. Even NSG mice, in which xenograft survival is further supported through transgenic cytokines, showed a reduced overall tumor load and an extension of median survival by 55%.

Due to the fact that signaling of BAFF and APRIL via BCMA is responsible for cell survival through up-regulation of anti-apoptotic Bcl-2 members such as Bcl-xL, Bcl-2 and Mcl-1 (Peperzak et al., 2013), the disruption of the ligand-receptor interaction should improve the therapeutic outcome in MM. To test this hypothesis, one group of mice was treated with deglycosylated J22.9-xi, which is unable to induce meaningful ADCC or CDC. The lifespan of these animals was indeed extended by 35% compared to isoAb treated mice. These results confirm that blocking the native ligands and/or the activation of NF-κB induced by J22.9-xi has a negative impact on tumor development, as a negative effect of J22.9-xi on MM.1S cells was also observed in cell culture.

In an experiment to address the functionality of J22.9-xi in a therapeutic setting, the treatment was delayed to day 5 post tumor challenge. The mode of treatment was also adjusted to better conform to a clinical setting by administration of the antibodies twice weekly over a period of 6 weeks. It further was decided to use 10 mg/kg body weight per injection, although the previous experiment showed that J22.9-xi was effective already at lower dosage. The tripling of the median survival of J22.9-xi treated animals demonstrates that this antibody is also beneficial in the treatment of established tumors. This finding was corroborated using cytokine transgenic NSG mice and delaying the start of antibody treatment to day 12.

In all *in vivo* studies all mice responded to J22.9-xi or J22.9-xi-N-glycan treatment and showed a substantially increased median survival that underlines the potential of this antibody in the treatment of MM. Eventually, J22.9-xi treated mice do die from the human tumors. However, xenografted mice do not possess a working adaptive immune system, since they lack functional B, T and NK cells. They therefore have no access to the main arm of the mammalian immune system, which is among other things important for the surveillance of the immune status of self cells and the immunological memory. Although NK cells lack the inhibitory FcγRIIB they seem not to play a major role in ADCC in mice (Nimmerjahn and Ravetch, 2007). Nevertheless, it is a missing cell population effective in the fight against the tumor cells. The absence of functional T cells is of great importance, since these cells are the central players regarding tumor regression. The uptake of tumor-specific antigens by APCs and their presentation via MHCI or MHCII molecules in these mice do not lead to an

induction of CD4- and CD8-positive effector T cells. CD4-positive cells are important for the coordination of the immune response and CD8-positive T cell can directly deplete tumor cells. In addition, these cell types form an immune memory which can help protect the body from relapses. As these immune responses cannot be initiated in SCID Beige or NSG mice, the anti-tumor effect is only effective while the mAb is present. Even though 22.9-xi was administered for six weeks in most experiments, some mice developed tumors within this time. In NSG mice, it is likely that the transgenic cytokines supported the tumor growth sufficiently such that the innate immune cells could not gain an advantage against tumor growth. With the SCID Beige mice one can speculate that the tumor cells, once exceeding a certain threshold growth, can no longer be curtailed by the immune system. One remaining the question is: why are the tumor cells not completely depleted by the antibody treatment? Perhaps some cells could escape the antibody therapy by down-regulation of BCMA and were therefore more resistant against J22.9-xi treatment. Alternatively, some cells found a niche in which they were otherwise protected from the therapy.

6.6 Summary and the therapeutic perspective of J22.9-xi

The generated BCMA-specific chimeric antibody J22.9-xi shows an exceptionally high affinity receptor-ligand interaction, induction of apoptosis in an MM cell line and significant efficacy in preclinical tumor mouse models. The solved structure of the J22.9-xi-F(ab):BCMA complex not only rationalizes the blocking and activation capacity of J22.9-xi, it will additionally facilitate humanization of the variable regions while keeping the high affinity interaction intact. With this, a necessary step towards clinical development can be fulfilled.

Although the median survival of MM patients has increased in recent years due to improvements in treatment regimens, MM remains incurable in most cases. New strategies for targeting the BM microenvironment or tumor cells directly (for example, by interfering with protein catabolism through vaccination or the use of mAbs) have evolved (Munshi and Anderson, 2013). Although the therapeutic use of mAbs holds promise, a multi-agent approach including mAbs might be necessary for overcoming the most difficult therapeutic challenges, such as those seen with Rituximab in the treatment of Non-Hodgkin's lymphoma (Cheson and Leonard, 2008). The BCMA-specific antibody J22.9-xi may provide a new potent tool for the treatment of MM.

Its use might not be restricted to MM since BCMA has also been shown to be expressed in Hodgkin's lymphoma (Chiu et al., 2007). BCMA may also be a suitable target for treating autoimmune diseases such as systemic lupus erythematosus or rheumatoid arthritis. This

antibody promises to be beneficial by depleting PCs or plasma blasts producing pathogenic autoantibodies, as both highly express BCMA on their cell surface (Benson et al., 2008; Darce et al., 2007; Good et al., 2009).

7. Abstract

Multiple myeloma (MM) is an aggressive and incurable plasma cell malignancy, in which patients suffer from bone pain, fractures, anemia and renal dysfunction. The current treatment of MM includes high-dose anti-angiogenesis, immunosuppressant or proteasome inhibitor regimens often followed by haematological stem cell transplantation. However, there is only a median life expectancy of less than seven years after diagnosis.

Although antibody-based therapies have demonstrated substantial clinical benefit for patients with hematological malignancies, there is still no approved antibody-based therapy available for MM. Therefore, the aim of this study was to generate an antibody directed against the B cell maturation antigen (BCMA). This receptor is important for the expression of anti-apoptotic genes and it is exclusively found on plasma cells and multiple myeloma cells.

The anti-BCMA antibody was generated in mice using standard hybridoma technology with subsequent amplification and cloning of the variable regions at 5' ends of the human IgG1 and kappa constant domains. This human-mouse chimeric antibody exhibits a high affinity towards BCMA and blocks the binding of the native ligands APRIL and BAFF. In addition, it activates NF-κB signaling upon binding to BCMA. Although NF-κB activation via BCMA is known to confer a survival advantage on the effected cells, the NF-κB activation upon binding of the antibody to BCMA promotes apoptosis in MM cells *in vitro*. The findings regarding binding, blocking and NF-κB activation are rationalized by the high resolution crystal structure of the F(ab) fragment in complex with the extracellular domain of BCMA.

The efficacy of the anti-BCMA antibody against MM cells was demonstrated in luciferase-based cytotoxicity assays *in vitro*. Most importantly, the antibody also effectively depletes BCMA-positive cells *in vivo* and substantially prolongs tumor-free survival under therapeutic conditions in a xenograft mouse model.

For all these reasons, the anti-BCMA antibody described herein is a promising option for the effective treatment of multiple myeloma. In addition, patients suffering from autoimmune diseases where auto-antibody secreting plasma cells are involved may benefit from such a therapeutic antibody approach.

8. Zusammenfassung

Das Multiple Myelom (MM) ist eine aggressive, unheilbare Tumorerkrankung, verursacht durch maligne Plasmazellen. Sie wird heutzutage mit Angiogenese-Inhibitoren und Immunsuppression oder Proteasom-Inhibitoren behandelt, häufig gefolgt von einer hämatologischen Stammzelltransplantation. Dennoch liegt die mittlere Lebenserwartung betroffener Patienten bei weniger als sieben Jahren.

Antikörperbasierte Therapien haben bereits bei hämatologischen Lymphomen und Leukämien einen klinischen Nutzen für Patienten gezeigt. Allerdings gibt es noch keine zugelassene Antikörpertherapie für die Behandlung von Multiplem Myelom. Deshalb wurde in dieser Arbeit das therapeutische Potential eines selbst generierten chimären human-maus Antikörpers untersucht, der das B cell maturation antigen (BCMA) bindet. Dieses Zielmolekül wird vor allem von Plasmazellen und Multiplen Myelomzellen exprimiert und spielt eine entscheidende Rolle für deren Überleben.

Der Antikörper wurde in Mäusen mit Hilfe von Standard Hybridomtechnologie generiert und anschließend wurden die variablen Regionen der schweren und leichten Kette vor die humanen konstanten IgG1- bzw. κ-Ketten kloniert. Der hochaffine Antikörper blockiert die natürlichen BCMA-Liganden APRIL und BAFF und aktiviert den NF-κB Signaltransduktionsweg. Diese Ergebnisse konnten mit Hilfe einer hochauflösenden Kristallstruktur des F(ab) Fragmentes im Komplex mit der extrazellulären Domäne von BCMA erklärt werden. Von größter Bedeutung ist jedoch die durch den Antikörper vermittelte, effektive Eliminierung von Multiple Myelom Zellen *in vitro* und *in vivo* und die damit einhergehende substantielle Verlängerung des Tumor-freien Überlebens von xenotransplantierten Mäusen selbst unter Therapie-ähnlichen experimentellen Bedingungen.

Aus den beschriebenen Gründen stellt der Antikörper eine viel versprechende Option für eine neuartige effektive Behandlung von Multiplen Myelomen und Autoimmunerkrankungen in Aussicht.

9. References

Achatz-Straussberger, G., Zaborsky, N., Konigsberger, S., Luger, E.O., Lamers, M., Crameri, R., and Achatz, G. (2008). Migration of antibody secreting cells towards CXCL12 depends on the isotype that forms the BCR. Eur J Immunol *38*, 3167-3177.

Adams, P.D., Afonine, P.V., Bunkoczi, G., Chen, V.B., Davis, I.W., Echols, N., Headd, J.J., Hung, L.W., Kapral, G.J., Grosse-Kunstleve, R.W., *et al.* (2010). PHENIX: a comprehensive Python-based system for macromolecular structure solution. Acta Crystallogr D Biol Crystallogr *66*, 213-221.

Alawadhi, A., Alawneh, K., and Alzahrani, Z.A. (2012). The effect of neutralizing antibodies on the sustainable efficacy of biologic therapies: what's in it for African and Middle Eastern rheumatologists. Clin Rheumatol *31*, 1281-1287.

Auer, S., Sturzebecher, A.S., Juttner, R., Santos-Torres, J., Hanack, C., Frahm, S., Liehl, B., and Ibanez-Tallon, I. (2010). Silencing neurotransmission with membrane-tethered toxins. Nat Methods *7*, 229-236.

Bellucci, R., Alyea, E.P., Chiaretti, S., Wu, C.J., Zorn, E., Weller, E., Wu, B., Canning, C., Schlossman, R., Munshi, N.C., *et al.* (2005). Graft-versus-tumor response in patients with multiple myeloma is associated with antibody response to BCMA, a plasma-cell membrane receptor. Blood *105*, 3945-3950.

Belnoue, E., Pihlgren, M., McGaha, T.L., Tougne, C., Rochat, A.F., Bossen, C., Schneider, P., Huard, B., Lambert, P.H., and Siegrist, C.A. (2008). APRIL is critical for plasmablast survival in the bone marrow and poorly expressed by early-life bone marrow stromal cells. Blood *111*, 2755-2764.

Benson, M.J., Dillon, S.R., Castigli, E., Geha, R.S., Xu, S., Lam, K.P., and Noelle, R.J. (2008). Cutting edge: the dependence of plasma cells and independence of memory B cells on BAFF and APRIL. J Immunol *180*, 3655-3659.

Bergsagel, D.E. (1962). Phase II trials of mitomycin C, AB-100, NSC-1026, L-sarcolysin, and meta-sarcolysin, in the treatment of multiple myeloma. Cancer Chemother Rep *16*, 261-266.

Bergsagel, P.L., and Kuehl, W.M. (2005). Molecular pathogenesis and a consequent classification of multiple myeloma. J Clin Oncol *23*, 6333-6338.

Boekel, E., Melchers, F., Rolink, A.G. (1998). Precursor B cells showing H chain allelic inclusion display allelic exclusion at the level of pre-B cell receptor surface expression. Immunity *8*, 199-207.

Bossen, C., Cachero, T.G., Tardivel, A., Ingold, K., Willen, L., Dobles, M., Scott, M.L., Maquelin, A., Belnoue, E., Siegrist, C.A., *et al.* (2008). TACI, unlike BAFF-R, is solely activated by oligomeric BAFF and APRIL to support survival of activated B cells and plasmablasts. Blood *111*, 1004-1012.

Bossen, C., and Schneider, P. (2006). BAFF, APRIL and their receptors: structure, function and signaling. Semin Immunol *18*, 263-275.

Bossen, C., Tardivel, A., Willen, L., Fletcher, C.A., Perroud, M., Beermann, F., Rolink, A.G., Scott, M.L., Mackay, F., and Schneider, P. (2011). Mutation of the BAFF furin cleavage site impairs B-cell homeostasis and antibody responses. Eur J Immunol *41*, 787-797.

Brunner, K.T., Mauel, J., Cerottini, J.C., and Chapuis, B. (1968). Quantitative assay of the lytic action of immune lymphoid cells on 51-Cr-labelled allogeneic target cells in vitro; inhibition by isoantibody and by drugs. Immunology *14*, 181-196.

Campoli, M., Ferris, R., Ferrone, S., and Wang, X. (2010). Immunotherapy of malignant disease with tumor antigen-specific monoclonal antibodies. Clin Cancer Res *16*, 11-20.

Carpenter, R.O., Evbuomwan, M.O., Pittaluga, S., Rose, J.J., Raffeld, M., Yang, S., Gress, R.E., Hakim, F.T., and Kochenderfer, J.N. (2013). B-cell maturation antigen is a promising target for adoptive T-cell therapy of multiple myeloma. Clin Cancer Res *19*, 2048-2060.

Castigli, E., Wilson, S.A., Scott, S., Dedeoglu, F., Xu, S., Lam, K.P., Bram, R.J., Jabara, H., and Geha, R.S. (2005). TACI and BAFF-R mediate isotype switching in B cells. J Exp Med *201*, 35-39.

Chan, V.S., Tsang, H.H., Tam, R.C., Lu, L., and Lau, C.S. (2013). B-cell-targeted therapies in systemic lupus erythematosus. Cell Mol Immunol *10*, 133-142.

Chavez-Galan, L., Arenas-Del Angel, M.C., Zenteno, E., Chavez, R., and Lascurain, R. (2009). Cell death mechanisms induced by cytotoxic lymphocytes. Cell Mol Immunol *6*, 15-25.

Chen, V.B., Arendall, W.B., 3rd, Headd, J.J., Keedy, D.A., Immormino, R.M., Kapral, G.J., Murray, L.W., Richardson, J.S., and Richardson, D.C. (2010). MolProbity: all-atom structure validation for macromolecular crystallography. Acta Crystallogr D Biol Crystallogr *66*, 12-21.

Cheson, B.D., and Leonard, J.P. (2008). Monoclonal antibody therapy for B-cell non-Hodgkin's lymphoma. N Engl J Med *359*, 613-626.

Chiu, A., Xu, W., He, B., Dillon, S.R., Gross, J.A., Sievers, E., Qiao, X., Santini, P., Hyjek, E., Lee, J.W., *et al.* (2007). Hodgkin lymphoma cells express TACI and BCMA receptors and generate survival and proliferation signals in response to BAFF and APRIL. Blood *109*, 729-739.

Chou, T. (2012). Multiple myeloma : recent progress in diagnosis and treatment. J Clin Exp Hematop *52*, 149-159.

Chu, V.T., Enghard, P., Riemekasten, G., and Berek, C. (2007). In vitro and in vivo activation induces BAFF and APRIL expression in B cells. J Immunol *179*, 5947-5957.

Chu, V.T., Frohlich, A., Steinhauser, G., Scheel, T., Roch, T., Fillatreau, S., Lee, J.J., Lohning, M., and Berek, C. (2011). Eosinophils are required for the maintenance of plasma cells in the bone marrow. Nat Immunol *12*, 151-159.

Claudio, J.O., Masih-Khan, E., Tang, H., Goncalves, J., Voralia, M., Li, Z.H., Nadeem, V., Cukerman, E., Francisco-Pabalan, O., Liew, C.C., *et al.* (2002). A molecular compendium of genes expressed in multiple myeloma. Blood *100*, 2175-2186.

Coquery, C.M., and Erickson, L.D. (2012). Regulatory roles of the tumor necrosis factor receptor BCMA. Crit Rev Immunol *32*, 287-305.

Darce, J.R., Arendt, B.K., Wu, X., and Jelinek, D.F. (2007). Regulated expression of BAFF-binding receptors during human B cell differentiation. J Immunol *179*, 7276-7286.

Deng, S., Yuan, T., Cheng, X., Jian, R., and Jiang, J. (2010). B-lymphocyte-induced maturation protein 1 up-regulates the expression of B-cell maturation antigen in mouse plasma cells. Mol Biol Rep *37*, 3747-3755.

DiDonato, J.A., Mercurio, F., and Karin, M. (1995). Phosphorylation of I kappa B alpha precedes but is not sufficient for its dissociation from NF-kappa B. Mol Cell Biol *15*, 1302-1311.

Dimopoulos, M.A., Palumbo, A., Attal, M., Beksac, M., Davies, F.E., Delforge, M., Einsele, H., Hajek, R., Harousseau, J.L., da Costa, F.L., *et al.* (2011). Optimizing the use of lenalidomide in relapsed or refractory multiple myeloma: consensus statement. Leukemia *25*, 749-760.

Donnelly, M.L., Luke, G., Mehrotra, A., Li, X., Hughes, L.E., Gani, D., and Ryan, M.D. (2001). Analysis of the aphthovirus 2A/2B polyprotein 'cleavage' mechanism indicates not a proteolytic reaction, but a novel translational effect: a putative ribosomal 'skip'. J Gen Virol *82*, 1013-1025.

Durie, B.G., Jacobson, J., Barlogie, B., and Crowley, J. (2004). Magnitude of response with myeloma frontline therapy does not predict outcome: importance of time to progression in southwest oncology group chemotherapy trials. J Clin Oncol *22*, 1857-1863.

Emsley, P., Lohkamp, B., Scott, W.G., and Cowtan, K. (2010). Features and development of Coot. Acta Crystallogr D Biol Crystallogr *66*, 486-501.

Fonseca, R., Bergsagel, P.L., Drach, J., Shaughnessy, J., Gutierrez, N., Stewart, A.K., Morgan,

G., Van Ness, B., Chesi, M., Minvielle, S., *et al.* (2009). International Myeloma Working Group molecular classification of multiple myeloma: spotlight review. Leukemia *23*, 2210-2221.

Forster, R., Schubel, A., Breitfeld, D., Kremmer, E., Renner-Muller, I., Wolf, E., and Lipp, M. (1999). CCR7 coordinates the primary immune response by establishing functional microenvironments in secondary lymphoid organs. Cell *99*, 23-33.

Fu, X., Tao, L., Rivera, A., Williamson, S., Song, X.T., Ahmed, N., and Zhang, X. (2010). A simple and sensitive method for measuring tumor-specific T cell cytotoxicity. PLoS One *5*, e11867.

Gatto, D., and Brink, R. (2010). The germinal center reaction. J Allergy Clin Immunol *126*, 898-907; quiz 908-899.

Getts, D.R., Getts, M.T., McCarthy, D.P., Chastain, E.M., Miller, S.D. (2010). Have we overestimated the benefit of human(ized) antibodies? Mabs *2*, 682-694.

Good, K.L., Avery, D.T., and Tangye, S.G. (2009). Resting human memory B cells are intrinsically programmed for enhanced survival and responsiveness to diverse stimuli compared to naive B cells. J Immunol *182*, 890-901.

Gordon, N.C., Pan, B., Hymowitz, S.G., Yin, J., Kelley, R.F., Cochran, A.G., Yan, M., Dixit, V.M., Fairbrother, W.J., and Starovasnik, M.A. (2003). BAFF/BLyS receptor 3 comprises a minimal TNF receptor-like module that encodes a highly focused ligand-binding site. Biochemistry *42*, 5977-5983.

Gras, M.P., Laabi, Y., Linares-Cruz, G., Blondel, M.O., Rigaut, J.P., Brouet, J.C., Leca, G., Haguenauer-Tsapis, R., and Tsapis, A. (1995). BCMAp: an integral membrane protein in the Golgi apparatus of human mature B lymphocytes. Int Immunol *7*, 1093-1106.

Gregersen, J.W., and Jayne, D.R. (2012). B-cell depletion in the treatment of lupus nephritis. Nat Rev Nephrol *8*, 505-514.

Greipp, P.R., San Miguel, J., Durie, B.G., Crowley, J.J., Barlogie, B., Blade, J., Boccadoro, M., Child, J.A., Avet-Loiseau, H., Kyle, R.A., *et al.* (2005). International staging system for multiple myeloma. J Clin Oncol *23*, 3412-3420.

Groom, J.R., Fletcher, C.A., Walters, S.N., Grey, S.T., Watt, S.V., Sweet, M.J., Smyth, M.J., Mackay, C.R., and Mackay, F. (2007). BAFF and MyD88 signals promote a lupuslike disease independent of T cells. J Exp Med *204*, 1959-1971.

Hatzoglou, A., Roussel, J., Bourgeade, M.F., Rogier, E., Madry, C., Inoue, J., Devergne, O., and Tsapis, A. (2000). TNF receptor family member BCMA (B cell maturation) associates with TNF receptor-associated factor (TRAF) 1, TRAF2, and TRAF3 and activates NF-kappa B, elk-1, c-Jun N-terminal kinase, and p38 mitogen-activated protein kinase. J Immunol *165*, 1322-1330.

Hauer, J., Puschner, S., Ramakrishnan, P., Simon, U., Bongers, M., Federle, C., and Engelmann, H. (2005). TNF receptor (TNFR)-associated factor (TRAF) 3 serves as an inhibitor of TRAF2/5-mediated activation of the noncanonical NF-kappaB pathway by TRAF-binding TNFRs. Proc Natl Acad Sci U S A *102*, 2874-2879.

Hideshima, T., and Anderson, K.C. (2002). Molecular mechanisms of novel therapeutic approaches for multiple myeloma. Nat Rev Cancer *2*, 927-937.

Hideshima, T., Mitsiades, C., Tonon, G., Richardson, P.G., and Anderson, K.C. (2007). Understanding multiple myeloma pathogenesis in the bone marrow to identify new therapeutic targets. Nat Rev Cancer *7*, 585-598.

Holliger, P., and Hudson, P.J. (2005). Engineered antibody fragments and the rise of single domains. Nat Biotechnol *23*, 1126-1136.

Hozumi, N., and Tonegawa, S. (1976). Evidence for somatic rearrangement of immunoglobulin genes coding for variable and constant regions. Proc Natl Acad Sci U S A *73*, 3628-3632.

Hsu, B.L., Harless, S.M., Lindsley, R.C., Hilbert, D.M., and Cancro, M.P. (2002). Cutting edge: BLyS enables survival of transitional and mature B cells through distinct

mediators. J Immunol *168*, 5993-5996.
Hymowitz, S.G., Patel, D.R., Wallweber, H.J., Runyon, S., Yan, M., Yin, J., Shriver, S.K., Gordon, N.C., Pan, B., Skelton, N.J.*, et al.* (2005). Structures of APRIL-receptor complexes: like BCMA, TACI employs only a single cysteine-rich domain for high affinity ligand binding. J Biol Chem *280*, 7218-7227.
Immunologylink.com (2013). FDA Approved Antibody-based Therapeutics, http://www.immunologylink.com/FDA-APP-Abs.html, (2013)
Ingold, K., Zumsteg, A., Tardivel, A., Huard, B., Steiner, Q.G., Cachero, T.G., Qiang, F., Gorelik, L., Kalled, S.L., Acha-Orbea, H.*, et al.* (2005). Identification of proteoglycans as the APRIL-specific binding partners. J Exp Med *201*, 1375-1383.
Inki, P., and Jalkanen, M. (1996). The role of syndecan-1 in malignancies. Ann Med *28*, 63-67.
Janeway, C.A., Travers, P., Walport, M., Shlomchik, M.J. (2001). *Immunobiology*, 5th edn (New York, Garland Science).
Jefferis, R. (2012). Isotype and glycoform selection for antibody therapeutics. Arch Biochem Biophys *526*, 159-166.
Jefferis, R., Lund, J., and Pound, J.D. (1998). IgG-Fc-mediated effector functions: molecular definition of interaction sites for effector ligands and the role of glycosylation. Immunol Rev *163*, 59-76.
Kabat, E.A., and Wu, T.T. (1991). Identical V region amino acid sequences and segments of sequences in antibodies of different specificities. Relative contributions of VH and VL genes, minigenes, and complementarity-determining regions to binding of antibody-combining sites. J Immunol *147*, 1709-1719.
Kabsch, W. (2010). Xds. Acta Crystallogr D Biol Crystallogr *66*, 125-132.
Klapproth, K., Sander, S., Marinkovic, D., Baumann, B., and Wirth, T. (2009). The IKK2/NF-{kappa}B pathway suppresses MYC-induced lymphomagenesis. Blood *114*, 2448-2458.
Klein, U., and Dalla-Favera, R. (2008). Germinal centres: role in B-cell physiology and malignancy. Nat Rev Immunol *8*, 22-33.
Kuehl, W.M., and Bergsagel, P.L. (2002). Multiple myeloma: evolving genetic events and host interactions. Nat Rev Cancer *2*, 175-187.
Kumar, S.K., Rajkumar, S.V., Dispenzieri, A., Lacy, M.Q., Hayman, S.R., Buadi, F.K., Zeldenrust, S.R., Dingli, D., Russell, S.J., Lust, J.A.*, et al.* (2008). Improved survival in multiple myeloma and the impact of novel therapies. Blood *111*, 2516-2520.
Kuroda, D., Shirai, H., Jacobson, M.P., Nakamura H. (2012). Computer-aided antibody design. Protein Eng Des Sel *25*, 507-522.
Kyle, R.A., and Kumar, S. (2009). The significance of monoclonal gammopathy of undetermined significance. Haematologica *94*, 1641-1644.
Leget, G.A., and Czuczman, M.S. (1998). Use of rituximab, the new FDA-approved antibody. Curr Opin Oncol *10*, 548-551.
Li, A., Rue, M., Zhou, J., Wang, H., Goldwasser, M.A., Neuberg, D., Dalton, V., Zuckerman, D., Lyons, C., Silverman, L.B.*, et al.* (2004). Utilization of Ig heavy chain variable, diversity, and joining gene segments in children with B-lineage acute lymphoblastic leukemia: implications for the mechanisms of VDJ recombination and for pathogenesis. Blood *103*, 4602-4609.
Liu, Y., Hong, X., Kappler, J., Jiang, L., Zhang, R., Xu, L., Pan, C.H., Martin, W.E., Murphy, R.C., Shu, H.B.*, et al.* (2003). Ligand-receptor binding revealed by the TNF family member TALL-1. Nature *423*, 49-56.
Lopez-Fraga, M., Fernandez, R., Albar, J.P., and Hahne, M. (2001). Biologically active APRIL is secreted following intracellular processing in the Golgi apparatus by furin convertase. EMBO Rep *2*, 945-951.
Luttman, W., Bratke, K., Küpper, M., Myrtek, D. (2006). *Experimentator: Immunologie*, 2. edn (München, Elsevier GmbH).

Ma, C., and Steinmetz, M.G. (2004). Substituent effects on competitive release of phenols and 1,3-rearrangement in alpha-keto amide photochemistry. Org Lett *6*, 629-632.
Mackay, F., Figgett, W.A., Saulep, D., Lepage, M., and Hibbs, M.L. (2010). B-cell stage and context-dependent requirements for survival signals from BAFF and the B-cell receptor. Immunol Rev *237*, 205-225.
Mackay, F., and Schneider, P. (2008). TACI, an enigmatic BAFF/APRIL receptor, with new unappreciated biochemical and biological properties. Cytokine Growth Factor Rev *19*, 263-276.
Mackay, F., and Schneider, P. (2009). Cracking the BAFF code. Nat Rev Immunol *9*, 491-502.
Mackay, F., Schneider, P., Rennert, P., and Browning, J. (2003). BAFF AND APRIL: a tutorial on B cell survival. Annu Rev Immunol *21*, 231-264.
Malavasi, F., Deaglio, S., Funaro, A., Ferrero, E., Horenstein, A.L., Ortolan, E., Vaisitti, T., and Aydin, S. (2008). Evolution and function of the ADP ribosyl cyclase/CD38 gene family in physiology and pathology. Physiol Rev *88*, 841-886.
Mantel, N. (1966). Evaluation of survival data and two new rank order statistics arising in its consideration. Cancer Chemother Rep *50*, 163-170.
Marsters, S.A., Yan, M., Pitti, R.M., Haas, P.E., Dixit, V.M., and Ashkenazi, A. (2000). Interaction of the TNF homologues BLyS and APRIL with the TNF receptor homologues BCMA and TACI. Curr Biol *10*, 785-788.
Matsuda, F., Ishii, K., Bourvagnet, P., Kuma, K., Hayashida, H., Miyata, T., and Honjo, T. (1998). The complete nucleotide sequence of the human immunoglobulin heavy chain variable region locus. J Exp Med *188*, 2151-2162.
Maul, R.W., Gearhart P.J. (2010). Controlling somatic hypermutation in immunoglobulin variable and switch regions. Immunol Res *47*, 113-122.
Meyer-Bahlburg, A., Andrews, S.F., Yu, K.O., Porcelli, S.A., and Rawlings, D.J. (2008). Characterization of a late transitional B cell population highly sensitive to BAFF-mediated homeostatic proliferation. J Exp Med *205*, 155-168.
Meyer, T.P., Zehnter, I., Hofmann, B., Zaisserer, J., Burkhart, J., Rapp, S., Weinauer, F., Schmitz, J., and Illert, W.E. (2005). Filter Buffy Coats (FBC): a source of peripheral blood leukocytes recovered from leukocyte depletion filters. J Immunol Methods *307*, 150-166.
Nilsson, B., Ekdahl, K.N. (2012). Complement diagnostics: concepts, indication, and practical guidelines. Clin Dev Immunol *2012*, 1-11.
Moore, P.A., Belvedere, O., Orr, A., Pieri, K., LaFleur, D.W., Feng, P., Soppet, D., Charters, M., Gentz, R., Parmelee, D.*, et al.* (1999). BLyS: member of the tumor necrosis factor family and B lymphocyte stimulator. Science *285*, 260-263.
Moreaux, J., Cremer, F.W., Reme, T., Raab, M., Mahtouk, K., Kaukel, P., Pantesco, V., De Vos, J., Jourdan, E., Jauch, A.*, et al.* (2005). The level of TACI gene expression in myeloma cells is associated with a signature of microenvironment dependence versus a plasmablastic signature. Blood *106*, 1021-1030.
Moreaux, J., Legouffe, E., Jourdan, E., Quittet, P., Reme, T., Lugagne, C., Moine, P., Rossi, J.F., Klein, B., and Tarte, K. (2004). BAFF and APRIL protect myeloma cells from apoptosis induced by interleukin 6 deprivation and dexamethasone. Blood *103*, 3148-3157.
Moreaux, J., Sprynski, A.C., Dillon, S.R., Mahtouk, K., Jourdan, M., Ythier, A., Moine, P., Robert, N., Jourdan, E., Rossi, J.F.*, et al.* (2009a). APRIL and TACI interact with syndecan-1 on the surface of multiple myeloma cells to form an essential survival loop. Eur J Haematol *83*, 119-129.
Moreaux, J., Veyrune, J.L., De Vos, J., and Klein, B. (2009b). APRIL is overexpressed in cancer: link with tumor progression. BMC Cancer *9*, 83.
Mülhardt, C. (2006). *Der Experimentator: Molekularbiologie/Genomics*, 5. edn (München, Elsevier GmbH).

Muller, G., Hopken, U.E., and Lipp, M. (2003). The impact of CCR7 and CXCR5 on lymphoid organ development and systemic immunity. Immunol Rev *195*, 117-135.
Munshi, N.C., and Anderson, K.C. (2013). New Strategies in the Treatment of Multiple Myeloma. Clin Cancer Res.
Muramatsu, M., Kinoshita, K., Fagarasan, S., Yamada, S., Shinkai, Y., and Honjo, T. (2000). Class switch recombination and hypermutation require activation-induced cytidine deaminase (AID), a potential RNA editing enzyme. Cell *102*, 553-563.
Nezlin, R., and Ghetie, V. (2004). Interactions of immunoglobulins outside the antigen-combining site. Adv Immunol *82*, 155-215.
Ng, L.G., Sutherland, A.P., Newton, R., Qian, F., Cachero, T.G., Scott, M.L., Thompson, J.S., Wheway, J., Chtanova, T., Groom, J.*, et al.* (2004). B cell-activating factor belonging to the TNF family (BAFF)-R is the principal BAFF receptor facilitating BAFF costimulation of circulating T and B cells. J Immunol *173*, 807-817.
Nimmerjahn, F., and Ravetch, J.V. (2007). Antibodies, Fc receptors and cancer. Curr Opin Immunol *19*, 239-245.
Nimmerjahn, F., and Ravetch, J.V. (2008). Fcgamma receptors as regulators of immune responses. Nat Rev Immunol *8*, 34-47.
Novak, A.J., Darce, J.R., Arendt, B.K., Harder, B., Henderson, K., Kindsvogel, W., Gross, J.A., Greipp, P.R., and Jelinek, D.F. (2004). Expression of BCMA, TACI, and BAFF-R in multiple myeloma: a mechanism for growth and survival. Blood *103*, 689-694.
O'Connor, B.P., Raman, V.S., Erickson, L.D., Cook, W.J., Weaver, L.K., Ahonen, C., Lin, L.L., Mantchev, G.T., Bram, R.J., and Noelle, R.J. (2004). BCMA is essential for the survival of long-lived bone marrow plasma cells. J Exp Med *199*, 91-98.
Palumbo, A., and Anderson, K. (2011). Multiple myeloma. N Engl J Med *364*, 1046-1060.
Palumbo, A., and Gay, F. (2011). A new combination for advanced multiple myeloma. Lancet Oncol *12*, 207-208.
Patel, D.R., Wallweber, H.J., Yin, J., Shriver, S.K., Marsters, S.A., Gordon, N.C., Starovasnik, M.A., and Kelley, R.F. (2004). Engineering an APRIL-specific B cell maturation antigen. J Biol Chem *279*, 16727-16735.
Paus, D., Phan, T.G., Chan, T.D., Gardam, S., Basten, A., and Brink, R. (2006). Antigen recognition strength regulates the choice between extrafollicular plasma cell and germinal center B cell differentiation. J Exp Med *203*, 1081-1091.
Peperzak, V., Vikstrom, I., Walker, J., Glaser, S.P., Lepage, M., Coquery, C.M., Erickson, L.D., Fairfax, K., Mackay, F., Strasser, A.*, et al.* (2013). Mcl-1 is essential for the survival of plasma cells. Nat Immunol *doi:10.1038/ni.2527*.
Perkins, N.D. (2007). Integrating cell-signalling pathways with NF-kappaB and IKK function. Nat Rev Mol Cell Biol *8*, 49-62.
Pham, P.L., Kamen, A., and Durocher, Y. (2006). Large-scale transfection of mammalian cells for the fast production of recombinant protein. Mol Biotechnol *34*, 225-237.
Pieper, K., Grimbacher, B., Hermann, E. (2013). B-cell biology and development J Allergy Clin Immunol *131*, 959-971.
Podar, K., Tai, Y.T., Cole, C.E., Hideshima, T., Sattler, M., Hamblin, A., Mitsiades, N., Schlossman, R.L., Davies, F.E., Morgan, G.J.*, et al.* (2003). Essential role of caveolae in interleukin-6- and insulin-like growth factor I-triggered Akt-1-mediated survival of multiple myeloma cells. J Biol Chem *278*, 5794-5801.
Raab, M.S., Podar, K., Breitkreutz, I., Richardson, P.G., and Anderson, K.C. (2009). Multiple myeloma. Lancet *374*, 324-339.
Ravetch, J.V., and Nussenzweig, M. (2007). Killing some to make way for others. Nat Immunol *8*, 337-339.
Rehm, H. (2006). *Experimentator: Proteinbiochemie/Proteomics*, 5. edn (München, Elsevier GmbH).
Reijmers, R.M., Groen, R.W., Kuil, A., Weijer, K., Kimberley, F.C., Medema, J.P., van

Kuppevelt, T.H., Li, J.P., Spaargaren, M., and Pals, S.T. (2011). Disruption of heparan sulfate proteoglycan conformation perturbs B-cell maturation and APRIL-mediated plasma cell survival. Blood *117*, 6162-6171.

Richardson, P.G., Barlogie, B., Berenson, J., Singhal, S., Jagannath, S., Irwin, D., Rajkumar, S.V., Srkalovic, G., Alsina, M., Alexanian, R.*, et al.* (2003). A phase 2 study of bortezomib in relapsed, refractory myeloma. N Engl J Med *348*, 2609-2617.

Rickert, R.C., Jellusova, J., and Miletic, A.V. (2011). Signaling by the tumor necrosis factor receptor superfamily in B-cell biology and disease. Immunol Rev *244*, 115-133.

Roccaro, A.M., Sacco, A., Thompson, B., Leleu, X., Azab, A.K., Azab, F., Runnels, J., Jia, X., Ngo, H.T., Melhem, M.R.*, et al.* (2009). MicroRNAs 15a and 16 regulate tumor proliferation in multiple myeloma. Blood *113*, 6669-6680.

Roopenian, D.C., and Akilesh, S. (2007). FcRn: the neonatal Fc receptor comes of age. Nat Rev Immunol *7*, 715-725.

Ryan, M.C., Hering, M., Peckham, D., McDonagh, C.F., Brown, L., Kim, K.M., Meyer, D.L., Zabinski, R.F., Grewal, I.S., and Carter, P.J. (2007). Antibody targeting of B-cell maturation antigen on malignant plasma cells. Mol Cancer Ther *6*, 3009-3018.

Salzer, U., Chapel, H.M., Webster, A.D., Pan-Hammarstrom, Q., Schmitt-Graeff, A., Schlesier, M., Peter, H.H., Rockstroh, J.K., Schneider, P., Schaffer, A.A.*, et al.* (2005). Mutations in TNFRSF13B encoding TACI are associated with common variable immunodeficiency in humans. Nat Genet *37*, 820-828.

Schatz, D.G., Oettinger, M.A., and Schlissel, M.S. (1992). V(D)J recombination: molecular biology and regulation. Annu Rev Immunol *10*, 359-383.

Schett, G., and Gravallese, E. (2012). Bone erosion in rheumatoid arthritis: mechanisms, diagnosis and treatment. Nat Rev Rheumatol *8*, 656-664.

Schmitz, S. (2009). *Experimentator: Zellkultur*, 2. edn (München, Elsevier GmbH).

Schneider, P., MacKay, F., Steiner, V., Hofmann, K., Bodmer, J.L., Holler, N., Ambrose, C., Lawton, P., Bixler, S., Acha-Orbea, H.*, et al.* (1999). BAFF, a novel ligand of the tumor necrosis factor family, stimulates B cell growth. J Exp Med *189*, 1747-1756.

Schroeder, H.W., Cavacini, L. (2010). Structure and function of immunoglobulins. J Allergy Clin Immunol *125*, 41-52.

Shapiro-Shelef, M., and Calame, K. (2005). Regulation of plasma-cell development. Nat Rev Immunol *5*, 230-242.

Shen, X., Zhu, W., Zhang, X., Xu, G., and Ju, S. (2011). A role of both NF-kappaB pathways in expression and transcription regulation of BAFF-R gene in multiple myeloma cells. Mol Cell Biochem *357*, 21-30.

Shields, R.L., Namenuk, A.K., Hong, K., Meng, Y.G., Rae, J., Briggs, J., Xie, D., Lai, J., Stadlen, A., Li, B.*, et al.* (2001). High resolution mapping of the binding site on human IgG1 for Fc gamma RI, Fc gamma RII, Fc gamma RIII, and FcRn and design of IgG1 variants with improved binding to the Fc gamma R. J Biol Chem *276*, 6591-6604.

Shlomchik, M.J., and Weisel, F. (2012). Germinal center selection and the development of memory B and plasma cells. Immunol Rev *247*, 52-63.

Sievers, E.L., and Senter, P.D. (2013). Antibody-drug conjugates in cancer therapy. Annu Rev Med *64*, 15-29.

Smith, S.L. (1996). Ten years of Orthoclone OKT3 (muromonab-CD3): a review. J Transpl Coord *6*, 109-119; quiz 120-101.

Stavnezer, J., Guikema, J.E.J., Schrader, C.E. (2008). Mechanism and Regulation of Class Switch Recombination. Annu Rev Immunol *26*, 261-292.

Tai, Y.T., and Anderson, K.C. (2011). Antibody-based therapies in multiple myeloma. Bone Marrow Res *2011*, 924058.

Tarlinton, D., Radbruch, A., Hiepe, F., and Dorner, T. (2008). Plasma cell differentiation and survival. Curr Opin Immunol *20*, 162-169.

Tassone, P., Goldmacher, V.S., Neri, P., Gozzini, A., Shammas, M.A., Whiteman, K.R.,

Hylander-Gans, L.L., Carrasco, D.R., Hideshima, T., Shringarpure, R., *et al.* (2004). Cytotoxic activity of the maytansinoid immunoconjugate B-B4-DM1 against CD138+ multiple myeloma cells. Blood *104*, 3688-3696.

Tiller, T., Busse, C.E., and Wardemann, H. (2009). Cloning and expression of murine Ig genes from single B cells. J Immunol Methods *350*, 183-193.

Uniprot.org (2013a). TN13B_HUMAN, http://www.uniprot.org/uniprot/Q9Y275, (2013a)

Uniprot.org (2013b). TNF13_HUMAN, http://www.uniprot.org/uniprot/O75888, (2013b)

Vagin, A., and Teplyakov, A. (2010). Molecular replacement with MOLREP. Acta Crystallogr D Biol Crystallogr *66*, 22-25.

Vale, A.M., Schroeder, H.W. (2010). Clinical consequences of defects in B-cell development. J Allergy Clin Immunol *125*, 778-787.

Vinuesa, C.G., Linterman, M.A., Goodnow, C.C., and Randall, K.L. (2010). T cells and follicular dendritic cells in germinal center B-cell formation and selection. Immunol Rev *237*, 72-89.

Vinuesa, C.G., Sanz, I., and Cook, M.C. (2009). Dysregulation of germinal centres in autoimmune disease. Nat Rev Immunol *9*, 845-857.

Wang, S.Y., and Weiner, G. (2008). Complement and cellular cytotoxicity in antibody therapy of cancer. Expert Opin Biol Ther *8*, 759-768.

Wofsy, D. (2013). Recent progress in conventional and biologic therapy for systemic lupus erythematosus. Ann Rheum Dis *72 Suppl 2*, ii66-68.

Xiang, Z., Cutler, A.J., Brownlie, R.J., Fairfax, K., Lawlor, K.E., Severinson, E., Walker, E.U., Manz, R.A., Tarlinton, D.M., and Smith, K.G. (2007). FcgammaRIIb controls bone marrow plasma cell persistence and apoptosis. Nat Immunol *8*, 419-429.

Xie, Z., Guo, N., Yu, M., Hu, M., and Shen, B. (2005). A new format of bispecific antibody: highly efficient heterodimerization, expression and tumor cell lysis. J Immunol Methods *296*, 95-101.

Xu, Z., Zan, H., Pone, E.J., Mai, T., Casali, P. (2013). Immunoglobulin class switch DNA recombination: induction, targeting and beyond. Nat Rev Immunol *12*, 517-531.

Yamane-Ohnuki, N., and Satoh, M. (2009). Production of therapeutic antibodies with controlled fucosylation. MAbs *1*, 230-236.

Yang, J., and Yi, Q. (2011). Therapeutic monoclonal antibodies for multiple myeloma: an update and future perspectives. Am J Blood Res *1*, 22-33.

Yokoyama, W.M. (2006). Production of monoclonal antibodies. Curr Protoc Cytom *Appendix 3*, Appendix 3J.

10. Curriculum vitae

For reasons of data protection, the curriculum vitae is not included in the online version.

11. Appendix

11.1 Abbreviations

A	Alanine
Å	Ångström (0.1 nm)
aa	Amino acid
ADCC	Antibody-dependent cellular cytotoxicity
AID	Activation-induced DNA-cytosine deaminase
APC	Antigen presenting cell
APC-conjugated	Allophycocyanin-conjugated
APRIL	A proliferation-inducing ligand
ASC	Antibody secreting cell
Asn	Asparagine
ATP	Adenosine triphosphate
BAFF	B cell activating factor
BAFF-R	BAFF receptor
Bcl	B cell lymphoma
BCMA	B cell maturation antigen
BCR	B cell receptor
Blimp-1	B-lymphocyte-induced maturation protein 1
BM	Bone marrow
CD	Cluster of differentiation
CDC	Complement-dependent cytotoxicity
CDR	Complementarity determining region
CH	Constant heavy
CL	Constant light
CLP	Common lymphoid progenitor
CRABO	Hypercalcemia (C), renal insufficiency (R), anemia (A), bone lesions (B) and other myeloma-related symptoms (O)
CRD	Cysteine-rich domain
CSR	Class switch recombination
CTL	Cytotoxic T lymphoicyte
CVID	Common variable immunodeficiency
D	Aspartic acid
D_H	Diversity (gene segment heavy chain)
DMEM	Dulbecco's Modified Eagle Medium
DNA	Deoxyribonucleic acid
E. coli	*Escherichia coli*
EDTA	Ethylendiaminetetraacetate
ELISA	Enzyme-linked immunosorbent assay
F(ab)	Fragment antigen binding

FACS	Fluorescence-activated cell sorting
FBC	Filter buffy coat
Fc	Fragment crystallizable
FcRn	Neotatal Fc receptor
FCS	Fetal calf serum
Fc□R	Fc gamma receptor
FDA	U.S. Food and Drug Administration
FDC	Follicular dendritic cell
FSC	Forward scattering
G418	Geneticin
GC	Germinal center
GFP	Green fluorescent protein
GST	Glutathione-S-transferase
GTP	Guanine triphosphate
H	Histidine
HAT	Hypoxantine-aminopterin-thymidine
HC	Heavy chain
HEPES	4-(2-Hydroxyethyl)-piperazin-1-ethan-sulfonic acid
HEV	High endothelial venule
HGPRT	Hypoxanthine-guanine phosphoribosyltransferase
HRP	Horseradish peroxidase
HSCT	Hematopoietic stem cell transplantation
HSPG	Heparin-sulfate proteoglycan
i.p.	intraperitoneal
i.v.	intravenous
ICOS	Inducible T cell costimulator
IFA	Incomplete Freund's adjuvant
Ig	Immunoglobulin
IGF	Insulin growth factor
IKK	Inhibitor NF-κB kinase
IL	Interleukin
IMWG	International Myeloma Working Group
IPTG	Isopropyl ß-D-1-thiogalactopyranoside
isoAb	Isotype control antibbody
IVIS	*In vivo* imaging system
IκB	Inhibitor of NF-κB
J_H, J_L	Joining (gene segment heavy chain, light chain)
kDa	kilo Dalton
KITLG	Stem cell factor
L	Leucine
LC	Light chain
mAb	Monoclonal antibody

Mcl-1	Induced myeloid leukemia cell differentiation protein 1
MGUS	Monoclonal gammopathy of undetermined clinical significance
MHC	Major histocampatibility complex
MM	Multiple myeloma
MP	Melphalan-prednisone
MW	Molecular weight
MZ	Mantel zone
N-addition	Nucleotide-addition
NF-κB	Nuclear factor kappa-light-chain-enhancer of activated B cells
NIK	NF-κB-inducing kinase
NK	Natural killer
NOD	Non-Obese Diabetic
O/N	Over night
OD_{600}	Optical density at 600 nm
P-addition	Palindromic-addition
PBMC	Peripheral blood mononuclear cell
PBS	Phosphate buffered saline
PC	Plasma cell
PCR	Polymerase chain reaction
PE	Phycoerythrin
PEG	Polyethylene glycol
PEI	Polyethylenimine
PI	Propidium iodide
pIgR	Polymeric immunoglobulin receptor
pre-B cell	precursor B cell
pre-BCR	precursor B cell receptor
pro-B cell	progenitor B cell
R	Arginine
RAG	Recombination activation gene
rmsd	Root-mean-square deviation
RNA	Ribonucleic acid
RPMI	Roswell Park Memorial Institute
RSS	Recombination signal sequence
RT	Room temperature
RT-PCR	Reverse transcription PCR
S	Serine
S2	Safety level 2
SCID	Severe combined immunodeficient
SDS-PAGE	Sodium dodecyl sulfate polyacrylamide gel electrophoresis
SEM	Standard error of the mean

SHM	Somatic hypermutation
SLO	Secondary lymphoid organ
SSC	Side scattering
TACI	Transmembrane activator and calcium modulator and cyclophilin ligand activator
TCR	T cell receptor
TdT	Terminal deoxynucleotidyl transferase
T_{FH}	Follicular B helper T cell
TLR	Toll-like receptor
TNF	Tumor necrosis factor
TNFLSF	Tumor necrosis factor ligand superfamily
TNFRSF	Tumor necrosis factor receptor superfamily
TRAF	TNF associated factor
TTP	Thymidine triphosphate
V_H, V_L	Variable (gene segment heavy chain, light chain)
VEGF	Vascular endothelial growth factor
VH	Variable heavy
VL	Variable light
VR	Variable region
W	Tryptophan
w/o	without
WB	Western blot
XBP1	X-box-binding protein 1
Y	Tyrosine

11.2 Primer list

Name	Sequence	Annealing temp (°C) used in PCR
1st PCR light chain		
5′ mKLP6, 8, 9	5′ ATGGAATCACAGRCYCWGGT 3′	50.0
5' mKLP3	5′ TGCTGCTGCTCTGGGTTCCAG 3′	50.0
5' mKLP4	5′ ATTWTCAGCTTCCTGCTAATC 3′	50.0
5' mKLP5	5′ TTTTGCTTTTCTGGATTYCAG 3′	50.0
5' mKLP6	5′ TCGTGTTKCTSTGGTTGTCTG 3′	50.0
5' mKLP14	5′ TCTTGTTGCTCTGGTTYCCAG 3′	50.0
5' mKLP19	5′ CAGTTCCTGGGGCTCTTGTTGTTC 3′	50.0
5' mKLP20	5′ CTCACTAGCTCTTCTCCTC 3′	50.0
3' mKCP	5′ TGGATGGTGGGAAGATG 3′	50.0
1st PCR heavy chain		
5' mHVP	5′ GGGAATTCGAGGTGCAGCTGCAGGAGTCTGG 3′	56.0
3' mHC1P	5′ GGAAGGTGTGCACACCGCTGGAC 3′	56.0
Sequencing primer for 1st PCR		
5' Absense	5′ GCTTCGTTAGAACGCGGCTAC 3′	
3' IgG	5′ GTTCGGGGAAGTAGTCCTTGAC 3′	
3' Cκ 494	5′ GTGCTGTCCTTGCTGTCCTGCT 3′	
2nd PCR light chain		
5′ AgeI P-mVK03	5′ CTGCAACCGGTGTACATTCCCAAATTGTTCTCACCCAGTCTCCA 3′	58.0
5′ AgeI P-mVK05	5′ CTGCAACCGGTGTACATTCCGAAAATGTTCTCACCCAGTCTCCA 3′	58.0
5′ AgeI P-mVK08	5′ CTGCAACCGGTGTACATTCCGACATCAAGATGACCCAGTCTCCA 3′	58.0
5′ AgeI P-mVK11	5′ CTGCAACCGGTGTACATTCCGACATTGTGATGACTCAGTCTC 3′	58.0
5′ AgeI P-mVK20	5′ CTGCAACCGGTGTACATTCCGACATTGTGCTCACCCAATCTCC 3′	58.0
3′ BsiWI P-mJK01	5′ GCCACCGTACGTTTGATTTCCAGCTTGGTG 3′	58.0
3′ BsiWI P-mJK02	5′ GCCACCGTACGTTTTATTTCCAGCTTGGTC 3′	58.0
3′ BsiWI P-mJK04	5′ GCCACCGTACGTTTTATTTCCAACTTTGTC 3′	58.0
3′ BsiWI P-mJK05	5′ GCCACCGTACGTTTCAGCTCCAGCTTGGTC 3′	58.0
2nd PCR heavy chain		
5′ AgeI P-mVH02	5′ CTGCAACCGGTGTACATTCCCAGGTGCAGCTGCAGCAGTCTGG 3′	60.0
3′ SalI P-mJH02	5′ TGCGAAGTCGACGCTGAGGAGACTGTGAGAGTGG 3′	60.0
3′ SalI P-mJH04	5′ TGCGAAGTCGACGCTGAGGAGACGGTGACTGAGG 3′	60.0
Sequencing primer for pTT5 vector		
5' pTT for	5′ GCGGGCATTACTTCTGCG 3′	
3' pTT rev	5′ TCCTTCCGAGTGAGAGACAC 3′	

S = G or C; W = A or T; Y = T or C